THE UNIVERSITY OF CALGARY

The Genomic Organisation and the Expression of the Calcium Ion Channel α1-subunit Gene *CACNA1F*

by

Margaret Jane Naylor

A THESIS SUBMITTED TO THE FACULTY OF GRADUATE STUDIES IN PARTIAL FULFILLMENT OF THE REQUIREMENTS FOR THE DEGREE OF MASTER OF SCIENCE

DEPARTMENT OF MEDICAL SCIENCE

CALGARY, ALBERTA

JUNE, 1999

© Margaret Jane Naylor 1999

National Library
of Canada

Acquisitions and
Bibliographic Services

395 Wellington Street
Ottawa ON K1A 0N4
Canada

Bibliothèque nationale
du Canada

Acquisitions et
services bibliographiques

395, rue Wellington
Ottawa ON K1A 0N4
Canada

Your file Votre référence

Our file Notre référence

The author has granted a non-exclusive licence allowing the National Library of Canada to reproduce, loan, distribute or sell copies of this thesis in microform, paper or electronic formats.

The author retains ownership of the copyright in this thesis. Neither the thesis nor substantial extracts from it may be printed or otherwise reproduced without the author's permission.

L'auteur a accordé une licence non exclusive permettant à la Bibliothèque nationale du Canada de reproduire, prêter, distribuer ou vendre des copies de cette thèse sous la forme de microfiche/film, de reproduction sur papier ou sur format électronique.

L'auteur conserve la propriété du droit d'auteur qui protège cette thèse. Ni la thèse ni des extraits substantiels de celle-ci ne doivent être imprimés ou autrement reproduits sans son autorisation.

0-612-48030-5

Canada

ABSTRACT

The gene for X-linked incomplete congenital stationary night blindness (CSNB) was mapped to a 1.2 Mb region within Xp11.23. Large-scale sequencing of this region identified several candidate genes for this retinal disorder, and subsequently, mutation analysis identified *CACNA1F*, a dihydropyridine-sensitive voltage-gated L-type calcium channel, as the gene responsible for incomplete CSNB. To begin the characterisation of *CACNA1F*, its genomic organisation was determined, its tissue expression pattern was defined, the mouse orthologue was identified, sequenced, and its spatial expression was determined.

The genomic organisation of *CACNA1F* was established by sequencing the cDNA and by comparison with the genomic sequence to identify the boundaries between the introns and exons. Furthermore, the cDNA sequence of the mouse orthologue of *CACNA1F*, *Cacna1f*, was amplified and sequenced. PCR amplification of a panel of cDNAs showed that expression of *CACNA1F* is restricted to the retina, while *in situ* hybridisation of *Cacna1f* probes in the mouse retina defined this expression within the retina.

Acknowledgments

I would like to thank Dr. N. Torben Bech-Hansen for providing me the opportunity to carry out this research in his laboratory. I am truly appreciative of his support of my goals and his encouragement to challenge myself and reach beyond those goals.

I would like to thank Dr. Derrick E. Rancourt for his enthusiastic support during my studies. The aspect that he brought to my project made it even more interesting and successful.

I would like to thank Tracy Maybaum for her unending support, both technical and emotional, and keeping me well supplied with both lab materials and candy!

I would like to thank Captain Picard for making it look easy and giving me a push when I needed it!

Last, but certainly not least, I would like to thank Brian, my family, and my friends for their words of encouragement and reminding me to maintain a healthy balance in my life.

This thesis is dedicated to my mother and father,

Åse and Gerald Naylor

TABLE OF CONTENTS

Title Page i

Approval Page ii

Abstract iii

Acknowledgements iv

Dedication v

Table of Contents vi

List of Tables x

List of Figures xi

Abbreviations xiii

CHAPTER ONE: INTRODUCTION 1

Clinical Definition of CSNB 2

Anatomy and physiology of the mammalian retina 9

The structure of the retina 9

The visual pathway 15

Genetic Aspects of CSNB 19

Genetic heterogeneity 19

The positional candidate approach to gene cloning 20

Identification of the gene for incomplete CSNB 24

Comparative Mapping 24

Definition of Linkage and Synteny 27

Linkage and Synteny Homologies Between Human and Mouse.. 27

Conserved Linkage and Synteny in Xp11.23..... 27

Expression studies in the mouse..... 28

The mouse as a model for retinal disorders..... 32

The Internet as a Resource..... 34

Summary..... 34

CHAPTER TWO: MATERIALS AND METHODS..... 37

General materials and methods..... 37

PCR conditions..... 37

Analysis of PCR products by gel electrophoresis..... 37

Isolation of DNA fragments from agarose gels..... 38

Quantitation of Oligonucleotide Primers..... 38

Restriction endonuclease digestion..... 39

Small-scale plasmid preparation..... 39

Small-scale BAC preparation..... 40

DNA sequencing..... 41

Acrylamide gel electrophoresis..... 41

RNA isolation..... 42

Determination of *CACNA1F* genomic structure..... 43

Design and synthesis of primers..... 43

PCR Amplification of *CACNA1F* from cDNAs representing various tissues..... 43

Analysis of PCR products..... 44
PCR-based expression analysis of *CACNA1F*..... 46
Clontech cDNA Panel..... 46
Identification and isolation of the mouse orthologue of *CACNA1F* (*Cacna1f*)..... 47
PCR-amplification using human primers..... 47
Sequencing of *Cacna1f* PCR products..... 47
5' and 3' RACE of *Cacna1f*..... 49
Computer analysis of *Cacna1f*..... 53
Analysis of expression *Cacna1f* in mouse retina using *in situ* hybridisation..... 53
Subcloning of mouse JMC8 fragments..... 53
Synthesis of riboprobes..... 54
Fixing, embedding, and sectioning of mouse eyes..... 54
In situ hybridisation..... 55
Prehybridisation..... 55
Hybridisation..... 55
Washing..... 56
Antibody conjugation..... 56
Antibody detection..... 56
Photography..... 57
Mapping of the mouse CACNA1F to the mouse X-chromosome..... 57

CHAPTER THREE: RESULTS 58

Determining the boundaries between the introns and exons 59

Genomic organisation of *CACNA1F* 59

Splice variants 66

CACNA1F cDNA sequence 75

Expression of *CACNA1F* 75

Tissue-specific expression of *CACNA1F* 75

Mouse orthologue of *CACNA1F* (*Cacna1f*) 78

PCR amplification and sequencing of *Cacna1f* 78

5' and 3' RACE of *CACNA1F* 88

Mapping of *Cacna1f* to the mouse X-chromosome 104

Spatial expression of *Cacna1f* in the mouse retina 104

CHAPTER 4: DISCUSSION 111

CACNA1F is a calcium ion channel α1 subunit 111

5'UTR 115

Splice variants 120

The mouse orthologue of *CACNA1F* 122

CACNA1F expression is localised to the retina 124

Spatial expression of *Cacna1f* in the mouse 125

The role of *CACNA1F* in night vision 127

Future studies 129

REFERENCES 131

LIST OF TABLES

Table		Page
1.	Internet Resources	35
2.	Human *CACNA1F* primer sets	45
3.	DNA panel for amplification of *CACNA1F*	44
4.	Human *CACNA1F* sequencing primers	46
5.	Mouse *Cacna1f* primer sets	48
6.	Mouse *Cacna1f* sequencing primers	49
7.	*Cacna1f* gene-specific primers for 5' and 3' RACE	52
8.	*CACNA1F* splice variant sequencing primers	72
9.	*Cacna1f* RACE product sequencing primers	89
10.	Primer sets for amplification of *Cacna1f* and *Syp* on BAC334I19	105

LIST OF FIGURES

Figure		Page
1.	Electroretinograms from unaffected individuals and patients with incomplete and complete CSNB	4
2.	Psychophysical Evaluations of patients with X-linked CSNB	7
3.	Cartoon of the human eye and retina	10
4.	The vertebrate rod photoreceptor cell	12
5.	The phototransduction cascade	16
6.	Schematic diagram of the X-chromosome	21
7.	The high resolution comparative map of the short arm of the X-chromosome between human and mouse	29
8.	Marathon cDNA adaptor and primer sequences	50
9.	cDNA sequence of CACNA1F and its predicted protein sequence	60
10.	Amplification of splice variants of the 5' end of *CACNA1F*	68
11.	Autoradiogram depicting sequence divergence at a *CACNA1F* splice junction	70
12.	Cartoon of variable sequences at the 5' end of *CACNA1F*	73
13.	The 5' end of the coding sequence showing the productive *CACNA1F* splice variant	76
14.	Tissue expression of *CACNA1F*	79
15.	Amplification of *Cacna1f*	81
16.	Fragments of *Cacna1f* amplified with human *CACNA1F* primers	83

17. Identification of amplified *Cacna1f* mouse segments..... 86

18. 5` and 3` RACE products..... 90

19. Alignment of *CACNA1F* and *Cacna1f* in the UTRs..... 93

20. Alignment of the mouse *Cacna1f* cDNA sequence with the human *CACNA1F* cDNA sequence..... 95

21. Amplification of *Syp* and *Cacna1f* on mouse BAC334I19..... 106

22. *in situ* hybridisation of *Cacna1f* transcripts in mouse retina..... 109

23. Cartoon of the topology of the predicted protein expressed from *CACNA1F*..... 113

24. Alignment of the mouse *Cacna1f* amino acid sequence with the human *CACNA1F* amino acid sequence..... 116

ABBREVIATIONS

BAC	bacterial artificial chromosome
BCIP	5-bromo-4-chloro-3-indoylyl phosphate
bp	base pair
cDNA	complementary DNA
cGMP	cyclic guanosine monophosphate
CHAPS	3-[(3-Cholamidopropyl)dimethylammonio] -1-propane-sulphonate
cm	centimetres
ddATP	dideoxyadenosine triphosphate
ddCTP	dideoxycytidine triphosphate
ddGTP	dideoxyguanosine triphosphate
ddNTP	dideoxynucleotide triphosphate
ddTTP	dideoxythymidine triphosphate
DHP	dihydropyridine
DIG	digoxigenin
DNA	deoxynucleic acid
DTT	dithiothreitol
e12.5	embryonic day 12.5
EDTA	ethylenediaminetetraacetic acid
EST	expressed sequence tag
EtBr	ethidium bromide

EtOH	ethanol
g	gravity
GDP	guanosine diphosphate
GTP	guanosine triphosphate
H_2O	water
hrs	hours
kb	kilobases
LB	luria broth
M	molar
mA	milliamperes
MABT	maleic acid/ sodium chloride / Tween20 solution
$MgCl_2$	magnesium chloride
min.	minutes
mL	millilitres
mM	millimolar
mV	millivolts
NaCl	sodium chloride
NaOH	sodium hydroxide
NBT	4-nitroblue tetrazolium chloride
ng	nanograms
NTE	sodium/ Tris/ EDTA solution
NTMT	sodium/ Tris/ magnesium/ Tween20

	solution
°C	degrees celcius
OD	optical density
PBS	phosphate buffered saline
pmol	picomoles
RNA	ribonucleic acid
RT	reverse transcription
s	seconds
SDS	sodium dodecyl sulphate
SSC	sodium chloride sodium citrate
TAE	Tris acetate EDTA
TBE	Tris borate EDTA
TBST	sodium/ potassium/ Tris/ Tween20 solution
TEMED	N.N.N'.N'-tetramethylethylenediamine
TNK	Tris sodium potassium
U	units
ug	micrograms
uL	microlitres
uM	micromolar
um	micrometre
UTP	uracil triphosphate
UTR	untranslated region

CHAPTER 1 - INTRODUCTION

X-linked congenital stationary night blindness (CSNB) is an inherited retinal disorder that is characterised by impaired night vision and reduced visual acuity and can be accompanied by other impairments such as myopia, nystagmus, and strabismus. Two clinical forms of CSNB, complete and incomplete, can be distinguished by performing electrophysiological and psychophysical examinations (Héon and Musarella, 1994). These two clinical forms of CSNB are genetically heterogeneous with the gene for incomplete CSNB (CSNB2) localising to Xp11.23 and the gene for complete CSNB (CSNB1) localising to Xp11.4 (Bech-Hansen and Pearce, 1993); (Bech-Hansen et al., 1998a); (Bergen et al., 1995); and (Boycott et al., 1998). The minimal region for CSNB2 was refined to 1.2Mb by haplotype analysis in affected individuals of Mennonite ancestry (Boycott et al., 1998). Large-scale sequencing covering approximately 900 kb of this region provided several candidate genes for incomplete CSNB.

Candidates for CSNB2 were screened for mutations in family members affected with incomplete CSNB by direct DNA sequencing. Mutations were identified in a gene predicted to encode a calcium channel α_1-subunit. At this point, it was clear that this gene, *CACNA1F*, was likely to be responsible for incomplete CSNB and necessitated the active establishment of its genomic organisation, hence setting the stage for my thesis work.

The first objective was to determine the genomic structure of the *CACNA1F* gene by defining the boundaries between the introns and the exons, including variably

expressed exons. The second objective was to identify the mouse orthologue of *CACNA1F* and determine its cDNA sequence to provide the basis for the development of a mouse model for incomplete CSNB. The third and final objective of this thesis was to determine expression pattern of *CACNA1F*. Information regarding the localisation of expression of *CACNA1F* will provide insight into the molecular mechanisms of the visual pathway that are affected in patients with incomplete CSNB.

Clinical Definition of CSNB

Congenital stationary night blindness (CSNB) refers to a group of non-progressive inherited retinal disorders in which the major symptom is inability to see in low levels of light. There are three Mendelian modes of inheritance for CSNB: autosomal dominant, autosomal recessive, and X-linked recessive, the latter of the three being the focal point of the research in the laboratory of Dr. Bech-Hansen (McKusick, 1992). Interestingly, the retinas in patients with CSNB appear normal, thus providing few clues to the molecular basis of this group of disorders (Héon and Musarella, 1994). The clinical manifestations of CSNB may include strabismus, fine or coarse nystagmus, decreased visual acuity ranging from 20/30 to 20/200 (20/200 constitutes legal blindness) or more, and the refractive error may range from mild hyperopia to severe myopia. The fundus usually appears normal upon examination, although it may be affected if severe myopia is present (Carr, 1974); (Khouri et al., 1988); (Krill, 1977); (Merin et al., 1970). Variations in these clinical features of CSNB are seen within individual families (Pearce et al., 1990).

CSNB patients are often misdiagnosed as some of the clinical symptoms are common in other ocular disorders such as nystagmus, which is found in patients with ocular albinism and congenital nystagmus (Pearce et al., 1990). Misdiagnosis also occurs in milder cases where the only manifestation is the inability to dark adapt, which is present at birth and may not be noticed by the patient until later in life (Héon and Musarella, 1994). For accurate diagnosis of CSNB, electrophysiological and psychophysical testing of the retina in dark and light adapted states is normally required.

Electroretinography is the measurement of the electrical response in the retina to a light stimulus. The electroretinogram (ERG) can be separated into components that allow for the distinction between retinal disorders involving either the rods or the cones (Héon and Musarella, 1994). The ERG in response to a flash of light is composed of three waves: the a-wave, the b-wave, and the c-wave (Héon and Musarella, 1994). The a-wave is generated by the photoreceptor layer, the b-wave is generated by the Müller cells and the bipolar cells within the inner nuclear layer, and the c-wave is generated by the retinal pigment epithelial cells (Fishman, 1985); (Jimenez-Sierra and Ogden, 1989).

For clinical diagnosis of CSNB both a- and b-wave amplitudes are measured. It is the b-wave that is most severely affected in CSNB patients suggesting the involvement of the bipolar or Müller cells in the pathogenesis of the disease (Figure 1) (Héon and Musarella, 1994). Electroretinography is used to differentiate between the two forms of X-linked CSNB, incomplete and complete CSNB (Figure 1). Rod function is reduced in incomplete CSNB, whereas it is completely diminished in complete CSNB. The oscillatory potentials normally seen on the ascending limb of the b-wave are present in patients with incomplete CSNB and absent in patients with complete CSNB (Figure 1)

Figure 1. Electroretinograms from unaffected individuals and patients with incomplete and complete CSNB. The response to bright white light demonstrates decreased rod function in CSNB patients, with a greater severity seen in patients with complete CSNB. This is observed as a decrease in b-wave amplitudes and implicit times in both complete and incomplete CSNB patients; and the absence of oscillatory potentials on the ascending limb of the b-wave in ERGs from complete CSNB patients. Response to the 30Hz flicker demonstrates the decreased functioning of cones in patients with incomplete CSNB, whereas the flicker response of patients with complete CSNB appears to be normal, suggesting the cones are unaffected. (Héon and Musarella, 1994)

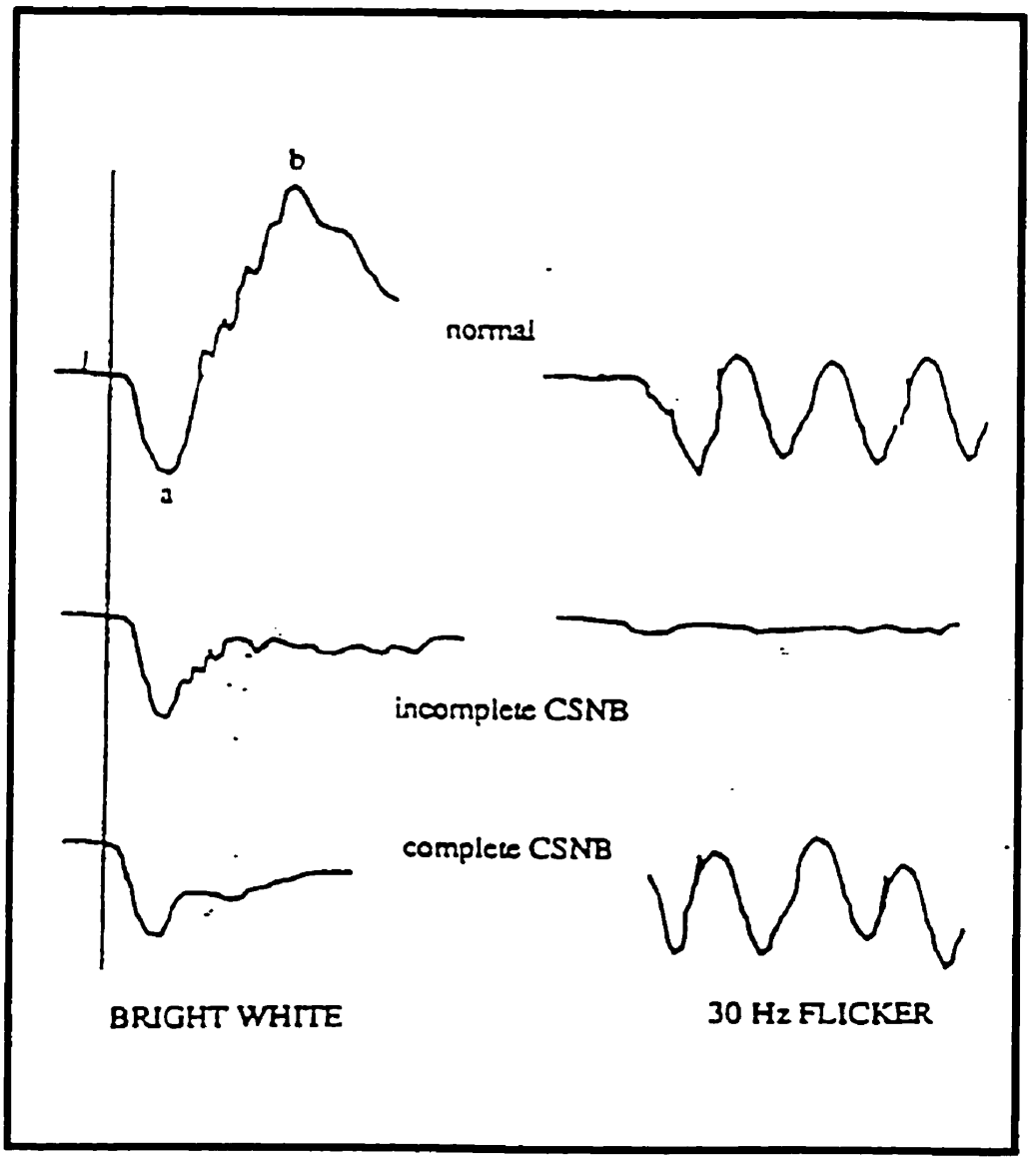
b
a
normal
incomplete CSNB
complete CSNB
BRIGHT WHITE
30 Hz FLICKER

(Heckenlively et al., 1983); (Miyake et al., 1987a). Although it is uncertain exactly where these oscillatory potentials originate, they originate from a different part of the retina compared with the origin of the a- and b- waves, confirming different mechanisms involved in incomplete and complete CSNB (as reviewed by (Wachtmeister, 1998). This is also confirmed by the response of the cones to a flickering red light stimulus where no response is elicited in patients with incomplete CSNB and a relatively normal response is elicited in patients with complete CSNB (Figure 1) (Héon and Musarella, 1994).

A second type of evaluation used to distinguish between the two forms of CSNB is psychophysical and is based on the ability of the photoreceptors to dark-adapt. The ability to dark-adapt is measured by identification of a test-target (a light source) by the patient, the intensity of which can be adjusted (Jimenez-Sierra and Ogden, 1989). The resulting dark adaptation curve for normal eyes is bipartite with the first part of the curve measuring cone adaptation and the second part measuring rod adaptation (Figure 2) (Héon and Musarella, 1994). In incomplete CSNB, the curve for rod adaptation is elevated, but the cone-rod break in the curve can still be seen, thus indicating partial functioning of the rods. The curve measuring rod adaptation is elevated even further in complete CSNB; and because the cone-rod break is not observed this curve is monophasic, indicating no rod adaptation (Figure 2) (Miyake et al., 1987b); (Miyake et al., 1986).

Figure 2. Psychophysical Evaluations of patients with X-linked CSNB. Dark adaptation curves in CSNB showing a bipartite curve for normal adaptation, an elevated curve for rod adaptation in incomplete CSNB, and the disappearance of the cone-rod break due to increased elevation of the rod adaptation curve in complete CSNB. (Héon and Musarella, 1994)

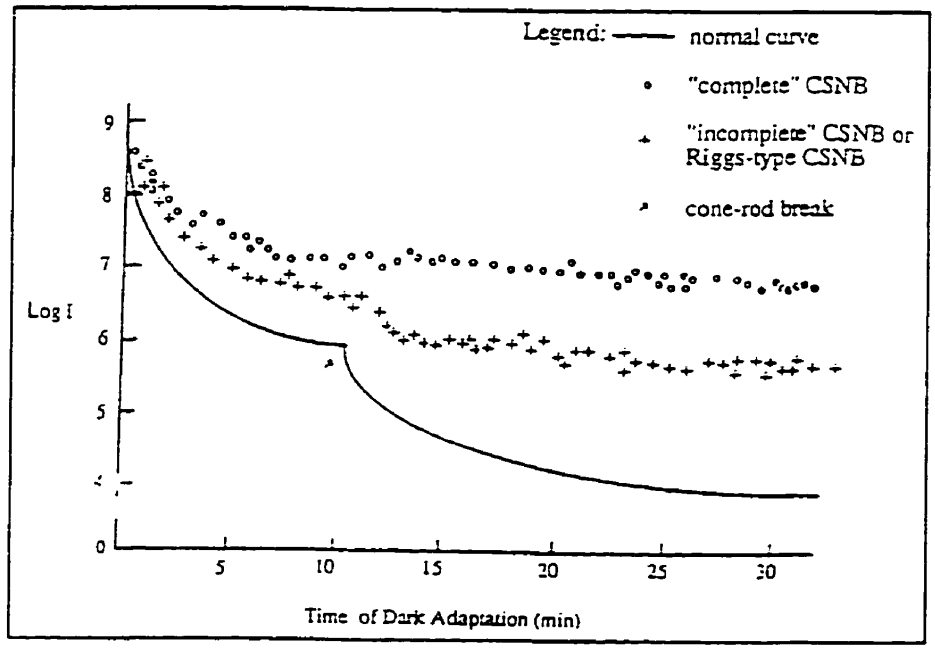
Legend: —— normal curve
"complete" CSNB
"incomplete" CSNB or Riggs-type CSNB
cone-rod break
Log I
9
8
7
6
5
0
5
10
15
20
25
30
Time of Dark Adaptation (min)

Anatomy and physiology of the mammalian retina

Crucial to understanding the molecular mechanisms behind a retinal disorder is the appreciation of the normal anatomy and physiology of the retina. An introduction to the anatomy of the mammalian retina and the differences and similarities between the mouse retina and the human retina will allow for a detailed discussion of the role that the calcium channel may play in incomplete CSNB.

The structure of the retina

Originating from the neurectoderm of the forebrain in development, the retina is the sensory tissue of the eyeball (Figure 3) (Williams, 1995). It is connected to the brain via the optic nerve, which is continuous with the ganglionic cells comprising the innermost layer of the retina. The retina is bounded externally by the choroid and internally by the hyaloid membrane of the vitreous body (as reviewed by (O'Brien, 1995).

The outermost layer of the retina is the retinal pigment epithelium which is a highly vascularised layer of simple cuboidal cells whose nuclei are located near the basal lamina that connects with the choroid via Bruch's membrane (as reviewed by (O'Brien, 1995). Toward the rods and cones the pigment epithelium projects microvilli that touch the outer segments (Figure 4). This epithelial layer has three major functions. Firstly, it is well known for the recycling of activated rhodopsin components and the phagocytosis and degradation of the ends of the rods and cones. Secondly, the pigment epithelium absorbs any light that hits it and prevents light from hitting the photoreceptors twice, hence allowing for a sharper image. Thirdly, the pigment epithelium functions as a

Figure 3. Cartoon of the human eye and a cross section through the retina showing the various structures and cell types (Copenhagen, 1996). The back of the retina is comprised of the retinal pigment epithelium. The next layer of cells toward the centre of the eye is the photoreceptor cell layer which is made up of both rod and cone photoreceptors and appears as four layers under the microscope. The outer segments, the inner segments, the cell nuclear bodies (outer nuclear layer) and the synaptic termini (the outer plexiform layer) make up these layers. The horizontal, bipolar, and amacrine cell bodies make up the inner nuclear layer, while their synaptic termini make up the inner plexiform layer. The innermost layer is comprised of ganglion cells (ganglion cell layer), the axons of which form the optic nerve. (O'Brien, 1995)

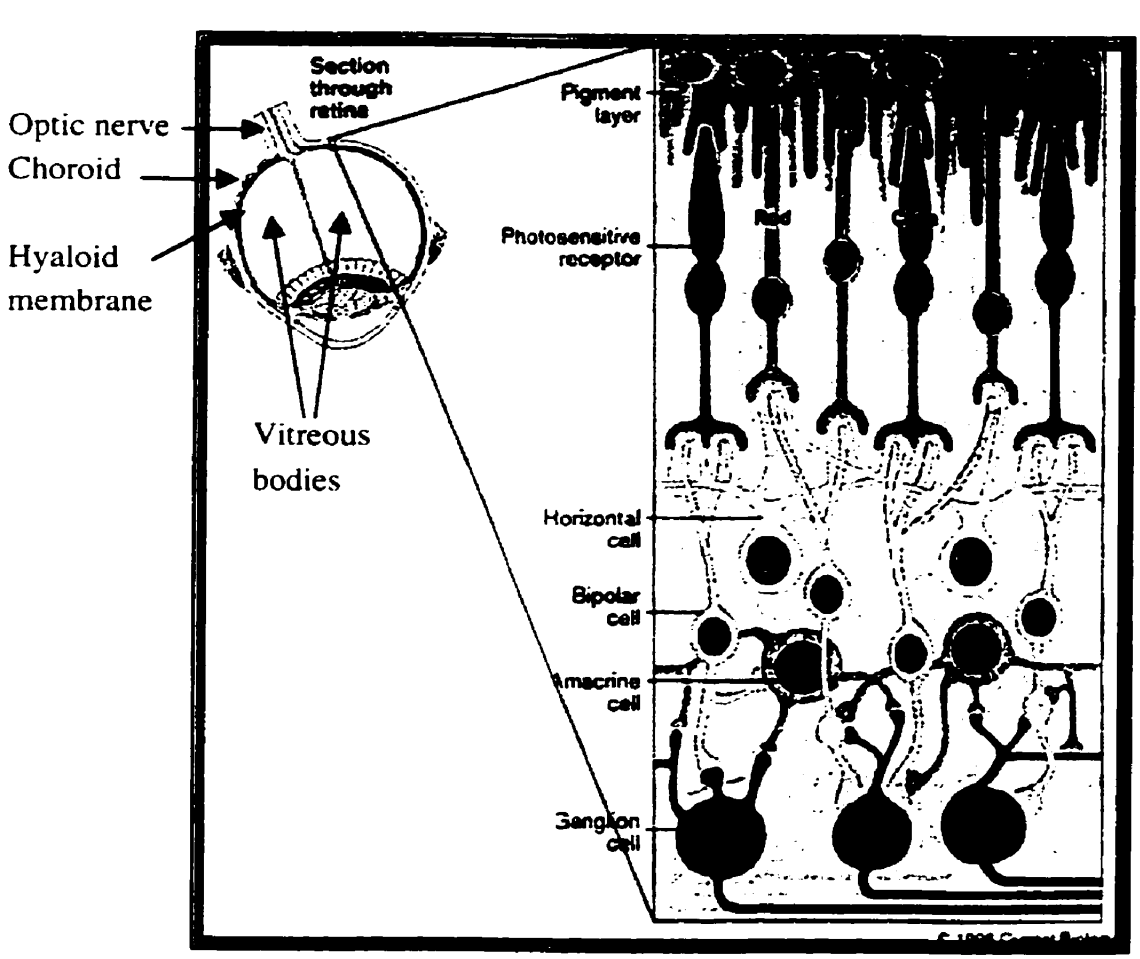
Optic nerve
Choroid
Hyaloid membrane
Vitreous bodies
Section through retina
Pigment layer
Photosensitive receptor
Horizontal cell
Bipolar cell
Amacrine cell
Ganglion cell
Retinal pigmen epithelium
Outer segments
Inner segments
Outer nuclear layer
Outer plexiform layer
Inner nuclear layer
Inner plexiform layer
Ganglion cell layer

Figure 4. The vertebrate rod photoreceptor cell. The outer segment is comprised of stacks of membranous sacs that provide the ultrastructure in which the components of the phototransduction cascade are embedded with rhodopsin being the major component. Microvilli are projected from the pigment epithelial cells and surround the outer segments of the rods and cones. (Farber and Danciger, 1994)

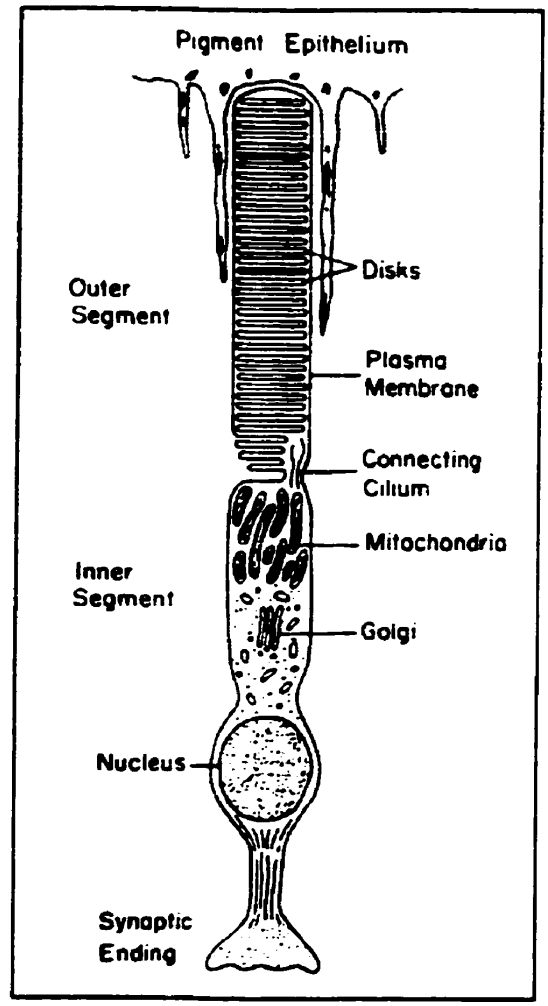
Pigment Epithelium
Disks
Outer Segment
Plasma Membrane
Connecting Cilium
Mitochondria
Inner Segment
Golgi
Nucleus
Synaptic Ending

blood-retinal barrier, regulating ion exchange as well as preventing the entry of leucocytes into the interior of the eye.

The photoreceptor cells comprise the next four layers of the retina (Figure 3) (as reviewed by (O'Brien, 1995). The outer segment layer is composed of the outer portion of the rod and cone processes called the lamellae (Figure 3). The lamellae are made up of stacks of discoidal membranous sacs that are embedded with rhodopsin molecules, which are photoreceptive molecules that initiate a phototransduction cascade involving second messengers (Figure 4). The inner segments of the rod and cone processes comprise the inner segment layer of the retina. These segments of the photoreceptor cells contain molecules that store energy for phototransduction. The third layer, the outer nuclear layer, is comprised of the cell bodies of the photoreceptor cells. The fourth layer, the outer plexiform layer is the region where the synaptic termini of the rod and cone cells interact with the synaptic termini of the bipolar and amacrine cells (Figure 3) (as reviewed by (O'Brien, 1995).

Next is the inner nuclear layer, an ordered array of nuclei and cell bodies of the horizontal cells, bipolar cells, and amacrine cells, with the horizontal cells being outermost and the amacrine cells being innermost (Figure 3). The inner plexiform layer is the layer where the ganglion cells synapse with the cells of the inner nuclear layer in a complex set of interactions. Ganglion cell bodies and nuclei make up the innermost neural cell layer in the retina called the ganglion cell layer (Figure 3). The axons of ganglion cells form the nerve fibre layer, which makes up the lamina on the inner surface of the retina and these fibres bundle to form the optic nerve at the optic disc.

The Müller (glial) cells span the thickness of the retina from the inner segments to the internal lamina (as reviewed by (O'Brien, 1995). These cells extend processes that wrap around the cell bodies of different cell types within the retina. Müller cell functioning is affected in patients with CSNB and plays a role in the diagnosis of this disorder.

The visual pathway

Once light (400-700 nm wavelength range) strikes the retina, a series of complex molecular interactions occurs in the outer segment of the photoreceptor cells that results in the closure of cGMP-gated ion channels and subsequently, the hyperpolarisation of these cells. This cascade of interactions is so sensitive that only a single photon is required to elicit a response in an individual rod (Rieke and Baylor, 1998). Figure 5 shows the details of this cascade. The hyperpolarisation of the photoreceptors causes the closure of L-type calcium channels in the inner segments and causes an inhibition in the release of glutamate, an excitatory amino acid, at the synaptic terminal of the photoreceptor cell (Schmitz and Witkovsky, 1997); (Tachibana et al., 1993). Prior to the closure of these channels, when the retina is in a dark-adapted state, the high Ca^{++} concentration maintains a continuous release of glutamate from the photoreceptor at this synapse (Rieke and Schwartz, 1994).

The visual signal from the rod photoreceptors is recognised by the rod bipolar cells because of the decrease in glutamate. The rod bipolar cells are maintained in a hyperpolarised or ON state in the dark-adapted retina when they are being stimulated by

Figure 5. The phototransduction cascade in the outer segments of the photoreceptor cells (Polans et al., 1996). The first molecule in the cascade that responds to light is rhodopsin (as reviewed by Rispoli, 1998). Rhodopsin ® is a visual pigment that is made up of the transmembrane protein opsin that is covalently linked to 11-cis-retinal by a protonated Schiff base linkage. This protonation changes the absorption wavelength (hv) from UV to visible (about 500 nm). Upon absorption of a photon, 11-cis-retinal isomerizes to all-trans-retinal which causes a series of changes in the Rhodopsin molecule. Of several intermediates that are formed from Rhodopsin, metarhodopsin II (R*) is the active molecule and initiates the amplification cascade. R* interacts with Transducin (T), a heterotrimeric G-protein, and catalyses the exchange of GDP for GTP (as reviewed by Koutalos and Yau, 1996 and Rispoli, 1998). The first stage of amplification occurs at this step (a single R* can activate 1000-5000 Transducin molecules per second). This uptake of GTP causes the dissociation of Transducin into two subunits, α and β. The α subunit carries the GTP and diffuses freely within the outer segment. This molecule acts on phosphodiesterase (PDE), also a heterotrimer, causing the release of the γ subunit, thus exposing the catalytic sites for cGMP. cGMP is rapidly

hydrolysed by activated PDE, hence its intracellular concentration decreases dramatically. This provides the second stage of the amplification cascade (PDE can hydrolyse cGMP at a rate of up to 4000 molecules per second). cGMP is required to maintain the outer segment in a depolarised state by maintaining the flow of Na^+ and Ca^{++} ions into the outer segment through cGMP-gated ion channels (CaM) (as reviewed by Rispoli, 1998).

This influx of Na^+ and Ca^{++} ions along with an efflux of Ca^{++} and K^+ through a Na^+: Ca^{++}, K^+ exchanger embedded in the cell membrane of the inner segment creates what is known as the dark current. The drop in the intracellular cGMP levels caused by hydrolysis through PDE leads to the closure of the cGMP-gated channels, and a subsequent decrease in flow of Na^+ and Ca^{++} into the outer segment. Although fewer Na^+ and Ca^{++} ions are entering the cell, the efflux of Ca^{++} and K^+ is maintained. This rapid decrease in intracellular ion concentration leads to the hyperpolarisation of the photoreceptor giving the rod an electrical potential more negative than –45mV, which in turn, causes the closure of voltage-gated L-type Ca^{++} channels in the inner segment of the photoreceptor (Witkovsky et al., 1997). Figure from Polans et al., 1996.

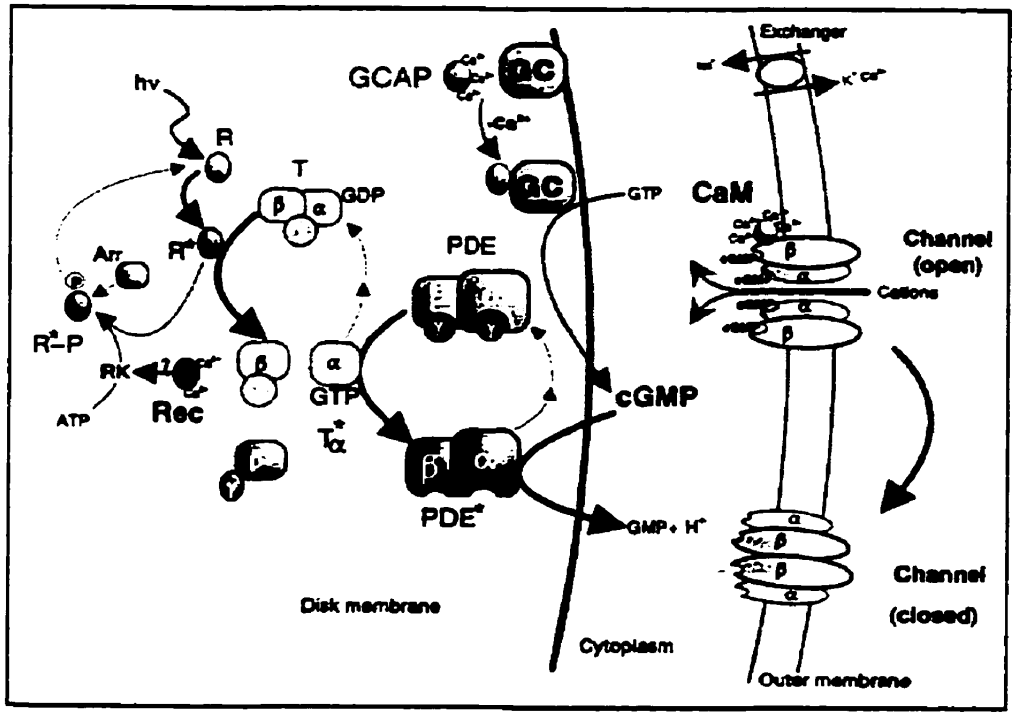

LEGEND

hv -wavelength	R -rhodopsin
R* -activated rhodopsin	R*-P -phosphorylated opsin
Arr -arrestin	RK -rhodopsin kinase
Rec -recoverin	T -transducin
T_α* -activated transducin	PDE -phosphodiesterase
GCAP - guanylate cyclase activating proteins	CaM -calmodulin

glutamate and depolarise when they are no longer stimulated by glutamate. Due to this, the rod bipolar cells are also known as a depolarising bipolar cells or DBCs. When DBCs become depolarised, potassium ions are released into the extracellular space and get taken up by Müller cells which also become depolarised (Stockton and Slaughter, 1989). This creates a transretinal electrical current that is believed to be responsible for a significant portion of the b-wave (Miller and Dowling, 1970). The visual signal is then transmitted to the brain through the ganglion cells and the optic nerve (as reviewed by (Sieving, 1993). The cone pathway, on the other hand, is more complex than the rod pathway, with connections to both depolarising and hyperpolarising cone-specific bipolar cells (DBC and HBC). However, as in the rod pathway, the DBCs form an ON pathway with the cones that is thought to function in a similar manner to the rod ON pathway. Yet, exclusive to the cones the connection with the HBCs form the OFF pathway which provides the cone its specialised function (as reviewed by (Sieving, 1993). An understanding of this pathway will enable us to determine a potential role for the gene responsible for incomplete CSNB.

Genetic Aspects of CSNB

Genetic heterogeneity

CSNB was first localised to the short arm of the X-chromosome (Xp11) by demonstrating linkage to markers DXS7 (Gal et al., 1989); (Musarella et al., 1989) and DXS255 (Bech-Hansen et al., 1990). CSNB was proven to be genetically heterogeneous (Bech-Hansen and Pearce, 1993); (Bergen et al., 1995); (Boycott et al., 1998), with

CSNB1 localised to Xp11.4 and CSNB2 localised to Xp11.23 (Figure 6) (Bech-Hansen et al., 1998); (Boycott et al., 1998). In addition to X-linked CSNB, the genes for retinitis pigmentosa (RP2) (Ott et al., 1990), Åland Island eye disease (ÅIED) (Alitalo et al., 1991); (Schwartz and Rosenberg, 1991), and a host of other disease genes also localised to the p11 region of the X-chromosome (Figure 6).

At one point the minimal regions for RP2, ÅIED and CSNB2 overlapped and the possibility that these disorders were caused by mutations in the same gene arose. Recent evidence from the laboratory of Dr. Bech-Hansen has shown that incomplete CSNB and Åland Island eye disease are due to alterations in the same gene (Bech-Hansen et al., unpublished data), whereas the recent identification of the RP2 gene demonstrated that a different gene was involved in retinitis pigmentosa (Figure 6) (Schwahn et al., 1998).

The positional candidate approach to gene cloning

A positional cloning strategy was carried out by the laboratory of Dr. Bech-Hansen in the search for CSNB2. Construction of haplotypes in families with incomplete CSNB localised CSNB2 to the region between markers DXS6849 and DXS8023 in Xp11.23 (Bech-Hansen et al., 1998a). Analysis of a set of Mennonite families narrowed the minimal region for CSNB2 to 1.2 Mb of DNA between markers DXS722 and DXS255 (Boycott et al., 1998).

Figure 6. Schematic diagram of the X-chromosome depicting the genetic heterogeneity of X-linked CSNB. CSNB1 lies in the Xp11.4 region and CSNB2 lies within Xp11.23. Loci for other retinal disease genes such as RP3, COD1, X-linked optic atrophy, Norrie disease, and RP2 also lie on the short arm of the X-chromosome. (Héon and Musarella, 1994).

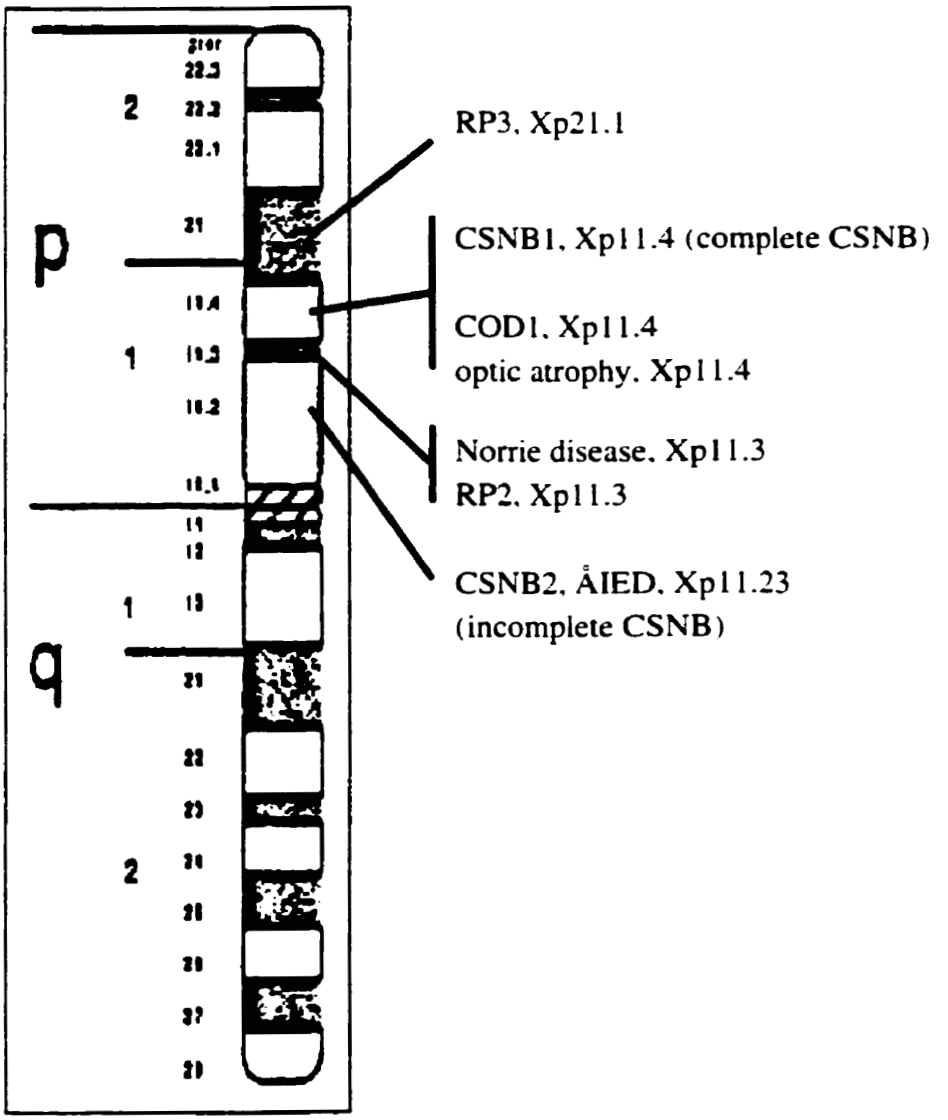
p
q
2
1
1
2
RP3, Xp21.1
CSNB1, Xp11.4 (complete CSNB)
COD1, Xp11.4
optic atrophy, Xp11.4
Norrie disease, Xp11.3
RP2, Xp11.3
CSNB2, ÅIED, Xp11.23
(incomplete CSNB)

With this refinement of the minimal region, the next step was to identify candidate genes for CSNB2. This approach called the positional candidate approach begins with positional mapping to define a minimal region and is followed by a search of databases for candidates (Collins, 1995). The candidates are chosen and prioritised based partially on their functionality as well as on their location (Collins, 1995). Function can be determined through identity with other genes in the databases or through the tissue source of the expressed gene.

The availability of regional genes and expressed sequence tags (ESTs), combined with the DNA sequencing effort as part of the Human Genome Project, make candidate genes more easily accessible to researchers. This reduces the effort of finding novel transcripts and allows for direct characterisation and analysis of the available genes. Another technique that provides candidate genes is large-scale sequencing of a minimal region for a disease gene. Computer-based analysis of genomic sequence derived from such efforts can predict genes within extended DNA sequence.

The Human Genome Project has focussed efforts of researchers and corporations worldwide on the sequencing of the entire human genome. High-throughput technologies are accelerating this process by generating huge amounts of sequence for analysis. Many of the regions targeted for this type of sequencing, at least initially, are minimal regions for disease genes. Genomic sequence covering 900kb of the minimal region for CSNB2 in Xp11.23 was done by large-scale DNA sequencing efforts in Jena (Germany) through the German Human Genome Project. This sequencing led to the identification of a set of genes in Xp11.23, thus providing us with a number of new candidate genes. Following

the positional candidate approach. these new genes were analysed for their potential function. One of the candidates that stood out was a gene predicted to encode a dihydropyridine-sensitive L-type calcium channel α_1-subunit. Known for playing a role in synaptic transmission. a calcium channel gene seemed like a good candidate. Additionally. a calcium channel gene in *Drosophila* was shown to be associated with electroretinographically determined night blindness (Smith et al.. 1996).

Identification of the gene for incomplete CSNB

With the prioritisation of the new candidate genes mutation analysis was carried out. Systematic sequencing of five genes was performed in affected individuals from families with incomplete CSNB. The gene for the dihydropyridine sensitive L-type calcium channel α_1-subunit (*CACNA1F*) was the first gene in which mutations were found (Bech-Hansen et al.. 1998).

Comparative Mapping

Comparative mapping is the comparison of the location of homologous genes between different species on their respective chromosomes. It is a useful strategy for identification of orthologous genes because it provides information regarding the location of these genes: hence their identity as a true orthologue can be confirmed. In the case of CSNB2. finding the mouse orthologue to *CACNA1F* would open the door for the study of this gene. its expression pattern and its function. which would prove difficult in the

human. Additionally, a mouse model for incomplete CSNB could be created with the orthologue of *CACNA1F* in hand.

Throughout mammalian evolution, chromosomal rearrangement has led to great phenotypic diversity amongst mammals (Eppig and Nadeau, 1995). Despite this diversity, the conservation in chromosomal organisation is vast, suggesting a limited number of chromosomal rearrangements since the start of mammalian divergence. Approximately 150 such rearrangements have been estimated (Eppig and Nadeau, 1995). Comparative maps with these conserved chromosomal segments are being constructed for many species and due to the intensive mapping efforts in both species are most complete between mice and humans.

There are five important applications of comparative mapping. Firstly, comparative maps can provide linkage information between different species. There is a tendency toward conservation of close linkage during evolution especially between mammals (Eppig and Nadeau, 1995). This linkage conservation allows the prediction of the location of a gene that has been mapped in one species, but not another. For example, the gene *Evi2*, encoding a murine ecotropic viral integration site, is found between the genes *Trp53* and *Hoxb* on mouse chromosome 11. Based on this information, the human homologue for *Evi2*, *EVI2* was found in the same relative position between *TRP53* and *HOXB* on human chromosome 17 (Buchberg et al., 1988), further demonstrating that linkage in one species can be used to determine linkage in another species.

Secondly, by using this type of linkage information, mapping of disease genes in one species could lead to the identification of the orthologous gene in the other species.

To continue with the above example, upon identification of *EVI2* in humans, this gene was considered a candidate for neurofibromatosis 1 (NF1) because it was located between two NF1 translocation breakpoints on chromosome 17 and had been implicated in the formation of myeloid tumours (Buchberg et al., 1988); (O'Connell et al., 1991). Another example is the gene for Waardenburg syndrome, which maps to chromosome 2. This gene was identified based on the identification of the mouse *Pax3* gene responsible for the 'splotch mutation' in a region of mouse chromosome 1 showing linkage conservation (Epstein et al., 1991).

A third application of comparative maps is the mapping of homologous markers, such as genes and ESTs, that could be used to build or add on to contigs in disease-gene minimal regions (Nadeau, 1989). These markers may also serve to identify the boundaries of the conserved linkages.

Fourthly, comparative mapping could lead to the identification of regions of homology to human genes in animals, which would allow for the study of complex disease traits and susceptibility genes. This is facilitated by the ability to control the environment and limit the genetic variability of laboratory animals (DeBry and Seldin, 1996).

Finally, the chromosomal distribution of homologous genes among different species will point out evolutionary patterns (Eppig and Nadeau, 1995).

Definition of Linkage and Synteny

Linkage and synteny homologies define the distribution of homologous genes on the chromosomes and the degree of conservation between two species (Nadeau and Taylor, 1984). Homology is the degree of similarity between two gene sequences. A single gene that is homologous between two species, regardless of any other genes on the chromosome, represents a homology segment. Synteny requires two or more homologous genes on the same chromosome in more. Synteny is conserved when these syntenic genes occur on the same chromosome in two or more species regardless of gene order. Conserved linkage requires both synteny and conservation of gene order between species (Nadeau, 1989) (Erhlich et al., 1997).

Linkage and Synteny Homologies Between Human and Mouse

The human and mouse genetic and physical maps are the most complete compared to other mammals, hence many of the evolutionary breakpoints between these two species have been defined. More than 1500 genes have been mapped in common with both human and mouse genomes. Of these genes, over 250 map to the X-chromosome.

Conserved Linkage and Synteny in Xp11.23

Ohno's law states that interchromosomal rearrangements between the X chromosome and the autosomes are strongly selected against, hence the majority of the genes on the X chromosome have conserved synteny (as reviewed by (Nadeau, 1989).

Supporting this law, most of the X-chromosome has conserved synteny, although linkage is not as highly conserved due to intrachromosomal rearrangements within these regions. Given the extensive mapping of both mouse and human X chromosome markers and genes, most of the evolutionary breakpoints on the X between these two species have been defined (as reviewed by (DeBry and Seldin, 1996).

Comparative mapping of the proximal region of the short arm of the human X-chromosome on the mouse X-chromosome shows that an evolutionary breakpoint occurs within Xp11.23, but not within the minimal region for CSNB2. Pedigree analysis has determined that there is conserved linkage of the mouse homologues of the genes *GATA1*, *TFE3*, *SYP*, and *CLCN5*. These genes lie within a subchromosomal block between the two evolutionary breakpoints within Xp11.23 (Figure 7) (Blair et al., 1995). Because the linkage of these genes is conserved and *CACNA1F* lies 5kb away from *SYP*, we would expect to find the mouse orthologue of *CACNA1F*, *Cacna1f*, near *Syp* on the mouse X-chromosome (Figure 7).

Expression studies in the mouse

Upon discovery of a gene, the first question asked is "what does this gene do?". In order to begin to elucidate the function of a gene, it is important to know in which tissue the gene is expressed. Knowing the cellular expression within that tissue would provide even more information with regard to function. Expression studies in the mouse can provide this information. The conserved linkage within the minimal region for

Figure 7. A comparative map of the proximal human X-chromosome short arm showing evolutionary breakpoints distal to *Gata1* and proximal to *Clcn5* in the mouse. This segment of the chromosome contains the mouse equivalent of Xp11.23 with conserved synteny. (Blair et al., 1995)

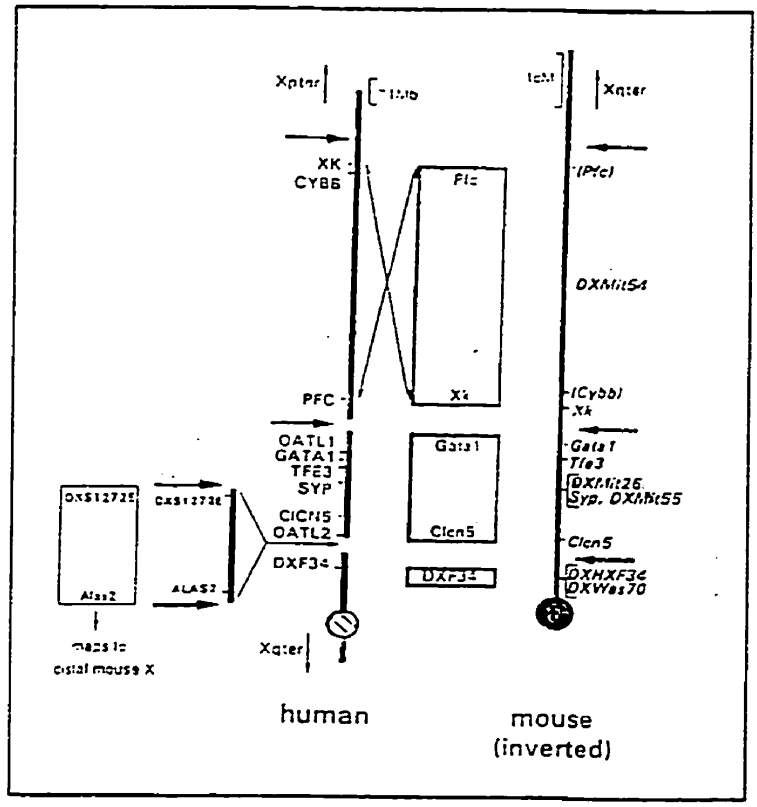
XK
CYBB
PFC
OATL1
GATA1
TFE3
SYP
CICN5
OATL2
DXF34
ALAS2
Xqter
Gata1
Clcn5
DXF34
Xqter
(Pfc)
DXMit54
(Cybb)
Xk
Gata1
Tfe3
DXMit26
Syp, DXMit55
Clcn5
DXHXF3C
DXWas70
human
mouse
(inverted)

CSNB2, as described in the previous section, suggests that there is a mouse gene that is orthologous to *CACNA1F*, therefore can be used in these studies.

Several methods of determining the expression patterns of a gene include RT-PCR, RNase protection, Northern blotting, and *in situ* hybridisation. *In situ* hybridisation, in which RNA is hybridised to a thin section of fixed tissue, can provide cellular resolution within that tissue (the retina in this case), whereas RT-PCR, RNase protection, and Northern blot analysis require the purification of RNA and are limited by the types of cells that can be isolated. Usually, the RNA comes from whole tissues (representing an entire structure) rather than from specific cell-types. In the study of gene expression in the retina, it would be very difficult to isolate retinal cells from surrounding eye cells. RT-PCR is an extremely sensitive technique for studying gene expression which may detect traces of RNA from contaminating cell-types and may even detect illegitimate transcription. Hence this method has the potential for providing misleading information with regard to the level of expression. *In situ* hybridisation provides a more realistic view of expression. Specific information on the location of gene expression derived from retinal *in situ* hybridisation in the mouse can be used to elicit functional information. Additionally, it is relatively easy to recruit the necessary tissues from the mouse. A potential limitation to using only *in situ* hybridisation in the mouse is that expression in some tissues may be missed. Northern blot analysis would allow for the confirmation of the average transcript size, detection of expression in other tissues, and quantitation of transcripts.

The mouse as a model for retinal disorders

The mouse retina contains the same major cell populations as seen in the human retina, though it has long been known that mice have a much greater percentage of rod photoreceptors compared to cone photoreceptors in their retinas (as reviewed by (Lyubarsky et al., 1999). In a recent study, Jeon et al. (1998) performed a quantitative analysis of the photoreceptors and other major cell populations in the mouse retina. Interestingly, they found the distribution of cones in the mouse retina to be similar to that in the human retina, approximately 12,400 cells/mm^2,with a region of higher density located 600 um from the optic nerve head. One major difference between the mouse and human retina lies in the density of the rod photoreceptors. Primate photoreceptor density is approximately 100,000 cells/mm^2, whereas mouse photoreceptor density is more than 400,000 cells/mm^2 (Jeon et al., 1998). Jeon et al. (1998) also state that the bipolar, horizontal, Müller and amacrine cells between different mammalian species are very similar and are present in comparable ratios. This group also found that the density of these cells was much greater in the mouse than in the rabbit (Jeon et al., 1998).

Due to the similarity between human and mouse retina and retinal specific genes, the study of the mouse has been imperative to the understanding of the underlying mechanisms of retinal disorders as well as the mechanisms of normal vision. Some of the mouse models that have already been studied and have provided much information regarding human retinal diseases include the *rd* (retinal degeneration) mouse (Bowes et al., 1990) and the *rds* (retinal degeneration slow) mouse (Travis and Hepler, 1993). These mice carry mutations in the β-subunit of the phosphodiesterase gene (*Pdeb*) and

the peripherin gene (*Prph2*), respectively. More recently, rhodopsin knockout mice have been created for the study of retinitis pigmentosa, and have been used to demonstrate the defect that might occur in the absence of rhodopsin in humans (Humphries et al., 1997). The mouse has even been used to demonstrate cone-driven responses, which further validates the mouse as a model for retinal disorders (Lyubarsky et al., 1999).

Another potential use of the mouse model is the study of modifying factors in disease, which are gaining importance in the understanding of many diseases. As stated earlier, patients with incomplete CSNB have a range of phenotypes, and variation is seen within a single family (Bech-Hansen et al., 1998). This is suggestive of the action of modifying genes. Mouse models would allow the study of the role of CSNB2 in different genetic backgrounds.

What makes the generation of the mouse model even more feasible are the advances in transgenics. Conventional transgenics involves injection of multiple copies of a normal or mutant gene into the male pronucleus of the zygote and relies on the gene getting integrated into the host chromosome (as reviewed by (Reeves, 1998). Targeted homologous recombination is a more direct approach to altering a specific gene, and can knock a gene out resulting in a null mutant. Phenotype rescue experiments or overexpression studies can be performed on these mice to test for gene function. Targeting vectors are now being designed for site-specific recombination and can be used to incorporate specific mutations, knock a gene out, or add a gene to the chromosome. Targeted disruption was used to knock out the rhodopsin gene for the study of retinitis pigmentosa (Humphries et al., 1997).

The Internet as a Resource

In the analysis of much of the data produced in a genetics laboratory, the internet has proven to be an invaluable resource. Due to the global nature of the Human Genome Project, many databases have been formed and made available through the internet. In addition to access to databases, programs that allow analysis of sequence information are available through the internet. For example, genes can be predicted from genomic sequence, open reading frames and amino acid sequence can be predicted from cDNA sequence, and secondary structure of proteins can be predicted based on amino acid sequence (see Table 1 for a list of websites used in analysis). Additionally, sequence similarity searches can be performed using BLAST (Basic Local Alignment Search Tool) (Table 1) to identify clones with homology to the cDNA or amino acid sequence of interest (see 'General Materials and Methods').

Summary

Upon discovery of the first few mutations in *CACNA1F* in affected members of families in which CSNB2 segregates, it was necessary to begin the characterisation of this gene. The objectives proposed in this thesis were designed to carry out this goal of the characterisation of *CACNA1F*. The initial objective was to determine the genomic structure of this gene by defining the boundaries between the introns and the exons, including variably expressed exons. The second objective was to identify the mouse orthologue of *CACNA1F* and determine its cDNA sequence, thus opening the door for the

Table 1 – Internet Resources

INTERNET TOOL	WEBSITE	PURPOSE
ALIGN	http://vega.igh.cnrs.fr/bin/align-guess.cgi	sequence alignment
Primer3	http://www-genome.wi.mit.edu/cgi-bin/primer/primer3_www.cgi	primer design
PRIMERS! for the world wide web	http://www.williamstone.com/primers/index.html	primer design and analysis
National Center for Biotechnology Information	http://www.ncbi.nlm.nih.gov/index.html	access to databases below
PubMed	http://www.ncbi.nlm.nih.gov/PubMed/	literature searches
ENTREZ	http://www.ncbi.nlm.nih.gov/Entrez/	nucleotide and amino acid sequence searches
BLAST	http://www.ncbi.nlm.nih.gov/BLAST/	sequence similarity searches
Human/Mouse Homology Relationships	http://www.ncbi.nlm.nih.gov/Homology/	homology comparison between mouse and human chromosomes
Sanger Centre	http://www.sanger.ac.uk/	access to large-scale sequence
GENSCAN	http://bioweb.pasteur.fr/seqanal/interfaces/genscan-simple.html	gene prediction program
Codon Usage	http://alces.med.umn.edu/cuse.html	DNA sequence translation

study of incomplete CSNB in a model organism. The third objective of this thesis was to determine expression pattern of *CACNA1F*. Information regarding the localisation of expression of *CACNA1F* will provide insight into the molecular mechanisms of the visual pathway that are affected in patients with incomplete CSNB.

CHAPTER 2 - MATERIALS AND METHODS

General materials and methods

PCR conditions

PCR was carried out on the MJR DNA Engine (Model#PTC200, Serial#AL006171). The TNK buffer system (Blanchard et al., 1993) was used for the reactions. One hundred ng of template DNA was used in a 25 uL reaction containing 10 mM Tris-HCl (pH8.3), 1.5 mM $MgCl_2$, 5 mM NH_4Cl, 100 mM KCl (TNK100), 0.4 uM of each primer, 100 uM each of dATP, dCTP, dTTP, and dGTP, and 0.5 U Taq DNA Polymerase (GIBCO/BRL). The reactions were run for 35 cycles of 94°C for 30 seconds, 55°C or 60°C for 45 seconds, and 72°C for 45 seconds, preceded by an initial denaturation step at 94°C for 7 min. and followed by a final extension step at 72°C for 7 min.

Analysis of PCR products by gel electrophoresis

PCR products were analysed on an agarose gel (0.5-1.5%) by electrophoresis, with 1X TAE (39 mM Tris, 20 mM acetic acid, 10 mM EDTA) as the buffer system. Loading dye was added to each sample for a final concentration of 5% glycerol and 0.035% Orange G. The samples were electrophoresed at a current of 8 mA per cm of gel for 30 min. The gels were stained with 0.5 ug ethidium bromide per mL of gel (added prior to casting). The products were visualised on an ultraviolet transilluminator set on 302 nm and were photographed with Polaroid Polapan 667 type film using a red filter.

Isolation of DNA fragments from agarose gels

PCR products and restriction fragments were excised from the agarose gel with a scalpel and placed in a 1.5 mL centrifuge tube. Each gel slice was then solubilised at 50°C for 10 min. in three volumes of Buffer QG, from the QIAquick Gel Extraction Kit by QIAGEN®. One gel volume of isopropanol was added and the sample was applied to the QIAquick column and centrifuged at >10.000 x g for one minute. The bound DNA was washed with Buffer PE and dried by centrifugation (same conditions as in previous step). The DNA products were then eluted from the QIAquick columns with 30 to 50 uL Buffer EB (10mM Tris-Cl, pH8.5) by centrifugation, and stored at 4°C.

Quantitation of Oligonucleotide Primers

To quantitate the primers, spectrophotometric readings were taken at wavelengths of 260 nm and 280 nm. The reading at 260 nm can be used to determine the DNA concentration; and the ratio between the 260 nm and 280 nm readings can be used to estimate the purity of the oligonucleotide. An optical density (OD) of 1 at 260 nm was taken to represent 30 ug/ml for the calculation of primer concentration and a A_{260}/A_{280} ratio of 1.8 signifies a pure preparation of DNA. Primers were diluted 40 times and the OD was measured at either 260 nm and 280 nm or just 260 nm on a Beckman DU®-65 spectrophotometer. Primers were synthesized on the Oligo 1000 DNA Synthesizer (serial#7070335, Beckman). Following their synthesis, the primers were cleaved from the synthesis columns using the Beckman DNA *Ultrafast* Cleavage and Deprotection Kit. The primers were dried in the Savant Speed Vac concentrator (Model#SVC100H, Serial#84-1015-115). The first twenty oligonucleotides that were synthesized and

cleaved were very pure, with an A_{260}/A_{280} ratio of approximately 1.8. Subsequent primers were assumed to be of good purity and the OD was measured only for A_{260} to quantitate the primers.

Restriction endonuclease digestion

Restriction digests were performed using 1-4 units of enzyme per ug of DNA. The reaction volumes were either 10 uL, containing 1ug of DNA (for visual analysis) or 50 uL, containing ≥5 ug of DNA (for purification of linearised products). Enzymes were purchased from either GIBCO-BRL or Boehringer-Mannheim. The buffer recommended by the manufacturer was used (normally one-tenth of the total reaction volume) and the reactions were brought to volume with sterile double-distilled H_2O. Incubations were carried out over 3 hours to overnight at 37°C. The products were either analysed on agarose gel (as described above) or purified for further use with the Qiagen gel purification kit (see 'Synthesis of riboprobes' section).

Small-scale plasmid preparation

Single bacterial colonies were picked with a sterile toothpick and used to inoculate 5 mL of LB medium supplemented with 50 ug/mL ampicillin. The cultures were incubated shaking at 225-300 rpm for 16 hrs at 37°C. The following day 1.5 mL of culture was added to a 1.5 mL centrifuge tube and the cells were pelleted by centrifugation at >10,000 x g for one minute. The supernatant was discarded and the pellet was resuspended in 200 uL GET (50 mM glucose, 10 mM EDTA, 25 mM Tris-HCl pH7.5) containing 250 ug/mL boiled RNase A. 400 uL of freshly-made lysis solution

(0.2 M NaOH, 1%SDS) was then added and the tube was gently inverted to mix the solutions. After four min. of incubation on ice, 300 uL of 7.5 M ammonium acetate (pH7.8) was added, the contents were mixed by inverting the tube and the sample was incubated on ice for 10 min. The precipitate was pelleted by centrifugation at >10,000 x g for 10 min. The supernatant was then transferred to a new micro-centrifuge tube containing 500 uL cold isopropanol. The samples were then vortexed and placed at -20°C from 30 min. to overnight. The DNA precipitate was pelleted by centrifugation for 10 min. at >10,000 x g. The supernatant was then decanted and the pellet was washed with 70% EtOH and the sample was centrifuged again for 2 min. The pellet was air-dried and resuspended in 50 uL sterile double-distilled H_2O.

Small-scale BAC preparation

Single bacterial colonies were cultured as described for the plasmid preparation (previous section), except the media was supplemented with 20 ug/mL chloramphenicol. In order to collect the cells, the cultures were centrifuged at 3,000 rpm in a Sorvall® model T6000B centrifuge (DuPont) for 10 min. The supernatant was decanted and the cell pellet was resuspended in 300 uL of P1 solution (15 mM Tris, pH8.0: 10 mM EDTA, 100 ug RNase A) and transferred to 1.5 mL centrifuge tubes. Next, 300 uL of lysis buffer (0.2 M NaOH, 1%SDS) was added and the contents were gently mixed and allowed to sit at room temperature for 5 min. until the mixture changed from turbid to translucent. 300 uL 3M potassium acetate (pH5.5) was then added and the tubes were vortexed in the inverted position and incubated on ice for 5 min. The samples were centrifuged at >10,000 x g for 10 min. and the DNA was precipitated as described for the plasmid

preparation (previous section). The DNA was resuspended by adding 30 uL sterile double-distilled H_2O without pipeting the sample in order to avoid shearing the DNA.

DNA sequencing

All sequencing was performed using Thermo Sequenase radiolabeled terminator cycle sequencing kit (Product #79750 Amersham Life Science, Inc.). 50-500 ng of DNA was added to a master mix containing 2.5 pmol primer, and 4 units of polymerase in 2.6 mM Tris-HCl, pH9.5, and 6.5 mM $MgCl_2$. This reaction mix was divided into four tubes, each containing termination mix with [α-^{33}P]ddNTP (G, A, T, or C). The samples were overlayed with mineral oil. The sequencing reaction was carried out on a Perkin-Elmer Thermocycler 480 using the following specific parameters: 45 cycles of 94°C for 30s, 55°C for 30s, and 72°C for 1 min. Upon completion of the sequencing reaction, 4 uL of stop solution was added to each reaction tube. The samples were then heated to 70°C for 2-10 min and 4 uL of each sample was loaded onto an acrylamide sequencing gel.

Acrylamide gel electrophoresis

All sequencing reactions were electrophoresed on 31.0 cm x 38.5 cm denaturing polyacrylamide gels using a model S2 apparatus (GIBCO/BRL). The acrylamide gels consisted of 8 M urea, 1X TBE, and 6% acrylamide (from a 40% acrylamide:bis-acrylamide (38:2) stock solution). The urea was dissolved in the acrylamide over low heat and the solution was subsequently filtered through a Nalgene sterilization filter unit with a 0.2 um cellulose nitrate membrane.

For each gel 60 mL of acrylamide was used to which 500 uL of a fresh 10% solution of ammonium persulfate to a final concentration of 0.1% with 0.032% v/v TEMED was added to initiate the cross-linking process. Each gel was cast between clean glass plates separated by 0.4 mm spacers and a 49-well sharkstooth comb was inserted between the plates at the top of the gel prior to solidification of the gel. The gels were run at 70 W for 1.5 hours for the initial read, and 6 hours to read the extended sequence. The gel was transferred to 3MM Whatman filter paper and dried under vacuum at 80°C for 20 min. on a Bio-Rad model 483 slab drier. The dried gels were exposed to Kodak BioMax^{TM} MR film at room temperature for one to five days prior to developing in a Fugi RGII X-ray developer.

RNA isolation

RNA was isolated from mouse eyes and brain. 12.5 day mouse embryo RNA was kindly provided by Dr. Susan Rancourt (Calgary). The RNA was extracted using the TRIZOL® RNA extraction reagent (GIBCO/BRL). The tissue was dissected from a CD1 mouse shortly after the mouse was sacrificed by cervical dislocation. The tissue was immediately weighed and the TRIZOL® was added. 1mL of TRIZOL® was added for every 150 mg of tissue. The tissue was homogenised using an Ultra-Turrax T25 tissue homogenizer (Janke and Kunkel IKA Labortechnik). The samples were centrifuged for 5 min. at 4°C and 12, 000 x g to remove the large tissue pieces. The liquid was transferred to a new tube, 200 uL of chloroform was added, and the tube was shaken for 15 seconds. The sample was incubated at room temperature for 2-3 min. then spun in the microcentrifuge for 15 min. at 4°C and 12, 000 x g. The aqueous layer was then

transferred to a new tube and 600 uL of isopropanol was added to precipitate the RNA. The sample was incubated at room temperature for 10 min. then centrifuged for 10 min. at 4°C and 12, 000 x g. The supernatant was poured off and the RNA was washed with 70% EtOH and the sample was centrifuged again for 2 min. The ethanol was removed and the pellet was air-dried. The pellet was resuspended in 200 uL H_2O. 5uL of the sample was run on a 1% agarose TAE gel and appeared to have residual DNA in the preparation, therefore 20 uL of React 3 from Gibco BRL was added, followed by 5 uL of RNase-free DNase. The sample was incubated at 37°C for 30 min., then the RNA was precipitated as described above. The RNA was finally resuspended in 100 uL of H_2O.

Determination of *CACNA1F* genomic structure

Design and synthesis of primers

Oligonucleotide primers were designed using either Primer3 or Primers! software (see Table 1 for website address). The primers were synthesised, cleaved, resuspended, and quantitated as described in the 'General Materials and Methods' section. The primers were then diluted to a 5 uM concentration for use in PCR reactions.

PCR Amplification of CACNA1F from cDNAs representing various tissues

Based on the GENSCAN-predicted intron/exon boundaries, primers were designed within the exons to yield products spanning several exons. To define the intron/exon boundaries in the genomic sequence of *CACNA1F* (also originally referred to as JMC8 and previously as JM8), the sequence of the cDNA had first to be determined. To establish this sequence, primer sets were based on the predicted cDNA sequence. The

primer sets were designed to yield overlapping PCR products, each spanning several exons, in the effort to cover the whole cDNA sequence (see Table 2 for a list of the primers). The synthesized primer sets were used to amplify cDNA, initially from a panel of cDNA sets or libraries which included cDNA synthesized from mouse RNA extracted from eye, brain, and 12.5 day embryo (Table 3), or just the JNR cDNA library and human retinal cDNA (HRET). RNA was extracted using TRIzol as described in 'General Materials and Methods'. The human retinal cDNA, kindly provided to us by Robert Winkfein (Calgary), was prepared from total RNA using random hexamers. PCR was carried out as described in 'General Materials and Methods'. The PCR products were sequenced following the protocol outlined in 'General Materials and Methods'. The start site at the 5' end of the cDNA was based on the predicted start site, which has been confirmed by 5' RACE by a group in Germany (Strom et al., 1998). The sequence of the 3' end of the cDNA was based on the sequence of a partial cDNA clone of *CACNA1F*.

Table 3 – DNA panel for amplification of JMC8

Name of sample	Description
FRET	random-primed cDNA library in λ zap
JNR	random-primed cDNA library in λ zap
FBRA	random-primed cDNA library in λ zap
human genome	genomic DNA
mouse brain cDNA	random-primed cDNA
mouse eye cDNA	random-primed cDNA
mouse embryo (e12.5)cDNA	random-primed cDNA
HRET cDNA	random-primed cDNA

Analysis of PCR products

PCR products were analysed by gel electrophoresis on an agarose TAE gel as described in 'General Materials and Methods'. The products that appeared to be of the

Table 2 – Human *CACNA1F* Primer Sets

Primer Set	Forward Primer Name	Forward Sequence	Reverse Primer Name	Reverse Sequence	Size (bp)
Exons 1-6	JM8-Ex1Fcod†	gagaatccttccatccctgc	JM8-Ex6Rcod	attcgtccaaggaacagctc	564
Exons 3-6	JMC8Ex3Fcod††	gtggagacggtgctcaagat	JM8-Ex6Rcod	attcgtccaaggaacagctc	371
Exons 6-10	JM8-Ex6Fcod	tcgtgctcttcgtcatcatc	JM8-Ex10Rcod	tggagtgtgtggagcgagta	663
Exons 10-15	JM8-Ex10Fcod	accaataggaggcgtggac	JM8-Ex15Rcod	ggtgtgggtctggtcaaagt	738
Exons 15-20	JM8-Ex15Fcod	ttctcctcttcctcttcatcatt	JM8-Ex20Rcod	ggtttggctgaggcagaag	590
Exons 20-27	JM8-Ex20Fcod	tgtaccccaaggagaaggtgg	JM8-Ex27(28)Rcod	aagtgatgatgacgaagccc	911
Exons 24-32	JM8-Ex24Fcod	ccatctcggtggtgaagatt	JM8-Ex32(33)Rcod	cggatcccttcacccttact	1060
Exons 27-36	JM8-Ex27(28)Fcod†††	taccgtgtggagatctcagtgt	JM8-Ex36(38)Rcod	caaccacatccaagtgtttgat	1126
Exons 32-36	JM8-Ex32(33)Fcod	gcatttccattaccttctttcg	JM8-Ex36(38)Rcod	caaccacatccaagtgtttgat	765
Exons 35-38	JM8-Ex35(37)IIFcod	caccagagattggtccatcc	JM8-Ex38(40)Rcod	ggggatgacctcatctagca	373
Exons 40-46	JM8-Ex40(42)Fcod	tgaaaaggacttggaaactaacaa	JM8-Ex46(48)Rcod	gccatctcgtctcccaagt	954

† "cod" in the primer name indicates the primer lies within coding sequence and is used to distinguish from the intronic primers made for mutation analysis

†† The original designation for the gene for CSNB2 was JM8 (Jena (J) and Munich (M) in Germany). We designated the true cDNA sequence JMC8 (Jena, Munich, Calgary) to distinguish the true cDNA sequence from the predicted cDNA sequence.

††† Upon determination of the boundaries between the introns and exons, some exons were renumbered. The exon number in brackets indicates the true exon, whereas the number in the primer name represents the predicted exon. The number in brackets is not part of the primer name.

expected size were isolated from the gel and sequenced with the forward and reverse primers used in the amplification of the products (see 'General Materials and Methods'). To sequence the entire length of the PCR products, it was necessary to design extra primers (Table 4).

Table 4 – Human Sequencing primers

Primer name	Primer Sequence
JM8Ex3Fcod	gtggagacggtgctcaagat
JM8Ex2Fcod	acatcctcatcctgctgacc
JM8Ex3Rcod	agtcgagtaggttccagcca
JM8Ex2Rcod	cagtgttggagtcgtcctca
JM8Ex24Fcod	ccatctcggtggtgaagatt
JM8Ex35IIFcod	caccagagattggtccatcc
JM8Ex38Rcod	ggggatgacctcatctagca
JM8Ex38Fcod	tgcggattgtcatcaaaaag
JM8Ex44Fcod	catgggaagaggggcagt
JMC8Ex44/45Fcod	tggaggctgtgcttatctca

PCR-based expression analysis of *CACNA1F*

Clontech cDNA Panel

Tissue expression of the *CACNA1F* gene was assessed by PCR amplification of a QUICK-Screen Human cDNA Library panel (Clontech) using primers from exons 24 and 33 which amplify a 1060 bp product (see Table 2 for primer sequence). PCR was performed as described in the 'General Materials and Methods' section with an annealing temperature of 55°C. The ubiquitously expressed EST, JRL4A1, (Boycott and Bech-Hansen, unpublished data) defined by the primers F-TTTCTCTCTGTCTACCTTGT; R-CTGCGGGCTCCCTTACTACTG, was used as an amplification control.

Identification and isolation of the mouse orthologue of *CACNA1F* (*Cacna1f*)

PCR-amplification using human primers

Mouse cDNA reverse-transcribed from RNA extracted from mouse eye, brain, and 12.5 day whole embryo was included in the panel of DNA used in the amplification of human *CACNA1F*. The initial segment of the mouse orthologue of *CACNA1F* was obtained from the amplification of this panel with human primers JM8Ex20Fcod and JM8Ex28Rcod (see Table 2 for primer sequence). All other human primer sets were subsequently used to attempt to amplify segments of the mouse orthologue (Table 2).

Upon determination of the sequence of these segments, mouse sequence-specific primer sets, whose products covered exons 15-21, 32-38 and 38-42, were designed. These primer sets were used to amplify the remaining orthologous sequence, apart from the 5' and 3' ends (Table 5). All PCR amplifications were carried out as described in 'General Materials and Methods'.

Sequencing of Cacna1f PCR products

To determine if PCR products amplified from the mouse cDNA were indeed part of the orthologous gene, the products were gel-isolated and sequenced as described in 'General Materials and Methods'. The sequencing was carried out using the primers used to amplify the PCR products. When sequencing from the PCR primers did not cover the entire PCR product, new mouse-specific primers were designed (Table 6).

Table 5 – Mouse *Cacna1f* primer sets

Primer Set	Forward Primer Name	Forward Sequence	Reverse Primer Name	Reverse Sequence	Product size (bp)
Exons 15-21	mJMC8Ex15F	atctggtggcatctttgctc	mJMC8Ex21R	agcagccagggacacactac	755
Exons32/33-38	mJMC8Ex32/33F	ggcgagagttcagaggacag	mJMC8Ex38R	ccacatccaagtgttgatgc	607
Exons 38-42	mJMC8Ex38(40)F†	ggatcaagccaaccagga	hJMC8Ex42(44)R	ctttggttcccttgggct	608
Exons 40N-48N	mJMC8Ex40N-F	ttccggagaaggaaagaaaa	mJMC8Ex48N-R	cacaaatcgtgggtcttgg	978

† Upon determination of the boundaries between the introns and exons, some exons were renumbered. The exon number in brackets indicates the true exon, whereas the number in the primer name represents the predicted exon. The number in brackets is not part of the primer name.

NB The mouse exon boundaries have not been defined, therefore for the purpose of naming the primers the exons are presumed to be the same in the mouse sequence.

Table 6 – Mouse Sequencing Primers	
Primer name	Primer Sequence
mJM8Ex20F2	actcaagatgacagtgtttg
mJM8Ex28R2	cctggtttccagcactgtgt
mJMC8Ex6-10(F2)	actgaaccataccgagtgcc
mJMC8Ex6-10(R2)	tcagcctgtgtgatccagtc
mJMC8Ex10-15(F2)	atgaaaacaaggatctgccg
mJMC8Ex10-15(R2)	gagacgtacacatcggagca
mJMC8Ex38-46F2	acacaggagaagctctgg
mJMC8Ex38-46F3	cacctcactggtccagca

5' and 3' RACE of Cacnalf

To determine the 5' and 3' sequences of *Cacnalf*, rapid amplification of cDNA ends (RACE) was performed using the CLONTECH Marathon cDNA Amplification Kit. Before the RACE reactions could be performed, double-stranded cDNA had to be synthesized and subsequently tagged on both ends with the Marathon Adaptor. Total RNA was extracted from mouse eyes following the procedure outlined in 'General Materials and Methods' and used to isolate polyA+ RNA. Double-stranded cDNA was synthesized, blunt-ended, and the Marathon Adaptor was ligated to the ends of the cDNA (see Figure 8). A radioactive tracer, α^{32}P-dCTP, was added to the cDNA synthesis reaction. Gel electrophoresis of the mouse eye cDNA and the control placental cDNA followed by exposure to film demonstrated sufficient quantities of mouse eye cDNA to carry out the ligation of the adaptors.

Two sets of primers specific for the 5' and 3' ends of *Cacnalf* cDNA were designed (Table 7). These sets included a primer that lay closer to each end of the cDNA for nested amplification. These primers were designed according to the specifications outlined in the CLONTECH manual for touchdown PCR: each are between 23 and 28

Figure 8. Marathon cDNA adaptor and primer sequences. The Marathon cDNA synthesis primer was used to synthesize oligo-dT cDNA and has an EcoRI and a NotI restriction site incorporated into an additional 20 bp at the 5' end. The Marathon cDNA Adaptor was linked to both ends of the blunt-ended cDNAs. Adaptor Primer 1 (AP1) and Nested Adaptor Primer 2 (AP2) were used with gene specific primers (GSPs) to amplify specific sequences from the adaptor-ligated cDNA. The RACE TFR Primers were used on control DNA as a positive touch-down PCR reaction.

Marathon cDNA Adaptor:

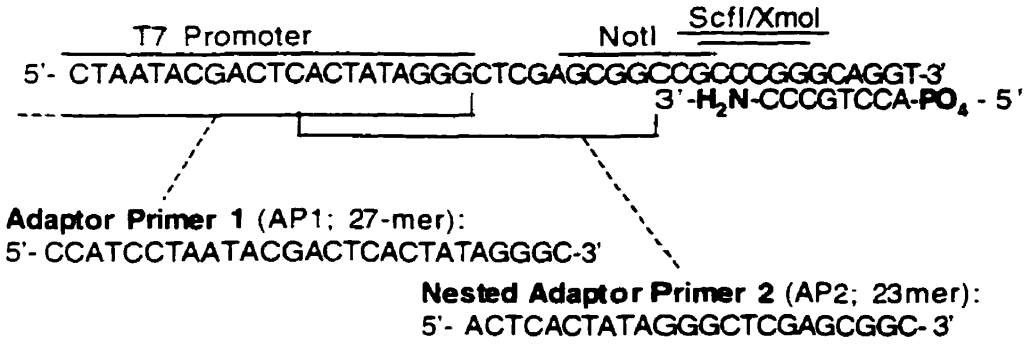

Marathon cDNA Synthesis Primer (52-mer):

5'- TTCTAGAATTCAGCGGCCGC$(T)_{30}N_{-1}N$- 3'

N_{-1}=G,A, or C. N=G,A,C, or T
Degenerate nucleotides anchor primer at base of poly-A tail

5'-RACE TFR Primer (24-mer):

5'-GTCAATGTCCCAAACGTCACCAGA-3'

3'-RACE TFR Primer (29-mer):

5'-ATTTCGGGAATGCTGAGAAAACAGACAGA-3'

Table 7 – *Cacna1f* gene-specific primers (GSPs) for 5' and 3' RACE

End of cDNA	GSP1 name	First gene-specific primer (GSP1)	GSP2 name	Nested GSP (GSP2)
5` end	mJMC8-5`-RACE-1	catggcatcctgcatccagtagagg	mJMC8-5'-RACE-2	gtccgaggaatagctcgagtccgatg
3` end	mJMC8-3`-RACE-1	ctcccaaccacacaggagaagctctg	mJMC8-3'-RACE-2	ccccctgttgttggtggaggaatctac

bases in length, each have a GC content of between 50 and 70%, and the Tm of each is greater than 65°C.

Computer analysis of Cacna1f

As each segment of *Cacna1f* DNA was analysed, its sequence was typed into the computer and compared with the *CACNA1F* sequence by aligning the two sequences. The program ALIGN found on the internet (Table 1) was used to perform the comparison and show the degree of homology between the sequences. The program BLAST (Table 1) was also used for similarity searches to identify any homologues and to ensure the sequence was novel.

Analysis of expression *Cacna1f* in mouse retina using *in situ* hybridisation

Subcloning of mouse JMC8 fragments

Several fragments of *Cacna1f* were subcloned in order to synthesize riboprobes representing those fragments. The fragments, subcloned for mouse retinal *in situ* hybridisation, spanned exons 15 to 21 and 40 to 48 (Table 5). PCR products were diluted to a concentration of approximately 10 ng/uL and 2 to 4 uL was used in the ligation reaction. The Invitrogen TOPO TA Cloning Kit (Version D) with the pCRII-TOPO vector was used for subcloning the fragments. The PCRII-TOPO vector has both T7 and SP6 ribosome binding sites enabling transcription of both sense and anti-sense riboprobes from the same vector.

Synthesis of riboprobes

The subclones were linearised with either *BamHI* or *SpeI* to be used for riboprobe synthesis with T7 RNA Polymerase; and *NotI*, *XbaI*, or *XhoI* to be used with SP6 RNA Polymerase. Each digestion reaction was then treated with 1 ug of protease (from the Qiagen DNA extraction kit) at 37°C for 30 min. The plasmids were then phenol/chloroform extracted followed by precipitation with one-tenth volume 3 M sodium acetate and 2 volumes isopropanol. Approximately 5 ug of each plasmid was added to each riboprobe synthesis reaction with a final concentration of each of the following: 10 mM DTT, 0.5 mM NTPs (including DIG-labeled UTP), 50-100 units of RNA polymerase, 40 mM Tris-HCl (pH8.0), 25 mM NaCl, 8 mM $MgCl_2$, 2 mM spermidine-$(HCl)_3$. The reactions were carried out at 37°C for 2 hours followed by a 20 minute digestion in 10 units of RNase-free-DNaseI at 37°C. The probes were then phenol/chloroform extracted and precipitated as described above. The probes were resuspended in 50 to 100 uL of H_2O.

Fixing, embedding, and sectioning of mouse eyes

Mouse eyes were removed from sacrificed mice with forceps. The eyes were placed in 4% paraformaldehyde PBS at 4°C and fixed overnight on a rotating platform. The following day the eyes were dehydrated by first washing in PBS then through an ethanol/PBS concentration series (25%, 50%, 75% and 100% ethanol). The eyes were then hemisected and kept in the freezer or embedded. Embedding of the eyes was done by washing once in 100% xylenes, two times in 50% xylenes/50% paraffin at 60°C, and two times in 100% paraffin under vacuum at 60°C. The eyes were then positioned in the

bottom of a sectioning block cup, covered in paraffin, and cooled overnight. The following day the eyes were cut into 5 um sections using a Reichert-Jung 1130/Biocut microtome, mounted on Superfrost-Plus microscope slides, and dried at least two days prior to use. The slides were stored at room temperature.

In situ hybridisation

The *in situ* hybridisation was carried out on mouse retinal sections using the riboprobes synthesized from the vectors containing the exon 15-21 and 40–48 regions of *Cacna1f*.

Prehybridisation: The wax was removed from the sections with two chloroform washes followed by two ethanol washes. The sections were then rehydrated in an ethanol/PBS series (95%, 90%, 80%, 70%, 50%, 30% EtOH) for 2 min. each, fixed in 4% paraformaldehyde in PBS for 30 min., treated with 10 ug/ml proteinase K (in 20 mM Tris, 1mM EDTA, pH7.2), and refixed in 4% paraformaldehyde in PBS for 30 min. The sections were washed in 1X PBS between each step after the rehydration. The sections were washed for 2 minutes twice in 2X SSC then incubated twice for 15 min. each in 1X Tris/Glycine.

Hybridisation: The slides were removed from the Tris/Glycine-buffer and excess liquid was removed. Hybridisation solution was made containing 50% formamide (deionized), 1.3X SSC, 5 mM EDTA, .5% CHAPS, 100 uM Heparin, and 0.2% Tween 20. The DIG-labeled riboprobe was added to the hybridisation solution to yield a 1/10 dilution, heated to 60°C and 20 uL was added to the sections, which were then covered

with Parafilm. The sections were placed in airtight containers lined with 2X SSC-soaked paper towels and incubated at 60°C overnight.

Washing: After hybridisation the slides were washed three times for twenty min. each time in 5X SSC at room temperature. The slides were then transferred to a solution of 0.5X SSC and 20% formamide. preheated to 60°C. This solution was changed once and allowed to cool to 37°C in a water bath. RNase treatment was carried out at 37°C for 30 min. in prewarmed NTE with 10 ug/ml RNase A. Prior to and proceeding Rnase treatment the sections were soaked in NTE. prewarmed for 15 min. at 37° C. After RNase treatment. the sections were washed in the 0.5X SSC/20% formamide solution at 60°C. then at room temperature for 30 min. in 2X SSC.

Antibody conjugation: The sections were preblocked in 1% blocking reagent in MABT for one hour at room temperature. The blocking solution was replaced with blocking solution containing a 1:5000 dilution of the Anti-DIG antibody AP and the slides were placed at 4°C overnight.

Antibody detection: The slides were washed four times for 10 min. each in 1X TBST at room temperature and once for 20 min.. and then washed three times for 10 min. each in NTMT with 2 mM levimasole. to prevent endogenous alkaline phosphatase activity. in the last wash. The colour reaction was started by adding 2% NBT/BCIP in MAB for 1-5 days. When the colour appeared in the sections. the reaction was stopped by washing the slides twice in NTMT for 15 min.. followed by a 10 minute wash in PBS. The slides were mounted with an aqueous mounting solution with a glass coverslip.

Photography: Sections were photographed with a bright-field microscope using Kodak Ektachrome 160 Tungsten film that was developed with a Kodak Q-lab developing system.

Mapping of *Cacna1f* to the mouse X-chromosome

The mouse primer set whose PCR product covers exons 40 to 48 was used to amplify a segment of *Cacna1f* to be used as a probe for screening of a mouse BAC library. The probe was sent to the MRC Genome Resource Facility (Department of Genetics, The Hospital for Sick Children, Toronto, Ontario) where it was used to screen the RPCI-22 (129/SvEvTACBr) Mouse BAC Library. Clone 334I19 was identified and upon receipt was streaked out onto an LB plate with 20 ug/mL chloramphenicol. Three single colonies were picked and used to inoculate 5 mL LB (20 ug/mL chloramphenicol) and grown at 37°C overnight. Additionally, one tube with 5 mL LB/chloramphenicol was inoculated with multiple colonies picked off the plate by 'sweeping' the sterile loop through the area of the plate with densely packed colonies. The following day 850 uL of each grown culture was added to 150 uL sterile glycerol, mixed and frozen at –80°C. The DNA was isolated from the remainder of the BAC cultures as described in 'General Materials and Methods'.

CHAPTER 3 – RESULTS

Following the positioning of the CSNB2 locus in the p11.23 region of the human X-chromosome (Bech-Hansen et al., 1998a); (Boycott et al., 1998) and the construction of physical maps of the CSNB2 minimal region (Boycott et al., 1998a); (Strom et al., 1998). DNA sequencing of overlapping cosmid clones covering this region was undertaken as part of the German Human Genome Project (see Table 1 for website address). This led to the identification of numerous genes, some of which represented candidates for the gene for incomplete CSNB (CSNB2). Mutation analysis of *SYP*, JM4, JM9, JM8, and KAT1 led to the identification of mutations only in the JM8 gene of patients with incomplete CSNB (Bech-Hansen et al., 1998). BLAST analysis indicated that the JM8 gene corresponded to a novel L-type voltage-gated calcium channel α_1-subunit. The 3' end of this gene was identified upon the genomic sequencing around the synaptophysin gene (Fisher et al., 1997).

The original genomic organisation of the JM8 gene (*CACNA1F*) was predicted by a GENSCAN analysis. GENSCAN is a web-based exon prediction program (see Table 1 for website address). 46 exons were predicted to be expressed from the genomic sequence. Although the prediction of the exons provided valuable information on which mutation analysis was originally based, the actual boundaries of the exons expressed in the retina needed to be established.

Determining the boundaries between the introns and exons

To define the boundaries between the introns and exons in the genomic sequence of *CACNA1F*, amplification and sequencing of *CACNA1F* from retinal cDNA was carried out. The amplification products from each set of primers overlapped each other by at least 20 bp. These products covered the length of the cDNA except for the 5' and 3' ends. While many primer sets were tried, only the primer sets JM8Ex1-6, 6-10, 10-15, 15-20, 20-28, 24-32, 32-36, 35-38, 38-46, and 40-46 yielded products (Table 2). The sequencing of these PCR products resulted in greater than 90% of the cDNA sequence of *CACNA1F*.

At this point, the 5' end and the 3' end of *CACNA1F* remained to be sequenced. Fortunately, a retinal cDNA clone was available in Genbank, (Genbank #3636203; AA019975), which provided the 3' sequence of the gene (Table 1), i.e. part of exon 46 and downstream to include the entire 3' UTR and part of the polyA tail. The 5' end of *CACNA1F* was determined using 5' RACE by Strom et al. (1998). Through these efforts, the entire length of the cDNA for *CACNA1F* was sequenced (Figure 9). The true boundaries between the exons and introns within the genomic region that encompasses *CACNA1F* were determined by comparing the cDNA sequence to the genomic sequence.

Genomic organisation of CACNA1F

From the analysis of the cDNA sequence, *CACNA1F* was shown to be comprised of 48 exons ranging from 21 bp to 305 bp which are distributed across 29 kb of genomic DNA. The exon boundaries are marked on the cDNA sequence in Figure 9. The length of

Figure 9. cDNA sequence of CACNA1F and its predicted protein sequence. The first base of each exon is marked with a vertical line. The predicted transmembrane domains are marked with a solid underline and each segment is numbered (e.g. IS3 for segment 3 of transmembrane domain I). The amino acids underscored with a dot in IIIS5, IIIS6, and IVS6 are conserved and are known to confer dihydropyridine sensitivity in other calcium channel α_1-subunits (Sinnegger et al., 1997). The EF-hand, another conserved feature of α_1-subunits is marked by a dashed underline. This segment of the protein has been shown to be a Ca^{++} binding site and initiates Ca^{++}-sensitive inactivation of the channel (de Leon et al., 1995). Mutations observed in DNA from patients with incomplete CSNB (Bech-Hansen et al., 1998) are shown in bold with a description of each mutation written above the DNA sequence.

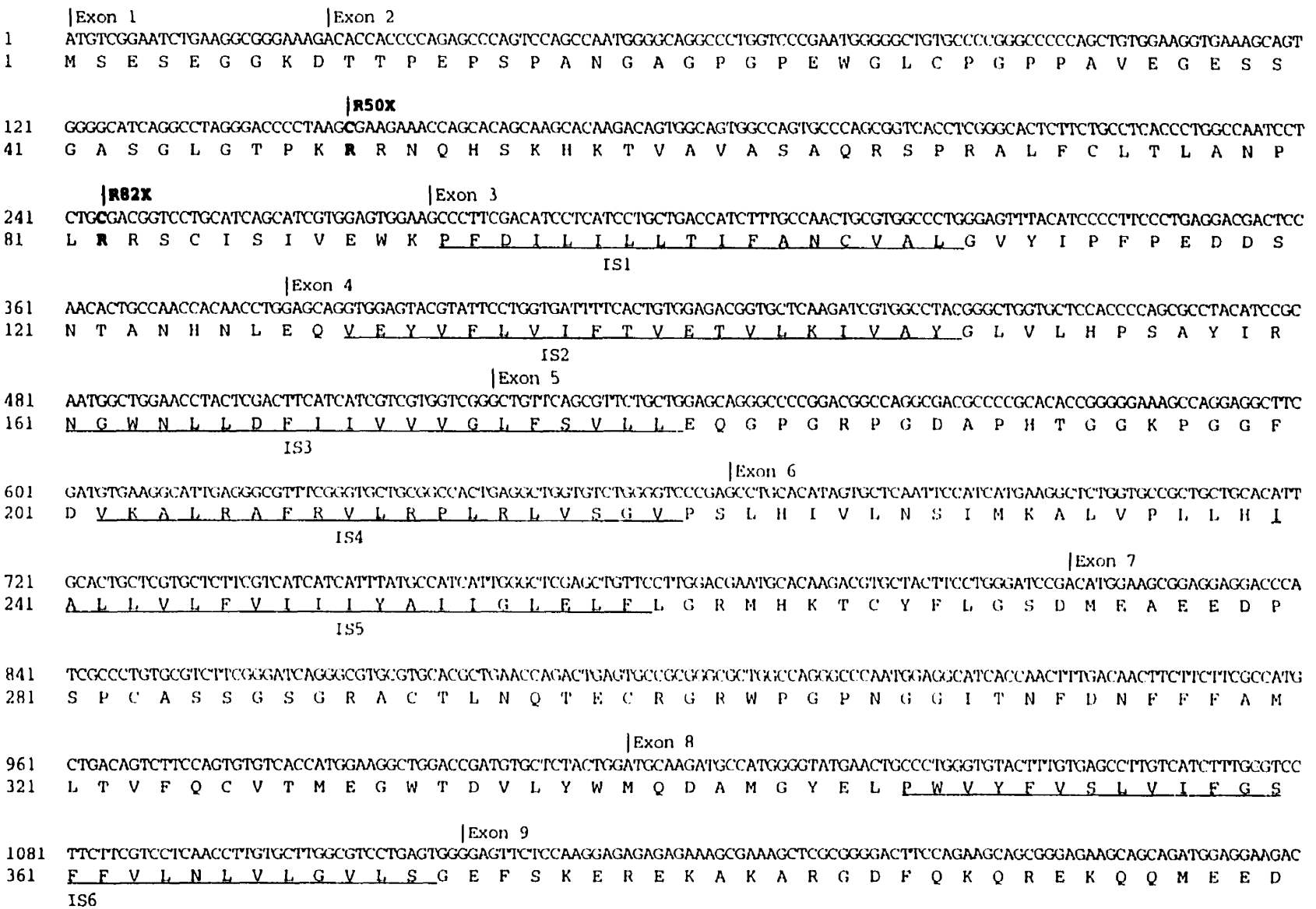
|Exon 1
|Exon 2
1 ATGTCGGAATCTGAAGGCGGGAAAGACACCACCCCAGAGCCCAGTCCAGCCAATGGGGCAGGCCCTGGTCCCGAATGGGGGCTGTGCCCCGGGCCCCCAGCTGTGGAAGGTGAAAGCAGT
1 M S E S E G G K D T T P E P S P A N G A G P G P E W G L C P G P P A V E G E S S
|R50X
121 GGGGCATCAGGCCTAGGGACCCCTAAGCGAAGAAACCAGCACAGCAAGCACAAGACAGTGGCAGTGGCCAGTGCCCAGCGGTCACCTCGGGCACTCTTCTGCCTCACCCTGGCCAATCCT
41 G A S G L G T P K R R N Q H S K H K T V A V A S A Q R S P R A L F C L T L A N P
|R82X
|Exon 3
241 CTGCGACGGTCCTGCATCAGCATCGTGGAGTGGAAGCCCTTCGACATCCTCATCCTGCTGACCATCTTTGCCAACTGCGTGGCCCTGGGAGTTTACATCCCCTTCCCTGAGGACGACTCC
81 L R R S C I S I V E W K P F D I L I L L T I F A N C V A L G V Y I P F P E D D S
IS1
|Exon 4
361 AACACTGCCAACCACAACCTGGAGCAGGTGGAGTACGTATTCCTGGTGATTTTCACTGTGGAGACGGTGCTCAAGATCGTGGCCTACGGGCTGGTGCTCCACCCCAGCGCCTACATCCGC
121 N T A N H N L E Q V E Y V F L V I F T V E T V L K I V A Y G L V L H P S A Y I R
IS2
|Exon 5
481 AATGGCTGGAACCTACTCGACTTCATCATCGTCGTGGTCGGGCTGTTCAGCGTTCTGCTGGAGCAGGGCCCCGGACGGCCAGGCGACGCCCCGCACACCGGGGGAAAGCCAGGAGGCTTC
161 N G W N L L D F I I V V V G L F S V L L E Q G P G R P G D A P H T G G K P G G F
IS3
|Exon 6
601 GATGTGAAGGCATTGACGGCGTTTCGGGTGCTGCGGCCACTGAGGCTGGTGTCTGGGGTCCCGAGCCTGCACATAGTGCTCAATTCCATCATGAAGGCTCTGGTGCCGCTGCTGCACATT
201 D V K A L R A F R V L R P L R L V S G V P S L H I V L N S I M K A L V P L L H I
IS4
|Exon 7
721 GCACTGCTCGTGCTCTTCGTCATCATCATTTATGCCATCATTGGGCTCGAGCTGTTCCTTGGACGAATGCACAAGACGTGCTACTTCCTGGGATCCGACATGGAAGCGGAGGAGGACCCA
241 A L L V L F V I I I Y A I I G L E L F L G R M H K T C Y F L G S D M E A E E D P
IS5
841 TCGCCCTGTGCGTCTTCGGGATCAGGGCGTGCGTGCACGCTGAACCAGACTGAGTGCCGCGGCGCTGGCCAGGGCCCAATGGAGGCATCACCAACTTTGACAACTTCTTCTTCGCCATG
281 S P C A S S G S G R A C T L N Q T E C R G R W P G P N G G I T N F D N F F F A M
|Exon 8
961 CTGACAGTCTTCCAGTGTGTCACCATGGAAGGCTGGACCGATGTGCTCTACTGGATGCAAGATGCCATGGGGTATGAACTGCCCTGGGTGTACTTTGTGAGCCTTGTCATCTTTGCGTCC
321 L T V F Q C V T M E G W T D V L Y W M Q D A M G Y E L P W V Y F V S L V I F G S
|Exon 9
1081 TTCTTCGTCCTCAACCTTGTGCTTGGCGTCCTGAGTGGGGAGTTCTCCAAGGAGAGAGAGAAAGCGAAAGCTCGCGGGGACTTCCAGAAGCAGCGGGAGAAGCAGCAGATGGAGGAAGAC
361 F F V L N L V L G V L S G E F S K E R E K A K A R G D F Q K Q R E K Q Q M E E D
IS6

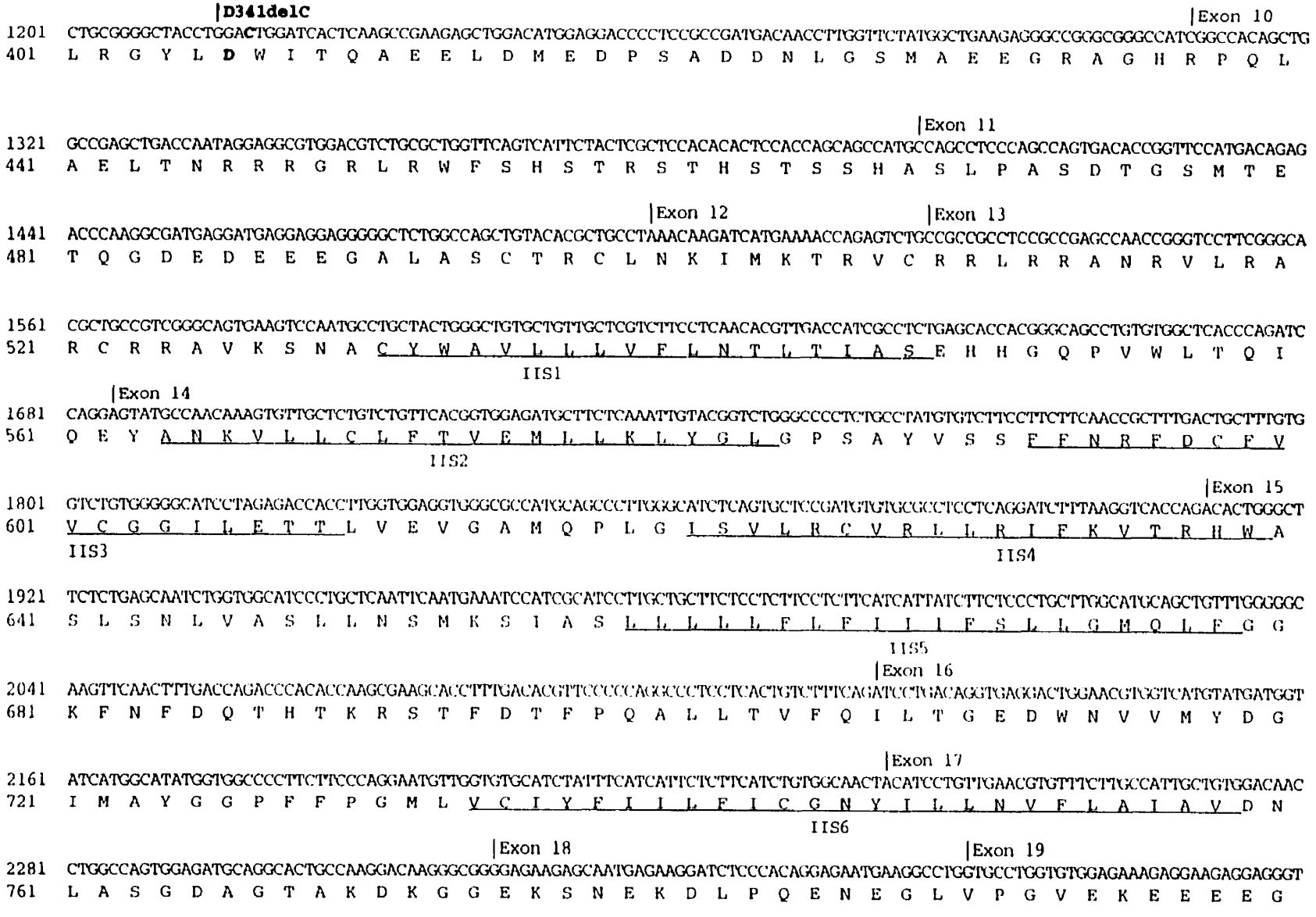
|D341delC
|Exon 10
1201 CTGCGGGGCTACCTGGACTGGATCACTCAAGCCGAAGAGCTGGACATGGAGGACCCCTCCGCCGATGACAACCTTGGTTCTATGGCTGAAGAGGGCCGCGCGGGCCATCGGCCACAGCTG
401 L R G Y L D W I T Q A E E L D M E D P S A D D N L G S M A E E G R A G H R P Q L
|Exon 11
1321 GCCGAGCTGACCAATAGGAGGCGTGGACGTCTGCGCTGGTTCAGTCATTCTACTCGCTCCACACACTCCACCAGCAGCCATGCCAGCCTCCCAGCCAGTGACACCGGTTCCATGACAGAG
441 A E L T N R R R G R L R W F S H S T R S T H S T S S H A S L P A S D T G S M T E
|Exon 12
|Exon 13
1441 ACCCAAGGCGATGAGGATGAGGAGGAGGGGGCTCTGGCCAGCTGTACACGCTGCCTAAACAAGATCATGAAAACCAGAGTCTGCCGCCGCCTCCGCCGAGCCAACCGGGTCCTTCGGGCA
481 T Q G D E D E E E G A L A S C T R C L N K I M K T R V C R R L R R A N R V L R A
1561 CGCTGCCGTCGGGCAGTGAAGTCCAATGCCTGCTACTGGGCTGTGCTGTTGCTCGTCTTCCTCAACACGTTGACCATCGCCTCTGAGCACCACGGGCAGCCTGTGTGGCTCACCCAGATC
521 R C R R A V K S N A C Y W A V L L L V F L N T L T I A S E H H G Q P V W L T Q I
IIS1
|Exon 14
1681 CAGGAGTATGCCAACAAAGTGTTGCTCTGTCTGTTCACGGTGGAGATGCTTCTCAAATTGTACGGTCTGGGCCCCTCTGCCTATGTGTCTTCCTTCTTCAACCGCTTTGACTGCTTTGTG
561 Q E Y A N K V L L C L F T V E M L L K L Y G L G P S A Y V S S F F N R F D C F V
IIS2
|Exon 15
1801 GTCTGTGGGGGCATCCTAGAGACCACCTTGGTGGAGGTGGGCGCCATGCAGCCCTTGGGCATCTCAGTGCTCCGATGTGTGCGCCTCCTCAGGATCTTTAAGGTCACCAGACACTGGGCT
601 V C G G I L E T T L V E V G A M Q P L G I S V L R C V R L L R I F K V T R H W A
IIS3
IIS4
1921 TCTCTGAGCAATCTGGTGGCATCCCTGCTCAATTCAATGAAATCCATCGCATCCTTGCTGCTTCTCCTCTTCCTCTTCATCATTATCTTCTCCCTGCTTGGCATGCAGCTGTTTGGGGGC
641 S L S N L V A S L L N S M K S I A S L L L L L F L F I I I F S L L G M Q L F G G
IIS5
|Exon 16
2041 AAGTTCAACTTTGACCAGACCCACACCAAGCGAAGCACCTTTGACACGTTCCCCCAGGCCCTCCTCACTGTCTTTCAGATCCTGACAGGTGAGGACTGGAACGTGGTCATGTATGATGGT
681 K F N F D Q T H T K R S T F D T F P Q A L L T V F Q I L T G E D W N V V M Y D G
|Exon 17
2161 ATCATGGCATATGGTGGCCCCTTCTTCCCAGGAATGTTGGTGTGCATCTATTTCATCATTCTCTTCATCTGTGGCAACTACATCCTGTTGAACGTGTTTCTTGCCATTGCTGTGGACAAC
721 I M A Y G G P F F P G M L V C I Y F I I L F I C G N Y I L L N V F L A I A V D N
IIS6
|Exon 18
|Exon 19
2281 CTGGCCAGTGGAGATGCAGGCACTGCCAAGGACAAGGGCGGGGAGAAGAGCAATGAGAAGGATCTCCCACAGGAGAATGAAGGCCTGGTGCCTGGTGTGGAGAAAGAGGAAGAGGAGGGT
761 L A S G D A G T A K D K G G E K S N E K D L P Q E N E G L V P G V E K E E E E G

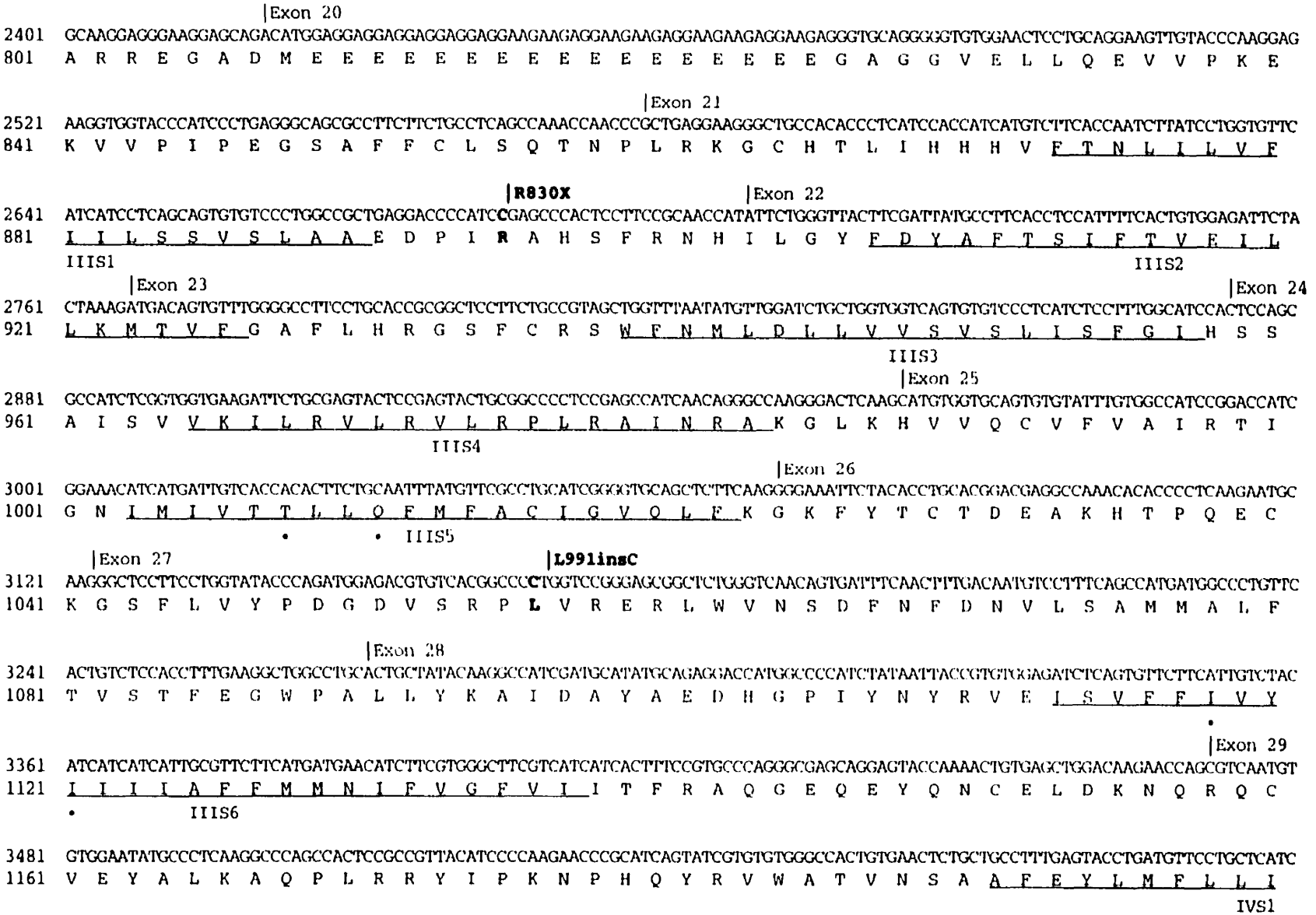
|Exon 20
2401 GCAACGAGGGAAGGAGCAGACATGGAGGAGGAGGAGGAGGAGGAAGAAGAGGAAGAAGAGGAAGAAGAGGAAGAGGGTGCAGGGGGTGTGGAACTCCTGCAGGAAGTTGTACCCAAGGAG
801 A R R E G A D M E E E E E E E E E E E E E E E E E E G A G G V E L L Q E V V P K E
|Exon 21
2521 AAGGTGGTACCCATCCCTGAGGGCAGCGCCTTCTTCTGCCTCAGCCAAACCAACCCGCTGAGGAAGGGCTGCCACACCCTCATCCACCATCATGTCTTCACCAATCTTATCCTGGTGTTC
841 K V V P I P E G S A F F C L S Q T N P L R K G C H T L I H H H V F T N L I L V F
|R830X
|Exon 22
2641 ATCATCCTCAGCAGTGTGTCCCTGGCCGCTGAGGACCCCATCCGAGCCCACTCCTTCCGCAACCATATTCTGGGTTACTTCGATTATGCCTTCACCTCCATTTTCACTGTGGAGATTCTA
881 I I L S S V S L A A E D P I R A H S F R N H I L G Y F D Y A F T S I F T V E I L
IIIS1
IIIS2
|Exon 23
|Exon 24
2761 CTAAAGATGACAGTGTTTGGGGCCTTCCTGCACCGCGGCTCCTTCTGCCGTAGCTGGTTTAATATGTTGGATCTGCTGGTGGTCAGTGTGTCCCTCATCTCCTTTGGCATCCACTCCAGC
921 L K M T V F G A F L H R G S F C R S W F N M L D L L V V S V S L I S F G I H S S
IIIS3
|Exon 25
2881 GCCATCTCCGTGGTGAAGATTCTGCGAGTACTCCGAGTACTGCGGCCCCTCCGAGCCATCAACAGGGCCAAGGGACTCAAGCATGTGGTGCAGTGTGTATTTGTGGCCATCCGGACCATC
961 A I S V V K I L R V L R V L R P L R A I N R A K G L K H V V Q C V F V A I R T I
IIIS4
|Exon 26
3001 GGAAACATCATGATTGTCACCACACTTCTGCAATTTATGTTCGCCTGCATCGGGGTGCAGCTCTTCAAGGGGAAAATTCTACACCTGCACGGACGAGGCCAAACACACCCCTCAAGAATGC
1001 G N I M I V T T L L Q F M F A C I G V Q L F K G K F Y T C T D E A K H T P Q E C
IIIS5
|Exon 27
|L991insC
3121 AAGGGCTCCTTCCTGGTATACCCAGATGGAGACGTGTCACGGCCCCTGGTCCGGGAGCGGCTCTGGGTCAACAGTGATTTCAACTTTGACAATGTCCTTTCAGCCATGATGGCCCTGTTC
1041 K G S F L V Y P D G D V S R P L V R E R L W V N S D F N F D N V L S A M M A L F
|Exon 28
3241 ACTGTCTCCACCTTTGAAGGCTGGCCTGCACTGCTATACAAGGCCATCGATGCATATGCAGAGGACCATGGCCCCATCTATAATTACCGTGTGGAGATCTCAGTGTTCTTCATTGTCTAC
1081 T V S T F E G W P A L L Y K A I D A Y A E D H G P I Y N Y R V E I S V F F I V Y
|Exon 29
3361 ATCATCATCATTGCGTTCTTCATGATGAACATCTTCGTGGGCTTCGTCATCATCACTTTCCGTGCCCAGGGCGAGCAGGAGTACCAAAACTGTGAGCTGGACAAGAACCAGCGTCAATGT
1121 I I I I A F F M M N I F V G F V I I T F R A Q G E Q E Y Q N C E L D K N Q R Q C
IIIS6
3481 GTGGAATATGCCCTCAAGGCCCAGCCACTCCGCCGTTACATCCCCAAGAACCCGCATCAGTATCGTGTGTGGGCCACTGTGAACTCTGCTGCCTTTGAGTACCTGATGTTCCTGCTCATC
1161 V E Y A L K A Q P L R R Y I P K N P H Q Y R V W A T V N S A A F E Y L M F L L I
IVS1

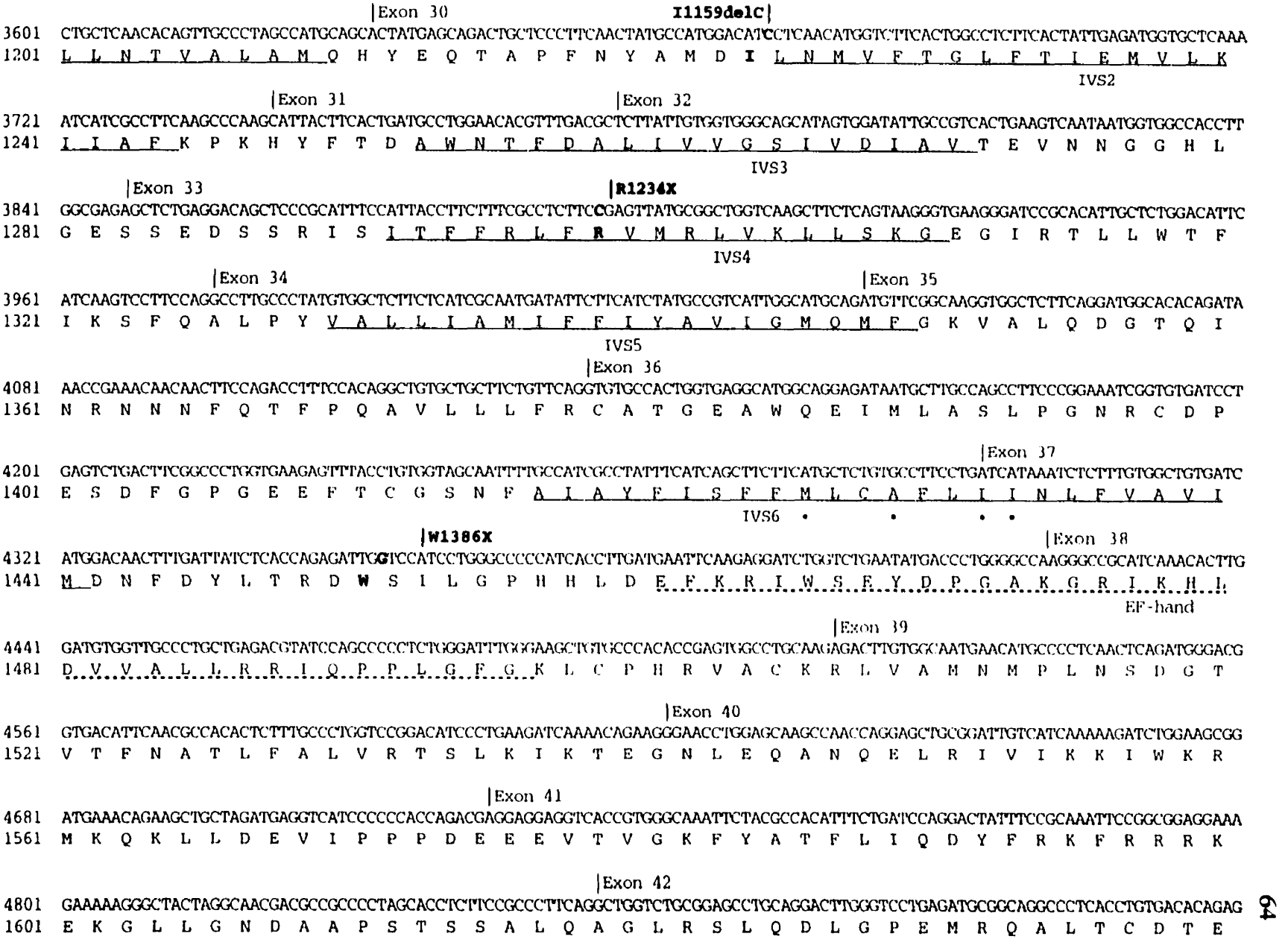
|Exon 30
I1159delC
IVS2
|Exon 31
|Exon 32
IVS3
|Exon 33
|R1234X
IVS4
|Exon 34
|Exon 35
IVS5
|Exon 36
|Exon 37
IVS6
|W1386X
|Exon 38
EF-hand
|Exon 39
|Exon 40
|Exon 41
|Exon 42

|Exon 43

4921 GAGGAGGAAGAAGAGGGGCAGGAGGGAGTGGAGGAGGAAGATGAAAAGGACTTGGAAACTAACAAAGCCACGATGGTCTCCCAGCCCTCAGCTCGCCGGGGCTCCGGGATTTCTGTGTCT

1641 E E E E E G Q E G V E E E D E K D L E T N K A T M V S Q P S A R R G S G I S V S

Exon 44|

5041 CTGCCTGTCGGGGACAGACTTCCAGATTCACTCTCCTTTGGGCCCAGTGATGATGACAGGGGGACTCCCACCTCCAGTCAGCCCAGTGTGCCCCAGGCTGGATCCAACACCCACAGGAGA

1681 L P V G D R L P D S L S F G P S D D D R G T P T S S Q P S V P Q A G S N T H R R

|Exon 45

5161 GGCTCTGGGGCTCTCATTTTCACCATCCCAGAAGAAGGAAATTCTCAGCCCAAGGGAACCAAAGGGCAAAACAAGCAAGATGAGGATGAGGAAGTCCCTGATCGGCTTTCCTACCTAGAT

1721 G S G A L I F T I P E E G N S Q P K G T K G Q N K Q D E D E E V P D R L S Y L D

|Exon 46

5281 GAGCAGGCAGGGACTCCCCCGTGCTCAGTCCTTTTGCCACCTCACAGAGCTCAGAGATACATGGATGGGCACCTGGTACCACGCCGCCGTCTGCTGCCCCCCACACCTGCAGGTCGGAAG

1761 E Q A G T P P C S V L L P P H R A Q R Y M D G H L V P R R R L L P P T P A G R K

|Exon 47

5401 CCCTCCTTCACCATCCAGTGTCTGCAGCGCCAGGGCAGTTGTGAGGATTTACCCATCCCAGGCACCTATCATCGTGGGCGAAATTCAGGGCCCAATAGGGCTCAGGGTTCCTGGGCAACA

1801 P S F T I Q C L Q R Q G S C E D L P I P G T Y H R G R N S G P N R A Q G S W A T

5521 CCACCTCAGCGGGGTCGGCTCCTGTATGCCCCGCTGTTGTTGGTGGAAGAGGGCGCAGCGGGGGAGGGGTACCTCGGCAGATCCAGTGGCCCACTGCGCACCTTCACCTGTCTGCACGTG

1841 P P Q R G R L L Y A P L L L V E E G A A G E G Y L G R S S G P L R T F T C L H V

|Exon 48

5641 CCTGGAACCCACTCGGACCCCAGCCATGGGAAGAGGGGCAGTGCCGACAGCTTGGTGGAGGCTGTGCTTATCTCAGAGGGTCTGGGCCTCTTTGCTCGAGACCCACGTTTCGTGGCCCTG

1881 P G T H S D P S H G K R G S A D S L V E A V L I S E G L G L F A R D P R F V A L

5761 GCCAAGCAGGAGATTGCAGATGCGTGTCGCCTGACGCTGGATGAGATGGACAATGCTGCCAGTGACCTGCTGGCACAGGGAACCAGCTCTCTCTATAGCGACGAGGAGTCCATCCTCTCC

1921 A K Q E I A D A C R L T L D E M D N A A S D L L A Q G T S S L Y S D E E S I L S

5881 CGCTTCGATGAGGAGGACTTGGGAGACGAGATGGCCTGCGTCCACGCCCTCTGAATTCCCACCCCTCCCCAACTGCTCAATAAACCTCCTGCCCTCCCCTCCCCAGCAGGAGGCAGGCAT

1961 R F D E E D L G D E M A C V H A L *

6001 GGACCACAAAAAAAAAAAAAAAAAAAAAAAAAAAAAAAAAAAAAAAAAAA

the introns ranges from 86 bp to 1672 bp. Every exon is invariably preceded, in order, by adenine and guanine and the first base of each exon is one of the following: guanine (46%), adenine (40%), or cytosine (14%). The 3' end of each exon is in all cases followed by guanine then by either a thymidine (94%) or cytosine (6%). Hence, splicing of the *CACNA1F* mRNA transcript follows the GT-AG rule in most cases (Stephens and Schneider, 1992).

To analyse the accuracy of the prediction of exons by GENSCAN, the number of predicted splice donor and acceptor sites were compared with the actual number of these sites. Overall the general location of 46/48 (96%) exons were predicted. More specifically, 44/48 (92%) of the intron/exon boundaries at the splice acceptor site (the 3' end of the intron) and 39/48 (81%) splice donor sites (the 5' end of the intron) were predicted by GENSCAN. Three full exons (exons 32, 34 and 45) were missed entirely by GENSCAN, and one predicted exon (between exons 3 and 4) was not found to be present in the expressed sequence. Several splice variants were found throughout the gene with greater variability near the 5' end of the cDNA.

Splice variants

During the splicing of pre-mRNA, different combinations of exons yield products that translate into functionally different proteins (as reviewed by (Sharp, 1994). Other combinations of exons may yield mRNAs whose reading frames are shifted and do not translate into functional proteins. Several splice variants of *CACNA1F* were identified during the characterisation of its genomic structure. These splice variants were

determined by amplification and sequencing. Amplification of a variable region of sequence of the splice variant, in this case, found within the genomic *CACNA1F* cDNA using a single primer set would yield multiple PCR products, whereas normally only a single product would be amplified. For example, PCR amplification with JM8Ex1Fcod and JM8Ex6Rcod (Table 2) resulted in at least three products (Figure 10). These products were separated by gel electrophoresis, excised and purified as described in 'General Materials and Methods'. Upon sequencing of these products, which showed that the sequence diverged at a splice junction, it was apparent that separation by gel electrophoresis was not sufficient to separate some isoforms that were close in size.

The autoradiogram in Figure 11 shows an example of how a sequence diverges at a splice junction. Single sequence can be read up to the splice junction, at which point two sequences overlap with each other, making reading of the sequences difficult. By marking the expected sequence (based on the predicted exons) with the number 1, the remaining sequence was deduced and marked with the number 2 (Figure 11). This sequence is just downstream from the predicted exon.

In order to sequence through the splice variants to the next junction, new primers were designed. These primers shared the first 10-13 bases from the 5' end, but the last 6-7 bases of each primer were specific for each variant (Table 8).

Figure 10. Amplification of splice variants of the 5' end of *CACNA1F*. Amplification of human retinal cDNA with Primer set JM8Ex1-6cod (Table 2) yielded at least three PCR products that can be seen in the third lane of the gel. In comparison, the amplification of human retinal cDNA with primer set JM8Ex20-28cod yielded a single PCR product (Lane 4). Amplification with the same primer sets with mouse eye cDNA as the template yielded a single PCR product for primer set JM8Ex20-28cod, but no PCR product for primer set JM8Ex1-6. The marker used was the 1 kb ladder from GIBCO/BRL.

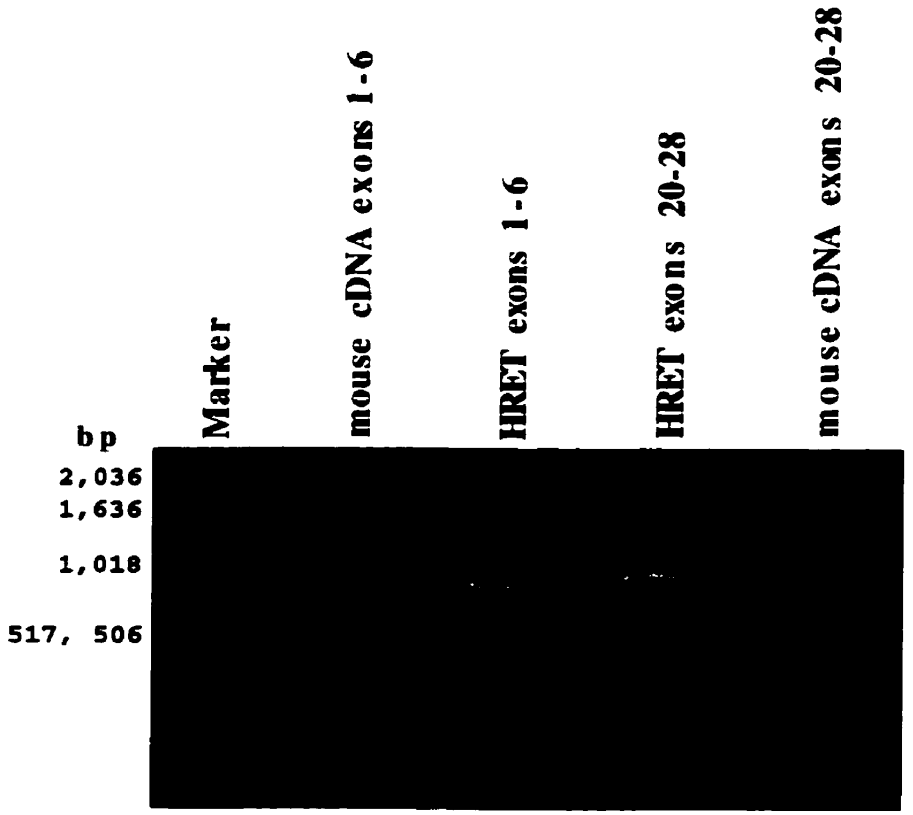
Marker
mouse cDNA exons 1-6
HRET exons 1-6
HRET exons 20-28
mouse cDNA exons 20-28
bp
2,036
1,636
1,018
517, 506

Figure 11. Autoradiogram depicting sequence divergence at a *CACNA1F* splice junction. The single sequence below the arrow represents the 5' portion of exon 33. The sequence diverges at the arrow and represents the junctions between the 5' end of exon 33 and the 3' ends of exons 31 and 32. Exon 31 was a predicted exon and is depicted by the number 1. Exon 32 was not a predicted exon, is variably expressed and is depicted by the number 2.

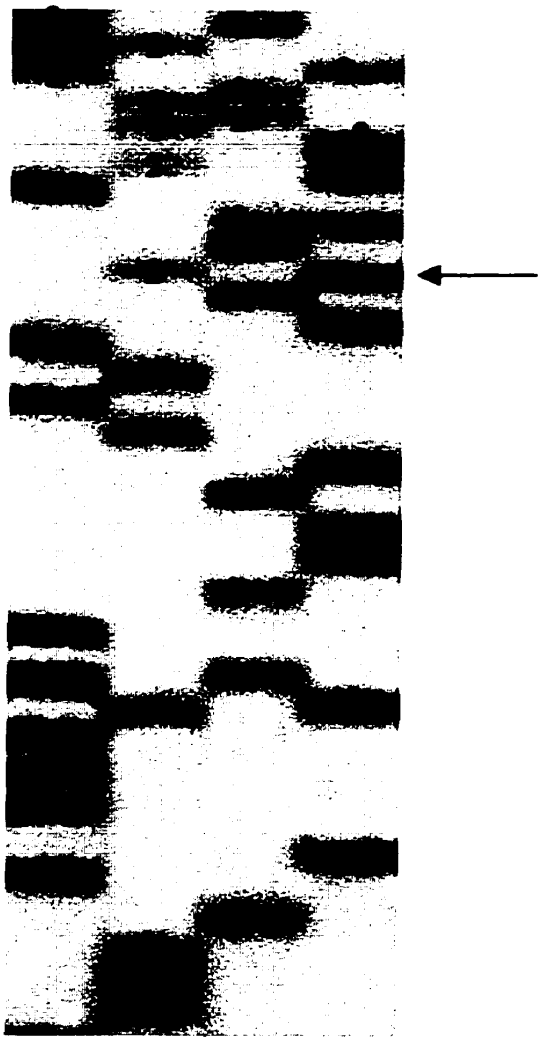

Table 8 – *CACNA1F* splice variant sequencing primers	
Primer name	Primer Sequence (5'-3')
JM8Ex31Rcod	tgtcctcagagctATTGAC
JM8Ex31aRcod	tgtcctcagagctCTCGCC
JM8Ex1b-longF	ttggagcaagTTTCTCC
JM8Ex1b-medF	ttggagcaagACACCAC
JM8Ex1b-shortF	ttggagcaagCATCGTG
JM8Ex2/1newR	gaagggcaggttagggt

The 5' end of *CACNA1F* cDNA is highly variable as was expected from the multiple PCR products yielded from the amplification with primers from exons 1 and 6 (Figure 10). From this work, two forms of exon 1 were identified, exon 1 and 1a. Exon 1a is 40 bp longer than exon 1 and both have the same start site (Figure 12). Exon 1 was originally described by Strom et al. (1998) and was confirmed in our lab. Five forms of exon 2 were identified and are called 2, 2a, b, c, and d. Exons 2, 2a, b and c contain some of the same sequence, which is roughly indicated by the position of the exons in Figure 12. Exon 2d, on the other hand originates from a region further upstream in the genomic sequence (Figure 12). Sequencing of these splice variants revealed that two combinations would yield productive sequences, i.e., the RNA coding sequence remained 'in frame'. These two combinations are the splicing of exons 1, 2 and 3, and the splicing of exons 1a, 2a and 3 (Figure 12). For reasons outlined in the discussion, the full-length cDNA with exons 1, 2 and 3 is considered the prototypical sequence.

Additional splice variants determined in this study were exon 3, exon 9, and exon 32. Exon 3 is 140 bp in length, therefore if it were removed the open reading frame would be disrupted; hence is required for a functional protein. Exon 9 has two forms, one thirty-three bases longer than the other, which would not disrupt the reading frame, and

Figure 12. Cartoon of variable sequences at the 5' end of *CACNA1F*. The thick bars represent exons determined to be expressed in isoforms of *CACNA1F*. The relative position of each exon reflects their location in the genomic DNA. Regions of the exons that overlap in the cartoon share the sequence that the overlapping region represents and differ in the non-overlapping regions. Variants that are predicted to yield functional proteins are marked with _ and variants that are not expected to yield functional proteins are marked with __

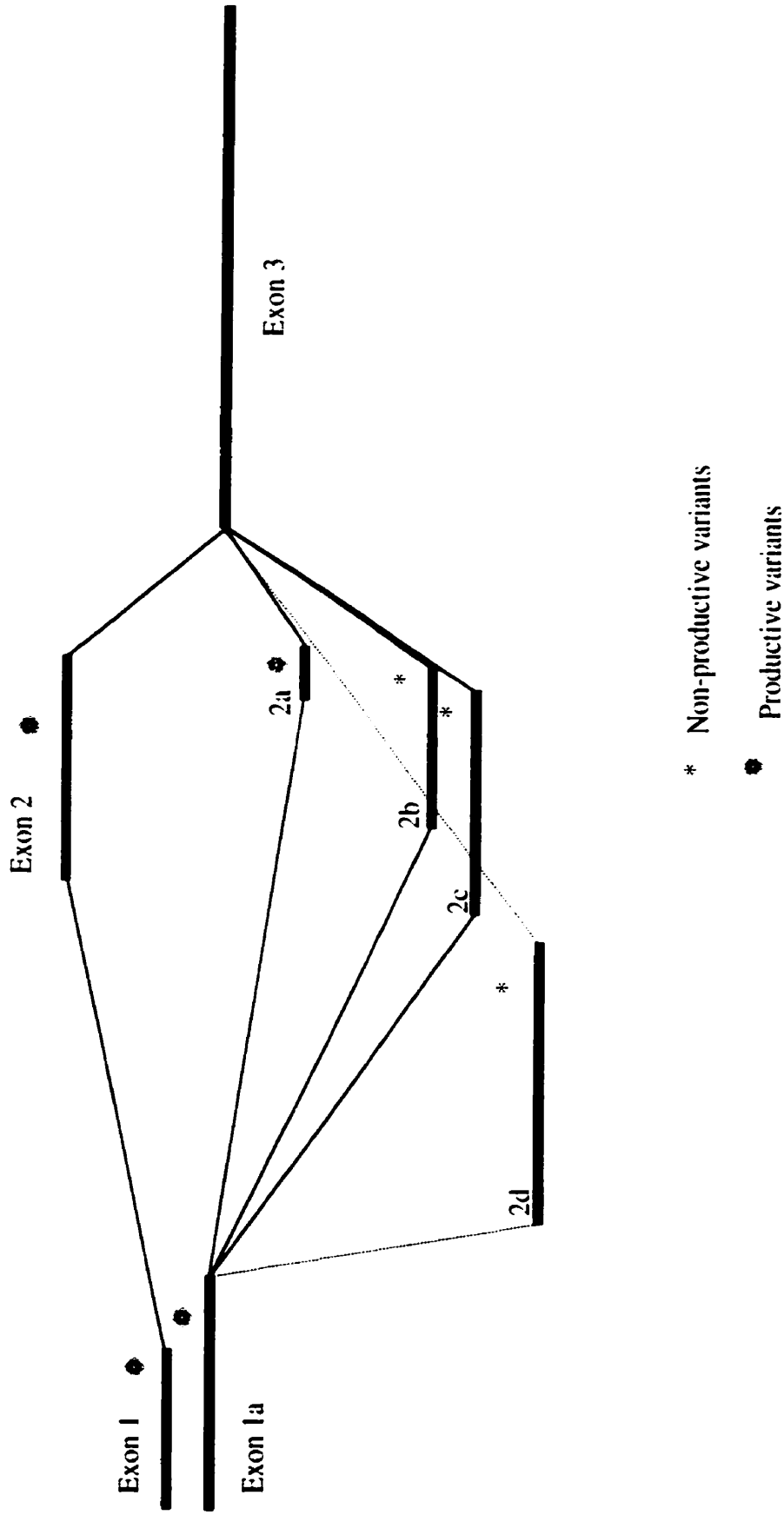
Exon 3
Exon 2
2a
2b
2c
2d
Exon 1
Exon 1a
* Non-productive variants
Productive variants

therefore both forms may be acceptable. The longer form was included in the prototypical *CACNA1F* cDNA. As was used in the example of separating the splice variants by using divergent primers, exon 32 was shown to be a splice variant, but was also included in the prototypical *CACNA1F* cDNA.

CACNA1F cDNA sequence

The cDNA sequence determined for *CACNA1F* was 6069 bp in length, including the 5' and 3' untranslated regions, with an open reading frame of 5931 bp, resulting in a protein of 1977 amino acids (Figure 9). The full-length of the isoform, including the longer exon 1 (1a) and the shorter exon 2 (2a) is 5875 bp with an open reading frame of 5736 bp and a predicted protein of 1912 amino acids in length (Figure 13). A northern blot analysis with a *CACNA1F* probe done by Strom et al. (1998) showed a transcript size of approximately 6.3kb. This size discrepancy could be due to the polyA tail on the RNA, which was not included in the cDNA sequence size. A more likely explanation is the inherent variation in measurement of the distance of the RNA bands on the gel compared to the autoradiogram.

Expression of *CACNA1F*

Tissue-specific expression of CACNA1F

To begin characterising *CACNA1F*, its tissue expression pattern was determined. To do this, a panel of human cDNAs representing nine different tissues was analysed by PCR amplification of *CACNA1F* segments. Primers amplifying a 1060 bp fragment

Figure 13. The 5' end of the coding sequence showing the productive *CACNA1F* splice variant containing exons 1a and 2a. The remainder of the sequence is identical to that of the prototypical sequence in Figure 9. The first transmembrane segment encoded in the cDNA (IS1) is marked with an underline.

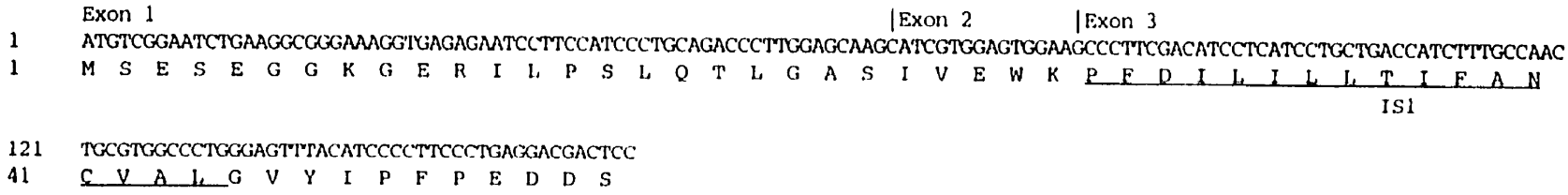
Exon 1
Exon 2
Exon 3
1 ATGTCGGAATCTGAAGGCGGGAAAGGTGAGAGAATCCTTCCATCCCTGCAGACCCTTGGAGCAAGCATCGTGGAGTGGAAGCCCTTCGACATCCTCATCCTGCTGACCATCTTTGCCAAC
1 M S E S E G G K G E R I L P S L Q T L G A S I V E W K P F D I L I L L T I F A N
IS1
121 TGCGTGGCCCTGGGAGTTTACATCCCCTTCCCTGAGGACGACTCC
41 C V A L G V Y I P F P E D D S

covering exons 24-33 (JM8Ex24Fcod and JM8Ex32Rcod) were used (Table 2). These primers amplified a product from the retinal cDNA pool, but not from any other of the eight cDNA pools indicating that the expression of *CACNA1F* was restricted to the retina (Figure 14a). The ubiquitously expressed EST, JRL4A1 was used as a positive control; and the PCR amplification product was observed in each of the cDNA sets from the nine tissues (Figure 14b).

Mouse orthologue of *CACNA1F* (*Cacna1f*)

PCR amplification and sequencing of Cacna1f

To determine whether the mouse orthologue of *CACNA1F*, designated *Cacna1f*, could be isolated using human primers, cDNAs representing several mouse tissues were included in the initial DNA panel used for amplifying the human *CACNA1F* (Table 3 in Materials and Methods section). Primer sets for exons 20 to 28 (JM8Ex20-28cod) first yielded a product from mouse eye cDNA (see Table 2 for primer sequences). This product was observed to be approximately the same size as the product from the human cDNA, which was 911 bp (Figure 15). No PCR products were observed with this primer pair from any other tissues including mouse and human brain (Figure 15), indicating that this method was a valid approach for isolating *Cacna1f*.

Since this portion of mouse *Cacna1f* amplified with human primers, other human primer sets were used to attempt the amplification of the remainder of *Cacna1f*. This strategy was met with relative success. Amplification of mouse eye cDNA with human primer sets JM8Ex6-10, JM8Ex10-15, JM8Ex24-32, and JM8Ex35-38 (Table 2) yielded PCR products from mouse eye cDNA (Figure 16).

Figure 14. Tissue expression of *CACNA1F*. a) Amplification of *CACNA1F* with primer set JM8Ex24-32cod (Table 2) yielded the 1060 bp product from retinal cDNA (lane 2), but not from brain, skeletal muscle, heart, liver, placenta, kidney, lung, or pancreas cDNA. b) Amplification of the ubiquitously expressed EST, JRL4A1 yielded the 281 bp product from all representative cDNAs. The marker in a) is lambda DNA digested with *HindIII* providing a comparison for the higher molecular weight PCR products. The marker in b) is bluescript digested with *HaeIII* and provides a comparison for lower molecular weight PCR products.

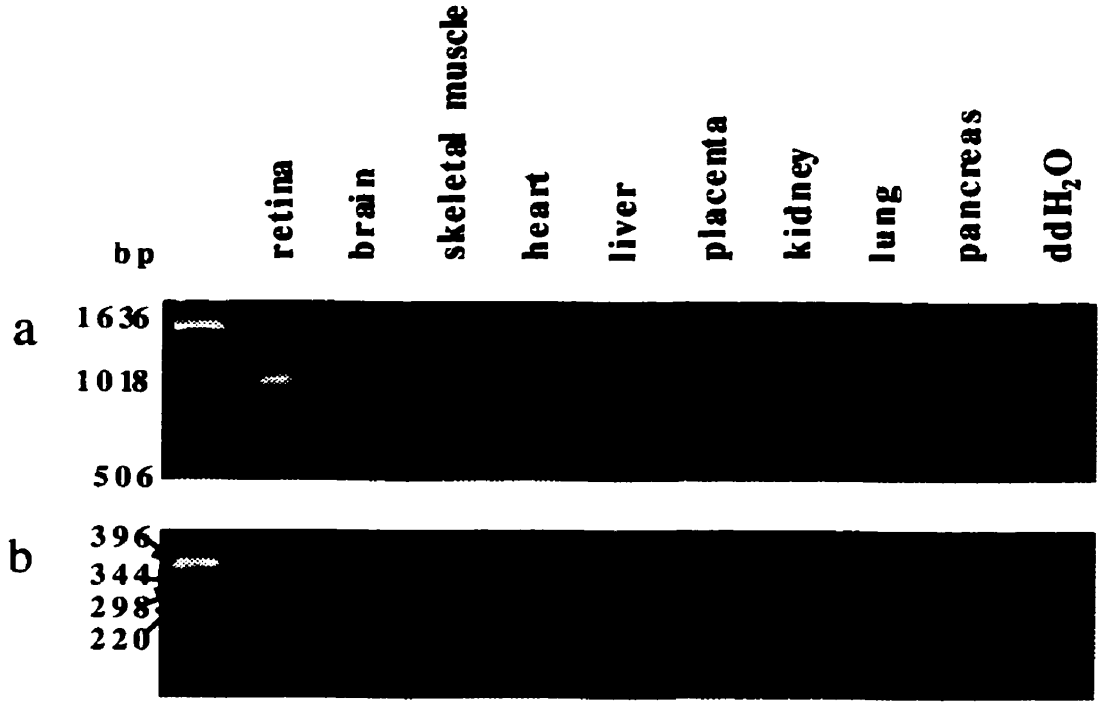
bp
retina
brain
skeletal muscle
heart
liver
placenta
kidney
lung
pancreas
ddH2O
a
1636
1018
506
b
396
344
298
220

Figure 15. Amplification of *Cacna1f*. Initial amplification of both genomic DNA and cDNA from a variety of human and mouse resources was used for isolation of *CACNA1F* with primers set in exons 20 and 28 (see Table 2 for primer sequences). A product can be seen only in the lanes containing mouse eye cDNA and human fetal retina cDNA. This product size is approximately 900 bp for both. The marker in lane 1 is lambda DNA digested with *HindIII* providing a comparison for the higher molecular weight PCR products. The marker in lane 2 is bluescript digested with *HaeIII* and provides a comparison for lower molecular weight PCR products.

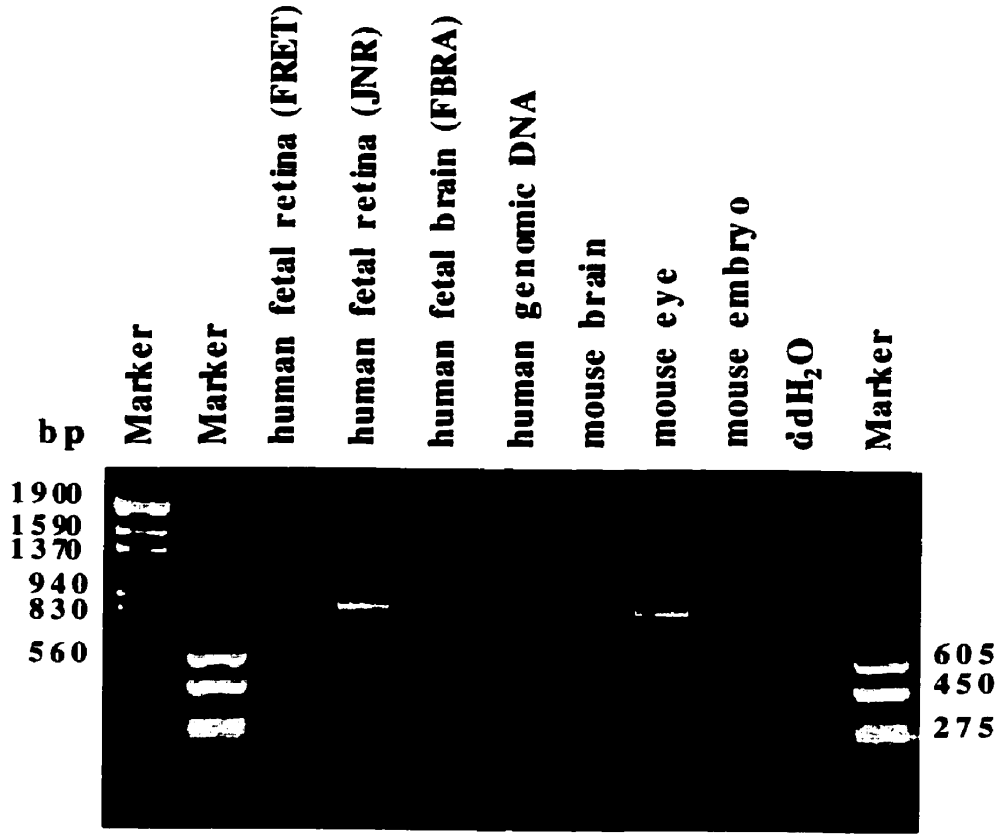
bp
Marker
Marker
human fetal retina (FRET)
human fetal retina (JNR)
human fetal brain (FBRA)
human genomic DNA
mouse brain
mouse eye
mouse embryo
ddH2O
Marker
1900
1590
1370
940
830
560
605
450
275

Figure 16. Fragments of *Cacna1f* amplified with human CACNA1F primers. Amplification of mouse eye cDNA with human primers sets JM8Ex6-10, JM8Ex10-15, JM8Ex20-28, and JM8Ex24-32 yielded *Cacna1f* products that spanned exons 6 through 15 and 20 through 28. The marker in lane 1 is lambda DNA digested with *HindIII* providing a comparison for the higher molecular weight PCR products. The marker in lane 2 is bluescript digested with *HaeIII* and provides a comparison for lower molecular weight PCR products.

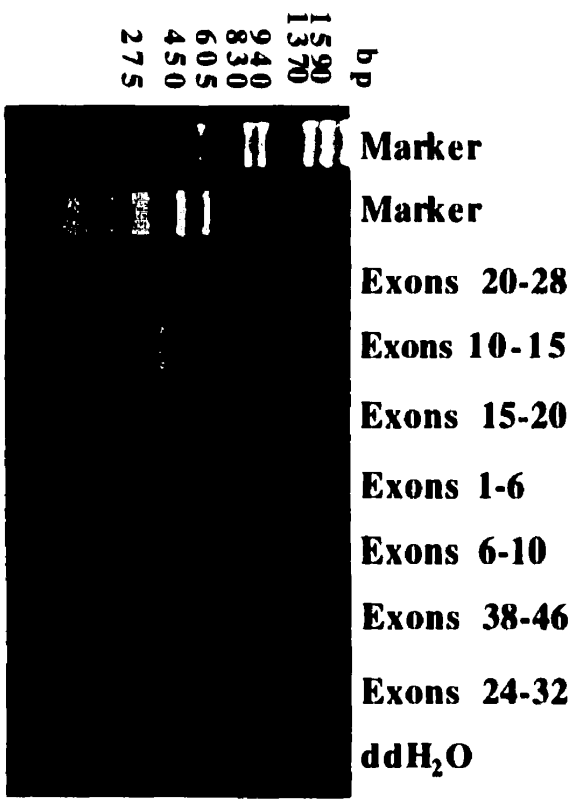
bp
1590
1370
940
830
605
450
275
Marker
Marker
Exons 20-28
Exons 10-15
Exons 15-20
Exons 1-6
Exons 6-10
Exons 38-46
Exons 24-32
ddH2O

There is a high degree of sequence homology amongst calcium channel α_1-subunits, and hence the PCR amplification products from the mouse eye cDNA were expected to be similar to the size of the PCR products from human retinal cDNA. In this study, primer set JM8Ex10-15 yielded two amplification products, one corresponding to the size of the human product, 738 bp, and one smaller than expected from both mouse brain cDNA and mouse embryo cDNA. Sequencing showed that only the PCR product amplified from mouse eye cDNA shared a high degree of homology with *CACNA1F*. This PCR products was approximately the same size as the human PCR products amplified with the same primer sets, as would be expected, whereas the smaller PCR products were not homologous with *CACNA1F*. Other human primer sets that yielded mouse products sharing high homology with *CACNA1F* were: JM8Ex6-10, JM8Ex10-15, JM8Ex24-32, JM8Ex35-38, and JM8Ex40-46.

To verify that these amplified segments were part of the same gene the overlapping segments were compared. If the sequences were identical then it was assumed that the two segments were both *Cacna1f*. On the other hand, if the overlapping portion of these sequences were not identical then one of these segments did not represent *Cacna1f*. For example, in the comparison of the overlapping segments between the JM8EX6-10 and JM8Ex10-15 mouse products illustrated in Figure 17, the sequences were identical, suggesting that the *Cacna1f* gene was amplified in both cases. Whereas the overlapping segment between the JM8Ex10-15 and JM8Ex15-20 mouse PCR products were not identical, therefore since JM8Ex15-20 also had lower homology to *CACNA1F*, it was assumed not to be part of the *Cacna1f* gene (Figure 17).

Figure 17. Identification of amplified mouse segments. Comparison of overlapping regions of mouse segments aided in the identification of the true *Cacnalf* sequence. a) Comparison of the overlapping sequence between segments covering exons 6-10 and 10-15 show identical sequences suggesting both are representative of *Cacnalf*. b) Comparison of the overlapping sequence between segments covering exons 10-15 and 15-20 show similar, but not identical sequences suggesting 15-20 is not part of *Cacnalf*.

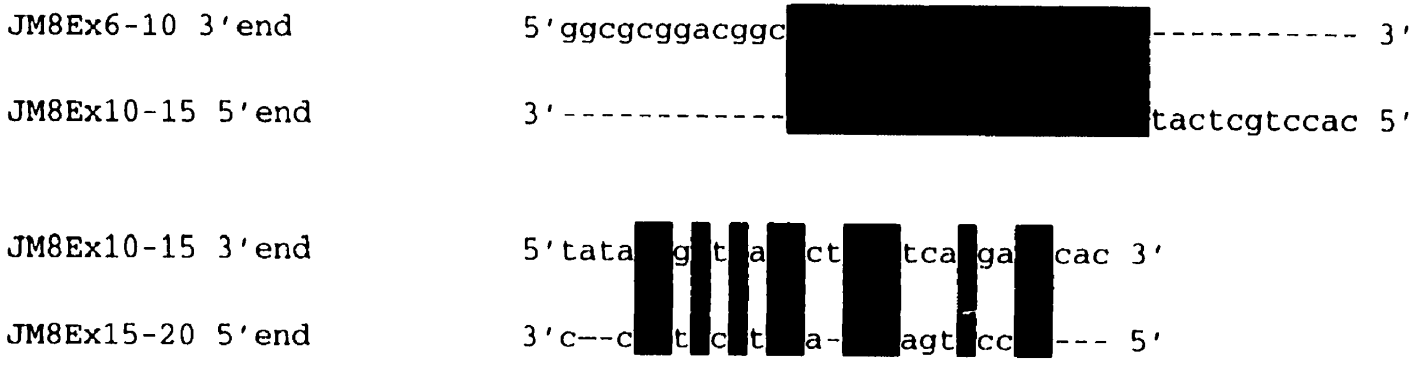
JM8Ex6-10 3'end
5'ggcgcggacggc
---------- 3'
JM8Ex10-15 5'end
3'----------
tactcgtccac 5'
JM8Ex10-15 3'end
5'tata
cac 3'
JM8Ex15-20 5'end
3'c--c
agt
--- 5'

The amplification and sequencing of *Cacna1f* with human primers yielded more than one half of the total cDNA sequence of the mouse gene. In order to obtain the remainder of the sequence, mouse specific primer sets (mJMC8Ex15-21, mJMC8Ex32/33-38, and mJMC8Ex38-42) (Table 5) were designed from derived mouse cDNA sequence and then were used to amplify across the additional regions of *Cacna1f*. This additional sequencing provided sequence coverage for the major gaps. However, the 5' end of *Cacna1f* proved difficult to amplify, most likely due to an increased variability in sequence at this end of the gene, which was also noticed in the sequencing of human *CACNA1F* sequence. To combat these difficulties and establish the sequence of the 5' end of the gene, PCR amplification was carried out using one mouse-specific primer (mJMC8Ex6-10R2) (Table 6) and one human-specific primer (JM8Ex3Fcod). The human primer was chosen from a region of *CACNA1F* bearing low homology with other calcium channel α_1-subunits. From this, the sequence as far 5' as the third exon was determined. At this point, all that was remaining were the 5' and 3' ends of the sequence.

5' and 3' RACE of CACNA1F

In order to determine the 5' and 3' sequences of *Cacna1f*, rapid amplification of cDNA ends (RACE) was performed using the CLONTECH Marathon cDNA Amplification Kit. Double-stranded cDNA was synthesized from polyA RNA isolated from mouse eyes and the adaptors were ligated on to both ends ('General Materials and Methods'). The primers for the adaptors were provided with the kit, Adaptor Primer 1 (AP1) and Adaptor Primer 2 (AP2), and overlap each other by 9 bases allowing for

nested amplification of the cDNA ends (Figure 8 in 'Materials and Methods'). Primers were synthesized to complement these Marathon RACE Adaptor Primers for amplification of the 5' and 3' ends. Touchdown PCR was carried out with these primers as described in 'Materials and Methods'.

3' RACE: Amplification with the primer mJMC8-3-RACE-1 (Table 7 in 'Materials and Methods') and the external adaptor primer (AP1) yielded a product of approximately 900 bp (Figure 18). The band was excised from the agarose gel, purified using the QIAquickTM Gel Extraction Kit (Qiagen), and sequenced using the mJMC8-3-RACE-seq primer (Table 9), as described in 'General Materials and Methods'. The 3' sequence of mouse cDNA of *Cacna1f* was the same length as the human cDNA and was approximately 85% homologous (Figure 14).

Table 9 – *Cacna1f* RACE product sequencing primers

Primer name	Primer Sequence
mJMC8 5'-RACE-seq	gacgatgatgaagtcgagca
mJMC8 5'-RACE-seq-II	gctgggtccttcttcttgg
mJMC8 5'-RACE-seq-III	gttggaggcccaggaca
mJMC8 5'-RACE-seq-IV	tgcacacagtcctcccaac
mJMC8 3'-RACE-seq	ccctggatgagatggacagt

5' RACE: Amplification with mJMC8-5'-RACE-1 (Table 7 in 'Materials and Methods') and AP1 yielded a product of approximately 1000 bp (Figure 18). The band was excised and, initially, sequenced using the mJMC8-5'-seq primer (Table 9). Three other primers were designed from the RACE sequence, as it was generated (Table 9). Sequencing with mJMC8-5'-RACE-seq-II and -III resulted in readable sequence.

Figure 18. 5' and 3' RACE products (depicted with arrows). Lane 1 shows the 1 kb ladder marker (GIBCO/BRL); lanes 2 and 3 show the products of the control amplifications for the 5' and 3' ends; lanes 4 and 5 show products for the 5' and 3' *Cacna1f* RACE reactions. The products were approximately 1000 and 800 bp in length, respectively.

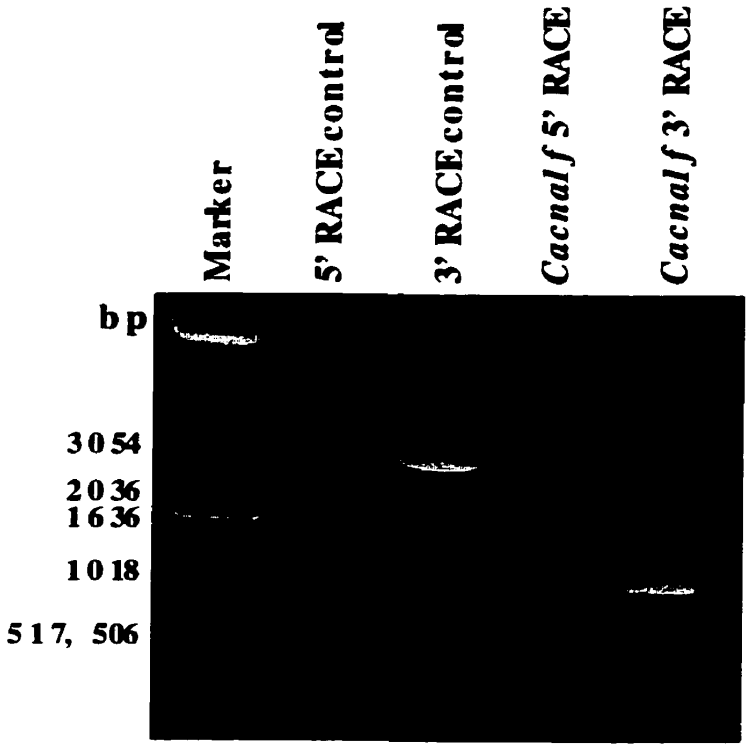
Marker
5' RACE contrd
3' RACE contrd
Cacnalf 5' RACE
Cacnalf 3' RACE
bp
3054
2036
1636
1018
517, 506

whereas sequencing with mJMC8-5'-RACE-seq-IV did not yield any further sequence. To read further toward the 5' end, the PCR products were subcloned into TOPO-TA cloning vector (Invitrogen) and colonies were screened using PCR amplification. Four clones were sequenced and all were shorter than the sequence that had been determined prior to cloning, therefore no further information was gained in the cloning of these PCR products. In summary, the 5'UTR of *Cacna1f* extends at least 48 bases upstream of the translation start site and has approximately 68% homology with the 5'UTR of the human cDNA sequence (Figure 19).

Overall, the entire cDNA sequence of the mouse orthologue of *CACNA1F* was determined to be 6078 bp in length with an open reading frame of 5956 bp that translates into a 1985 amino acid protein (Figure 20). The degree of homology between the mouse *Cacna1f* cDNA sequence and the human *CACNA1F* cDNA sequence ranged from 80% to 95% depending on the region of comparison (Figure 20). Greatest homology was observed in the regions encoding the transmembrane segments, whereas less homology was observed in regions encoding the 3' end, 5' end and cytoplasmic loops. In comparison with the two isoforms of *CACNA1F* that were described in the 'splice variants' section of 'Genomic organisation of *CACNA1F*', *Cacna1f* has greatest homology with the prototypical cDNA of *CACNA1F*. There is an even greater similarity between *CACNA1F* and *Cacna1f* in the comparison of the amino acid sequence with a 90% identity and this identity would be even higher if the conserved amino acid changes were taken into consideration (Figure 24 in 'Discussion').

Figure 19. Alignment of *CACNA1F* and *Cacna1f* in the UTRs. a) Alignment of the 3' UTR shows 81.8% identity between the mouse and human cDNAs. Both UTRs are the same length (76bp). b) Alignment of the 5' UTR shows 68.1% identity between the mouse and human sequences. The human UTR extends 15 bp past the 5' end of the established mouse UTR. The ATG start site is 48 bases from the beginning of the *Cacna1f* cDNA.

a

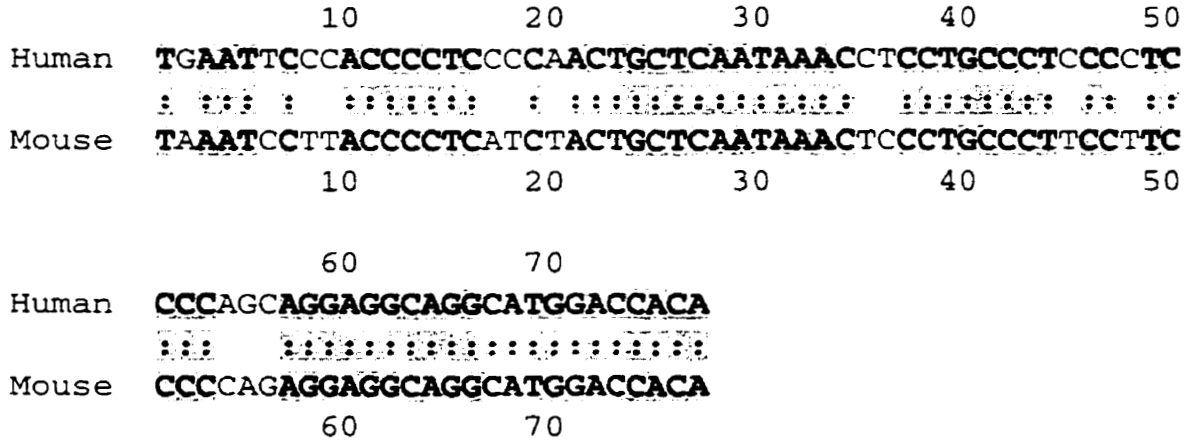
10 20 30 40 50
Human TGAATTCCCACCCCTCCCCAACTGCTCAATAAACCTCCTGCCCTCCCCTC
Mouse TAAATCCTTACCCCTCATCTACTGCTCAATAAACTCCCTGCCCTTCCTTC
10 20 30 40 50
60 70
Human CCCAGCAGGAGGCAGGCATGGACCACA
Mouse CCCCAGAGGAGGCAGGCATGGACCACA
60 70

b

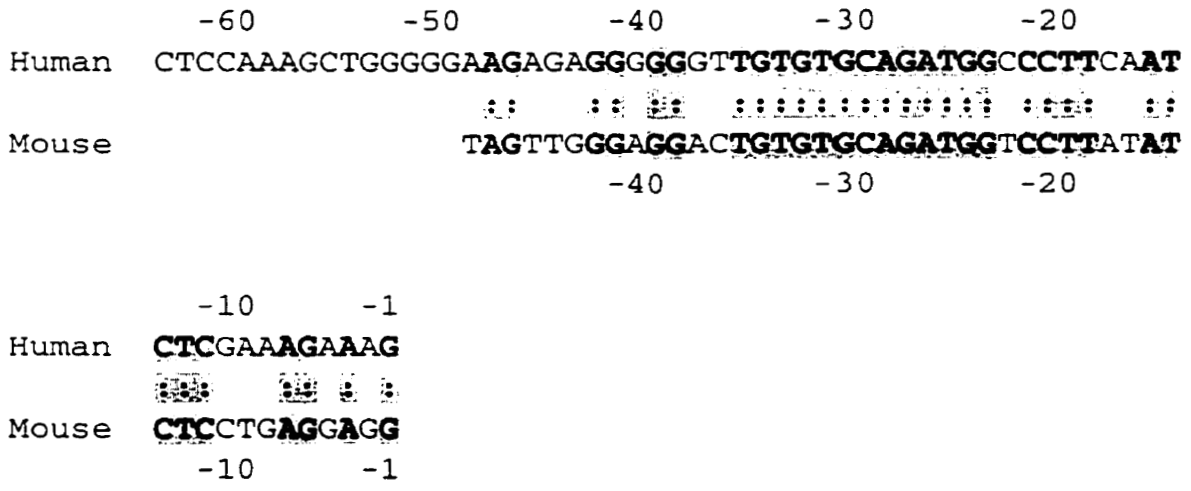
-60 -50 -40 -30 -20
Human CTCCAAAGCTGGGGGAAGAGAGGGGGGTTGTGTGCAGATGGCCCTTCAAT
Mouse TAGTTGGGAGGACTGTGTGCAGATGGTCCTTATAT
-40 -30 -20
-10 -1
Human CTCGAAAGAAAG
Mouse CTCCTGAGGAGG
-10 -1

Figure 20. Alignment of the mouse *Cacna1f* cDNA sequence with the human *CACNA1F* cDNA sequence. The numbering begins at the predicted transcription start sites and corresponds to the numbering of the translated *CACNA1F* in Figure 9. The upper sequence represents human *CACNA1F* (h) and the lower sequence represents mouse *Cacna1f* (m). The transmembrane segments are marked with an underline and labeled. The EF-hand is marked with a dotted underline and labeled.

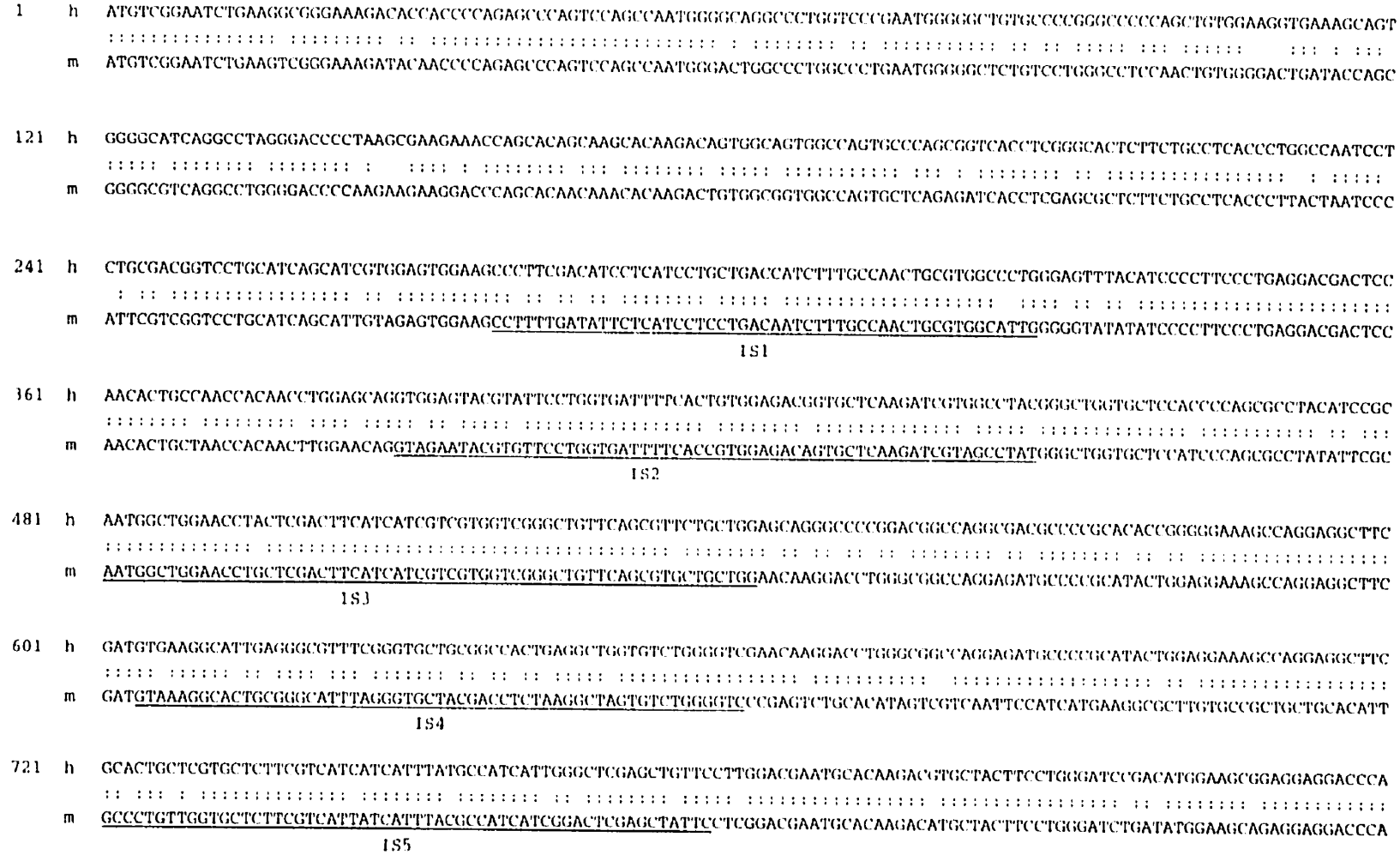
1 h ATGTCGGAATCTGAAGGCGGGAAAGACACCACCCCAGAGCCCAGTCCAGCCAATGGGGCAGGCCCTGGTCCCGAATGGGGGCTGTGCCCCGGGCCCCCAGCTGTGGAAGGTGAAAGCAGT
m ATGTCGGAATCTGAAGTCGGGAAAGATACAACCCCAGAGCCCAGTCCAGCCAATGGGACTGGCCCTGGCCCTGAATGGGGGCTCTGTCCTGGGCCTCCAACTGTGGGGACTGATACCAGC
121 h GGGGCATCAGGCCTAGGGACCCCTAAGCGAAGAAACCAGCACAGCAAGCACAAGACAGTGGCAGTGGCCAGTGCCCAGCGGTCACCTCGGGCACTCTTCTGCCTCACCCTGGCCAATCCT
m GGGGCGTCAGGCCTGGGGACCCCAAGAAGAAGGACCCAGCACAACAAACACAAGACTGTGGCGGTGGCCAGTGCTCAGAGATCACCTCGAGCGCTCTTCTGCCTCACCCTTACTAATCCC
241 h CTGCGACGGTCCTGCATCAGCATCGTGGAGTGGAAGCCCTTCGACATCCTCATCCTGCTGACCATCTTTGCCAACTGCGTGGCCCTGGGAGTTTACATCCCCTTCCCTGAGGACGACTCC
m ATTCGTCGGTCCTGCATCAGCATTGTAGAGTGGAAGCCTTTTGATATTCTCATCCTCCTGACAATCTTTGCCAACTGCGTGGCATTGGGGGTATATATCCCCTTCCCTGAGGACGACTCC
IS1
361 h AACACTGCCAACCACAACCTGGAGCAGGTGGAGTACGTATTCCTGGTGATTTTCACTGTGGAGACGGTGCTCAAGATCGTGGCCTACGGGCTGGTGCTCCACCCCAGCGCCTACATCCGC
m AACACTGCTAACCACAACTTGGAACAGGTAGAATACGTGTTCCTGGTGATTTTCACCGTGGAGACAGTGCTCAAGATCGTAGCCTATGGGCTGGTGCTCCATCCCAGCGCCTATATTCGC
IS2
481 h AATGGCTGGAACCTACTCGACTTCATCATCGTCGTGGTCGGGCTGTTCAGCGTTCTGCTGGAGCAGGGCCCCGGACGGCCAGGCGACGCCCCGCACACCGGGGGAAAGCCAGGAGGCTTC
m AATGGCTGGAACCTGCTCGACTTCATCATCGTCGTGGTCGGGCTGTTCAGCGTGCTGCTGGAACAAGGACCTGGGCGGCCAGGAGATGCCCCGCATACTGGAGGAAAGCCAGGAGGCTTC
IS3
601 h GATGTGAAGGCATTGAGGGCGTTTCGGGTGCTGCGGCCACTGAGGCTGGTGTCTGGGGTCGAACAAGGACCTGGGCGGCCAGGAGATGCCCCGCATACTGGAGGAAAGCCAGGAGGCTTC
m GATGTAAAGGCACTGCGGGCATTTAGGGTGCTACGACCTCTAAGGCTAGTGTCTGGGGTCCCGAGTCTGCACATAGTCGTCAATTCCATCATGAAGGCGCTTGTGCCGCTGCTGCACATT
IS4
721 h GCACTGCTCGTGCTCTTCGTCATCATCATTTATGCCATCATTGGGCTCGAGCTGTTCCTTGGACGAATGCACAAGACGTGCTACTTCCTGGGATCCGACATGGAAGCGGAGGAGGACCCA
m GCCCTGTTGGTGCTCTTCGTCATTATCATTTACGCCATCATCGGACTCGAGCTATTCCTCGGACGAATGCACAAGACATGCTACTTCCTGGGATCTGATATGGAAGCAGAGGAGGACCCA
IS5

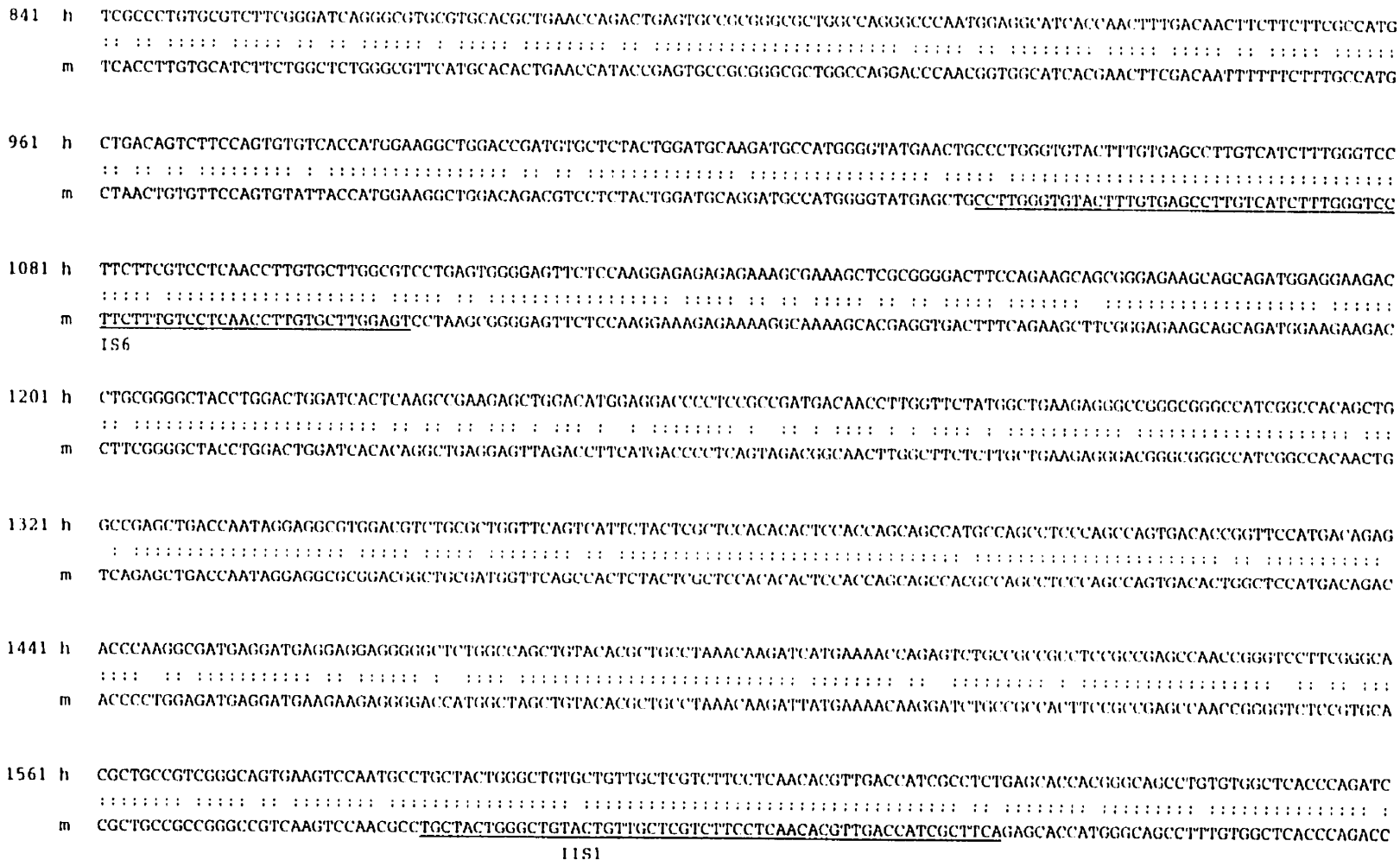
841 h TCGCCCTGTGCGTCTTCGGGATCAGGGCGTGCGTGCACGCTGAACCAGACTGAGTGCCCGCGGGCGCTGGCCAGGGCCCAATGGAGGCATCACCAACTTTGACAACTTCTTCTTCGCCATG
m TCACCTTGTGCATCTTCTGGCTCTGGGCGTTCATGCACACTGAACCATACCGAGTGCCGCGGGCGCTGGCCAGGACCCAACGGTGGCATCACGAACTTCGACAATTTTTTCTTTGCCATG
961 h CTGACAGTCTTCCAGTGTGTCACCATGGAAGGCTGGACCGATGTGCTCTACTGGATGCAAGATGCCATGGGGTATGAACTGCCCTGGGTGTACTTTGTGAGCCTTGTCATCTTTGGGTCC
m CTAACTGTGTTCCAGTGTATTACCATGGAAGGCTGGACAGACGTCCTCTACTGGATGCAGGATGCCATGGGGTATGAGCTGCCTTGGGTGTACTTTGTGAGCCTTGTCATCTTTGGGTCC
1081 h TTCTTCGTCCTCAACCTTGTGCTTGGCGTCCTGAGTGGGGAGTTCTCCAAGGAGAGAGAGAAAGCGAAAGCTCGCGGGGACTTCCAGAAGCAGCGGGAGAAGCAGCAGATGGAGGAAGAC
m TTCTTTGTCCTCAACCTTGTGCTTGGAGTCCTAAGCGGGGAGTTCTCCAAGGAAAGAGAAAAGGCAAAAGCACGAGGTGACTTTCAGAAGCTTCGGGAGAAGCAGCAGATGGAAGAAGAC
IS6
1201 h CTGCGGGGCTACCTGGACTGGATCACTCAAGCCGAAGAGCTGGACATGGAGGACCCCTCCGCCGATGACAACCTTGGTTCTATGGCTGAAGAGGGCCGGGCGGGCCATCGGCCACAGCTG
m CTTCGGGGCTACCTGGACTGGATCACACAGGCTGAGGAGTTAGACCTTCATGACCCCTCAGTAGACGGCAACTTGGCTTCTCTTGCTGAAGAGGGACGGGCGGGCCATCGGCCACAACTG
1321 h GCCGAGCTGACCAATAGGAGGCGTGGACGTCTGCGCTGGTTCAGTCATTCTACTCGCTCCACACACTCCACCAGCAGCCATGCCAGCCTCCCAGCCAGTGACACCGGTTCCATGACAGAG
m TCAGAGCTGACCAATAGGAGGCGCGGACGGCTGCGATGGTTCAGCCACTCTACTCGCTCCACACACTCCACCAGCAGCCACGCCAGCCTCCCAGCCAGTGACACTGGCTCCATGACAGAC
1441 h ACCCAAGGCGATGAGGATGAGGAGGAGGGGGCTCTGGCCAGCTGTACACGCTGCCTAAACAAGATCATGAAAACCAGAGTCTGCCGCCGCCTCCGCCGAGCCAACCGGGTCCTTCGGGCA
m ACCCCTGGAGATGAGGATGAAGAAGAGGGGACCATGGCTAGCTGTACACGCTGCCTAAACAAGATTATGAAAACAAGGATCTGCCGCCACTTCCGCCGAGCCAACCGGGGTCTCCGTGCA
1561 h CGCTGCCGTCGGGCAGTGAAGTCCAATGCCTGCTACTGGGCTGTGCTGTTGCTCGTCTTCCTCAACACGTTGACCATCGCCTCTGAGCACCACGGGCAGCCTGTGTGGCTCACCCAGATC
m CGCTGCCGCCGGGCCGTCAAGTCCAACGCCTGCTACTGGGCTGTACTGTTGCTCGTCTTCCTCAACACGTTGACCATCGCTTCAGAGCACCATGGGCAGCCTTTGTGGCTCACCCAGACC
IIS1

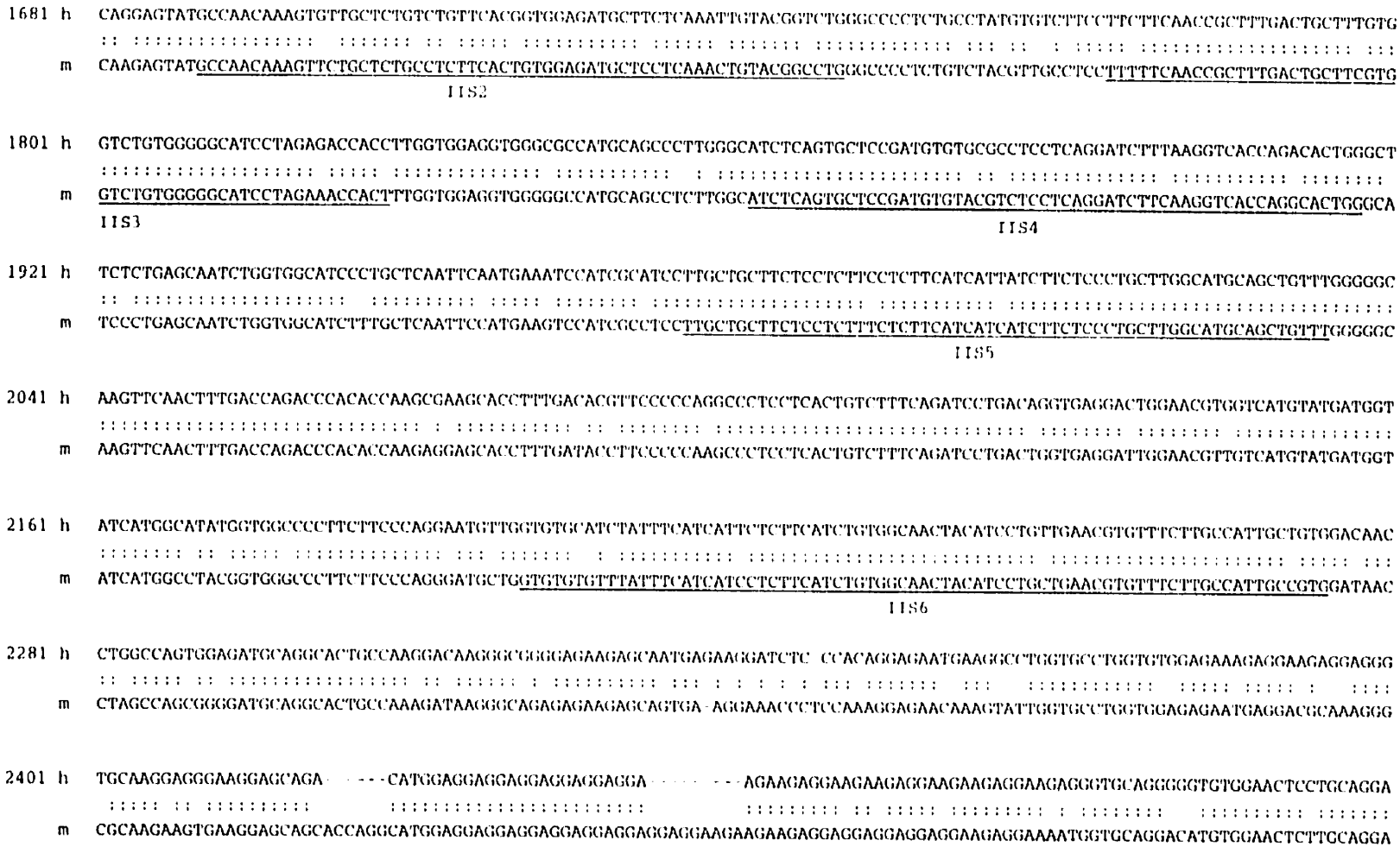
1681 h CAGGAGTATGCCAACAAAGTGTTGCTCTGTCTGTTCACGGTGGAGATGCTTCTCAAATTGTACGGTCTGGGCCCCTCTGCCTATGTGTCTTCCTTCTTCAACCGCTTTGACTGCTTTGTG
m CAAGAGTATGCCAACAAAGTTCTGCTCTGCCTCTTCACTGTGGAGATGCTCCTCAAACTGTACGGCCTGGGCCCCTCTGTCTACGTTGCCTCCTTTTTCAACCGCTTTGACTGCTTCGTG
IIS2
1801 h GTCTGTGGGGGCATCCTAGAGACCACCTTGGTGGAGGTGGGCGCCATGCAGCCCTTGGGCATCTCAGTGCTCCGATGTGTGCGCCTCCTCAGGATCTTTAAGGTCACCAGACACTGGGCT
m GTCTGTGGGGGCATCCTAGAAACCACTTTGGTGGAGGTGGGGGCCATGCAGCCTCTTGGCATCTCAGTGCTCCGATGTGTACGTCTCCTCAGGATCTTCAAGGTCACCAGGCACTGGGCA
IIS3
IIS4
1921 h TCTCTGAGCAATCTGGTGGCATCCCTGCTCAATTCAATGAAATCCATCGCATCCTTGCTGCTTCTCCTCTTCCTCTTCATCATTATCTTCTCCCTGCTTGGCATGCAGCTGTTTGGGGGC
m TCCCTGAGCAATCTGGTGGCATCTTTGCTCAATTCCATGAAGTCCATCGCCTCCTTGCTGCTTCTCCTCTTTCTCTTCATCATCATCTTCTCCCTGCTTGGCATGCAGCTGTTTGGGGGC
IIS5
2041 h AAGTTCAACTTTGACCAGACCCACACCAAGCGAAGCACCTTTGACACGTTCCCCCAGGCCCTCCTCACTGTCTTTCAGATCCTGACAGGTGAGGACTGGAACGTGGTCATGTATGATGGT
m AAGTTCAACTTTGACCAGACCCACACCAAGAGGAGCACCTTTGATACCTTCCCCCAAGCCCTCCTCACTGTCTTTCAGATCCTGACTGGTGAGGATTGGAACGTTGTCATGTATGATGGT
2161 h ATCATGGCATATGGTGGCCCCTTCTTCCCAGGAATGTTGGTGTGCATCTATTTCATCATTCTCTTCATCTGTGGCAACTACATCCTGTTGAACGTGTTTCTTGCCATTGCTGTGGACAAC
m ATCATGGCCTACGGTGGGCCCTTCTTCCCAGGGATGCTGGTGTGTGTTTATTTCATCATCCTCTTCATCTGTGGCAACTACATCCTGCTGAACGTGTTTCTTGCCATTGCCGTGGATAAC
IIS6
2281 h CTGGCCAGTGGAGATGCAGGCACTGCCAAGGACAAGGGCGGGGAGAAGAGCAATGAGAAGGATCTC CCACAGGAGAATGAAGGCCTGGTGCCTGGTGTGGAGAAAGAGGAAGAGGAGGG
m CTAGCCAGCGGGGATGCAGGCACTGCCAAAGATAAGGGCAGAGAGAAGAGCAGTGA AGGAAACCCTCCAAAGGAGAACAAAGTATTGGTGCCTGGTGGAGAGAATGAGGACGCAAAGGG
2401 h TGCAAGGAGGGAAGGAGCAGA CATGGAGGAGGAGGAGGAGGA AGAAGAGGAAGAAGAGGAAGAAGAGGAAGAGGGTGCAGGGGGTGTGGAACTCCTGCAGGA
m CGCAAGAAGTGAAGGAGCAGCACCAGGCATGGAGGAGGAGGAGGAGGAGGAAGAAGAAGAGGAGGAGGAGGAAGAGGAAAATGGTGCAGGACATGTGGAACTCTTGCAGGA

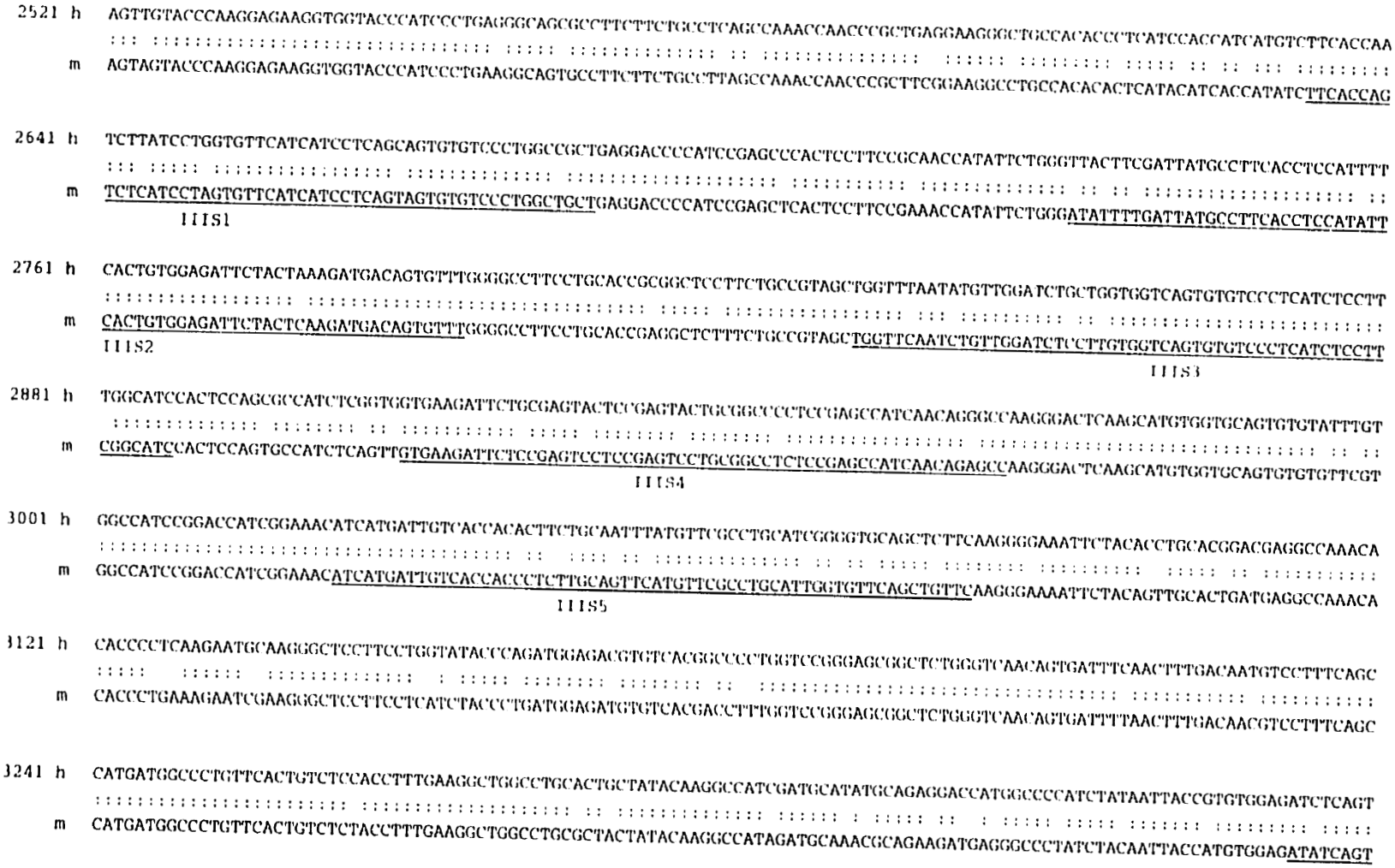
2521 h
AGTTGTACCCAAGGAGAAGGTGGTACCCATCCCTGAGGGCAGCGCCTTCTTCTGCCTCAGCCAAACCAACCCGCTGAGGAAGGGCTGCCACACCCTCATCCACCATCATGTCTTCACCAA
m
AGTAGTACCCAAGGAGAAGGTGGTACCCATCCCTGAAGGCAGTGCCTTCTTCTGCCTTAGCCAAACCAACCCGCTTCGGAAGGCCTGCCACACACTCATACATCACCATATCTTCACCAG
2641 h
TCTTATCCTGGTGTTCATCATCCTCAGCAGTGTGTCCCTGGCCGCTGAGGACCCCATCCGAGCCCACTCCTTCCGCAACCATATTCTGGGTTACTTCGATTATGCCTTCACCTCCATTTT
m
TCTCATCCTAGTGTTCATCATCCTCAGTAGTGTGTCCCTGGCTGCTGAGGACCCCATCCGAGCTCACTCCTTCCGAAACCATATTCTGGGATATTTTGATTATGCCTTCACCTCCATATT
IIIS1
2761 h
CACTGTGGAGATTCTACTAAAGATGACAGTGTTTGGGGCCTTCCTGCACCGCGGCTCCTTCTGCCGTAGCTGGTTTAATATGTTGGATCTGCTGGTGGTCAGTGTGTCCCTCATCTCCTT
m
CACTGTGGAGATTCTACTCAAGATGACAGTGTTTGGGGCCTTCCTGCACCGAGGCTCTTTCTGCCGTAGCTGGTTCAATCTGTTGGATCTCCTTGTGGTCAGTGTGTCCCTCATCTCCTT
IIIS2
IIIS3
2881 h
TGGCATCCACTCCAGCGCCATCTCGGTGGTGAAGATTCTGCGAGTACTCCGAGTACTGCGGCCCCTCCGAGCCATCAACAGGGCCAAGGGACTCAAGCATGTGGTGCAGTGTGTATTTGT
m
CGGCATCCACTCCAGTGCCATCTCAGTTGTGAAGATTCTCCGAGTCCTCCGAGTCCTGCGGCCTCTCCGAGCCATCAACAGAGCCAAGGGACTCAAGCATGTGGTGCAGTGTGTGTTCGT
IIIS4
3001 h
GGCCATCCGGACCATCGGAAACATCATGATTGTCACCACACTTCTGCAATTTATGTTCGCCTGCATCGGGGTGCAGCTCTTCAAGGGGAAATTCTACACCTGCACGGACGAGGCCAAACA
m
GGCCATCCGGACCATCGGAAACATCATGATTGTCACCACCCTCTTGCAGTTCATGTTCGCCTGCATTGGTGTTCAGCTGTTCAAGGGAAAATTCTACAGTTGCACTGATGAGGCCAAACA
IIIS5
3121 h
CACCCCTCAAGAATGCAAGGGCTCCTTCCTGGTATACCCAGATGGAGACGTGTCACGGCCCCTGGTCCGGGAGCGGCTCTGGGTCAACAGTGATTTCAACTTTGACAATGTCCTTTCAGC
m
CACCCTGAAAGAATCGAAGGGCTCCTTCCTCATCTACCCTGATGGAGATGTGTCACGACCTTTGGTCCGGGAGCGGCTCTGGGTCAACAGTGATTTTAACTTTGACAACGTCCTTTCAGC
3241 h
CATGATGGCCCTGTTCACTGTCTCCACCTTTGAAGGCTGGCCTGCACTGCTATACAAGGCCATCGATGCATATGCAGAGGACCATGGCCCCATCTATAATTACCGTGTGGAGATCTCAGT
m
CATGATGGCCCTGTTCACTGTCTCTACCTTTGAAGGCTGGCCTGCGCTACTATACAAGGCCATAGATGCAAACGCAGAAGATGAGGGCCCTATCTACAATTACCATGTGGAGATATCAGT

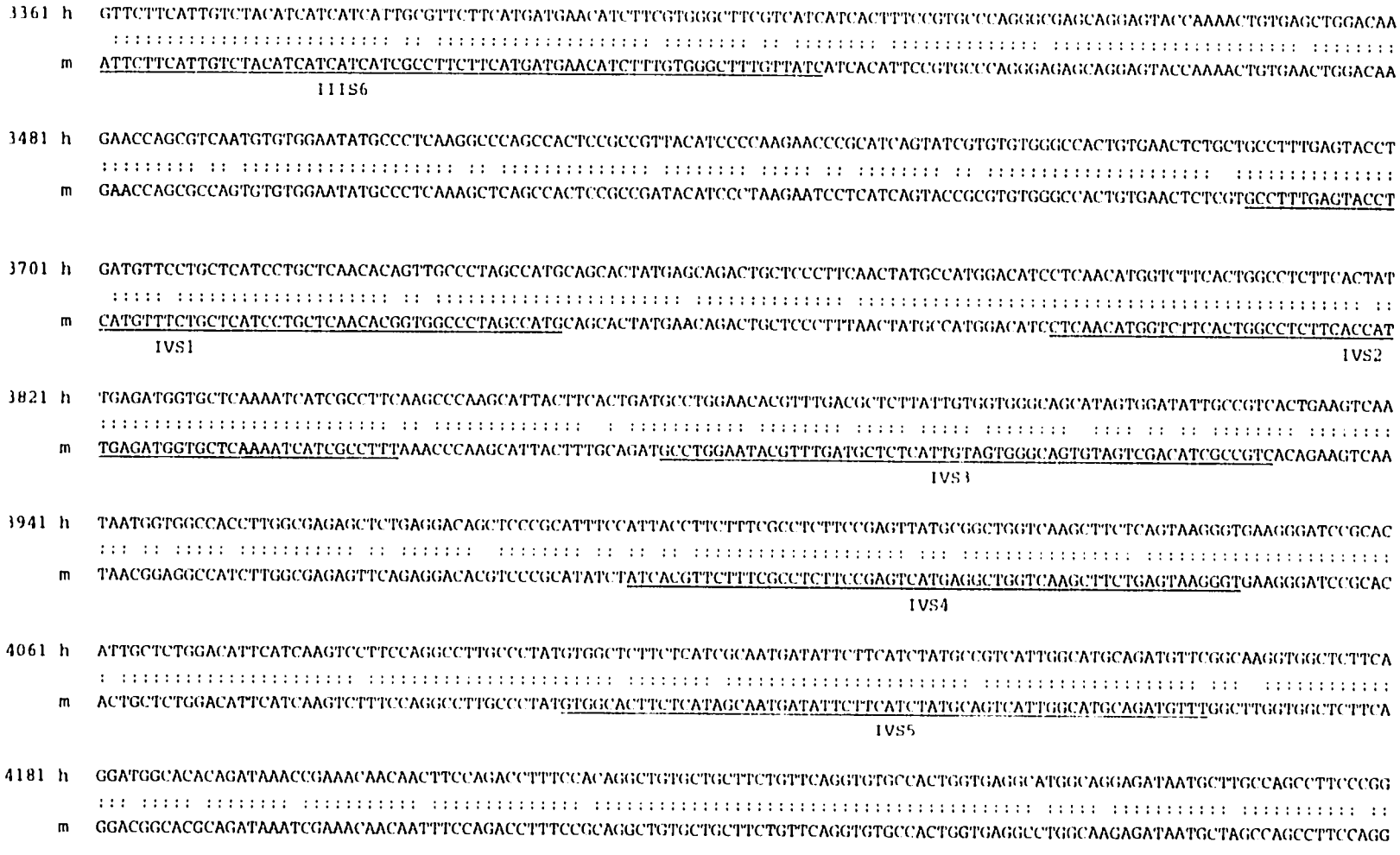
3361 h GTTCTTCATTGTCTACATCATCATCATTGCGTTCTTCATGATGAACATCTTCGTGGGCTTCGTCATCATCACTTTCCGTGCCCAGGGCGAGCAGGAGTACCAAAACTGTGAGCTGGACAA
m ATTCTTCATTGTCTACATCATCATCATCGCCTTCTTCATGATGAACATCTTTGTGGGCTTTGTTATCATCACATTCCGTGCCCAGGGAGAGCAGGAGTACCAAAACTGTGAACTGGACAA
IIIS6
3481 h GAACCAGCGTCAATGTGTGGAATATGCCCTCAAGGCCCAGCCACTCCGCCGTTACATCCCCAAGAACCCGCATCAGTATCGTGTGTGGGCCACTGTGAACTCTGCTGCCTTTGAGTACCT
m GAACCAGCGCCAGTGTGTGGAATATGCCCTCAAAGCTCAGCCACTCCGCCGATACATCCCTAAGAATCCTCATCAGTACCGCGTGTGGGCCACTGTGAACTCTCGTGCCTTTGAGTACCT
3701 h GATGTTCCTGCTCATCCTGCTCAACACAGTTGCCCTAGCCATGCAGCACTATGAGCAGACTGCTCCCTTCAACTATGCCATGGACATCCTCAACATGGTCTTCACTGGCCTCTTCACTAT
m CATGTTTCTGCTCATCCTGCTCAACACGGTGGCCCTAGCCATGCAGCACTATGAACAGACTGCTCCCTTTAACTATGCCATGGACATCCTCAACATGGTCTTCACTGGCCTCTTCACCAT
IVS1
IVS2
3821 h TGAGATGGTGCTCAAAATCATCGCCTTCAAGCCCAAGCATTACTTCACTGATGCCTGGAACACGTTTGACGCTCTTATTGTGGTGGGCAGCATAGTGGATATTGCCGTCACTGAAGTCAA
m TGAGATGGTGCTCAAAATCATCGCCTTTAAACCCAAGCATTACTTTGCAGATGCCTGGAATACGTTTGATGCTCTCATTGTAGTGGGCAGTGTAGTCGACATCGCCGTCACAGAAGTCAA
IVS3
3941 h TAATGGTGGCCACCTTGGCGAGAGCTCTGAGGACAGCTCCCGCATTTCCATTACCTTCTTTCGCCTCTTCCGAGTTATGCGGCTGGTCAAGCTTCTCAGTAAGGGTGAAGGGATCCGCAC
m TAACGGAGGCCATCTTGGCGAGAGTTCAGAGGACACGTCCCGCATATCTATCACGTTCTTTCGCCTCTTCCGAGTCATGAGGCTGGTCAAGCTTCTGAGTAAGGGTGAAGGGATCCGCAC
IVS4
4061 h ATTGCTCTGGACATTCATCAAGTCCTTCCAGGCCTTGCCCTATGTGGCTCTTCTCATCGCAATGATATTCTTCATCTATGCCGTCATTGGCATGCAGATGTTCGGCAAGGTGGCTCTTCA
m ACTGCTCTGGACATTCATCAAGTCTTTCCAGGCCTTGCCCTATGTGGCACTTCTCATAGCAATGATATTCTTCATCTATGCAGTCATTGGCATGCAGATGTTTGGCTTGGTGGCTCTTCA
IVS5
4181 h GGATGGCACACAGATAAACCGAAACAACAACTTCCAGACCTTTCCACAGGCTGTGCTGCTTCTGTTCAGGTGTGCCACTGGTGAGGCATGGCAGGAGATAATGCTTGCCAGCCTTCCCGG
m GGACGGCACGCAGATAAATCGAAACAACAATTTCCAGACCTTTCCGCAGGCTGTGCTGCTTCTGTTCAGGTGTGCCACTGGTGAGGCCTGGCAAGAGATAATGCTAGCCAGCCTTCCAGG

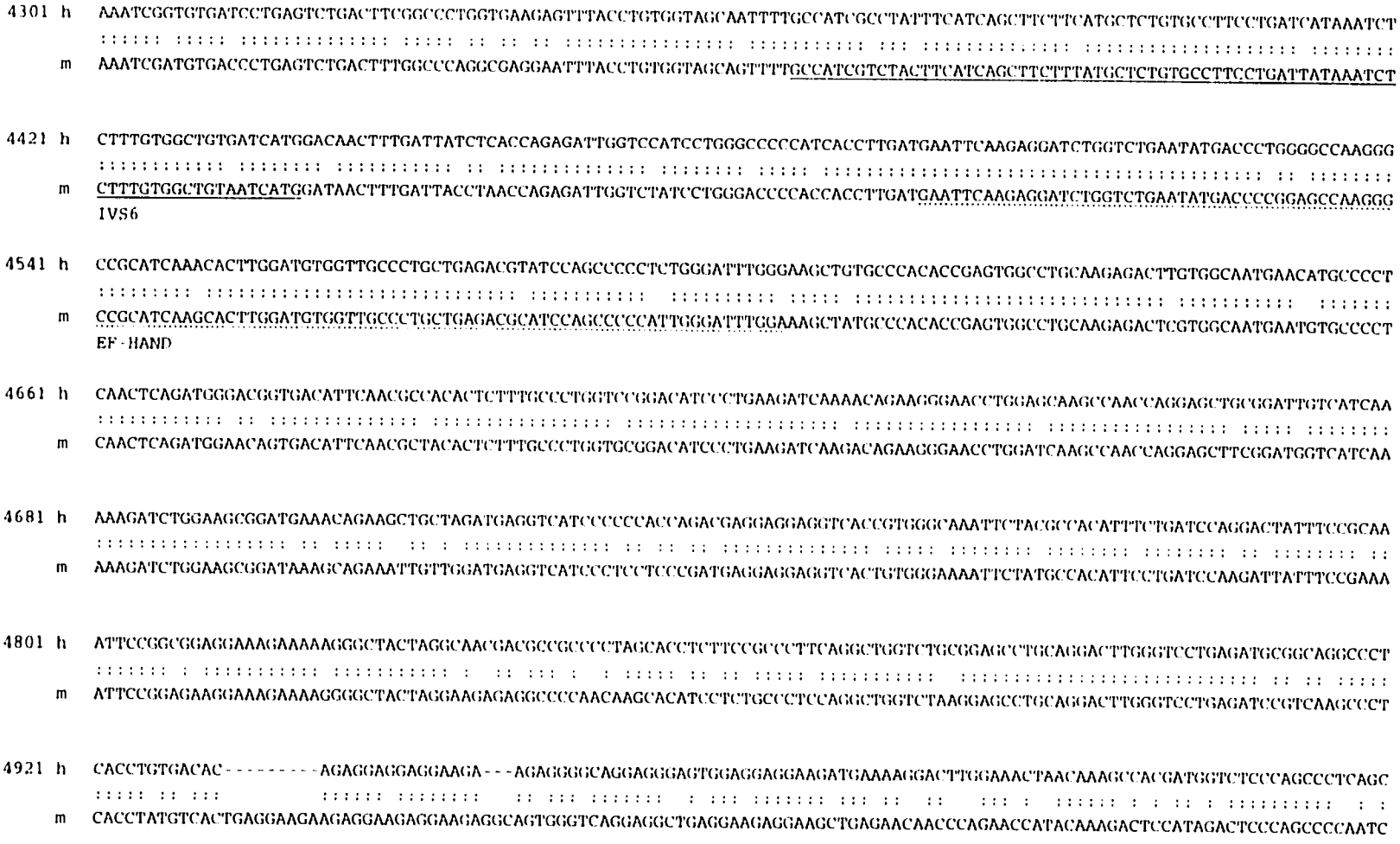
4301 h AAATCGGTGTGATCCTGAGTCTGACTTCGGCCCTGGTGAAGAGTTTACCTGTGGTAGCAATTTTGCCATCGCCTATTTCATCAGCTTCTTCATGCTCTGTGCCTTCCTGATCATAAATCT
m AAATCGATGTGACCCTGAGTCTGACTTTGGCCCAGGCGAGGAATTTACCTGTGGTAGCAGTTTTGCCATCGTCTACTTCATCAGCTTCTTTATGCTCTGTGCCTTCCTGATTATAAATCT
4421 h CTTTGTGGCTGTGATCATGGACAACTTTGATTATCTCACCAGAGATTGGTCCATCCTGGGCCCCCATCACCTTGATGAATTCAAGAGGATCTGGTCTGAATATGACCCTGGGGCCAAGGG
m CTTTGTGGCTGTAATCATGGATAACTTTGATTACCTAACCAGAGATTGGTCTATCCTGGGACCCCACCACCTTGATGAATTCAAGAGGATCTGGTCTGAATATGACCCCGGAGCCAAGGG
IVS6
4541 h CCGCATCAAACACTTGGATGTGGTTGCCCTGCTGAGACGTATCCAGCCCCCTCTGGGATTTGGGAAGCTGTGCCCACACCGAGTGGCCTGCAAGAGACTTGTGGCAATGAACATGCCCCT
m CCGCATCAAGCACTTGGATGTGGTTGCCCTGCTGAGACGCATCCAGCCCCCATTGGGATTTGGAAAGCTATGCCCACACCGAGTGGCCTGCAAGAGACTCGTGGCAATGAATGTGCCCCT
EF-HAND
4661 h CAACTCAGATGGGACGGTGACATTCAACGCCACACTCTTTGCCCTGGTCCGGACATCCCTGAAGATCAAAACAGAAGGGAACCTGGAGCAAGCCAACCAGGAGCTGCGGATTGTCATCAA
m CAACTCAGATGGAACAGTGACATTCAACGCTACACTCTTTGCCCTGGTGCGGACATCCCTGAAGATCAAGACAGAAGGGAACCTGGATCAAGCCAACCAGGAGCTTCGGATGGTCATCAA
4681 h AAAGATCTGGAAGCGGATGAAACAGAAGCTGCTAGATGAGGTCATCCCCCCACCAGACGAGGAGGAGGTCACCGTGGGCAAATTCTACGCCACATTTCTGATCCAGGACTATTTCCGCAA
m AAAGATCTGGAAGCGGATAAAGCAGAAATTGTTGGATGAGGTCATCCCTCCTCCCGATGAGGAGGAGGTCACTGTGGGAAAATTCTATGCCACATTCCTGATCCAAGATTATTTCCGAAA
4801 h ATTCCGGCGGAGGAAAGAAAAAGGGCTACTAGGCAACGACGCCGCCCCTAGCACCTCTTTCCGCCCTTCAGGCTGGTCTGCGGAGCCTGCAGGACTTGGGTCCTGAGATGCGGCAGGCCCT
m ATTCCGGAGAAGGAAAGAAAAGGGGCTACTAGGAAGAGAGGCCCCAACAAGCACATCCTCTGCCCTCCAGGCTGGTCTAAGGAGCCTGCAGGACTTGGGTCCTGAGATCCGTCAAGCCCT
4921 h CACCTGTGACAC---------AGAGGAGGAGGAAGA---AGAGGGGCAGGAGGGAGTGGAGGAGGAAGATGAAAAGGACTTGGAAACTAACAAAGCCACGATGGTCTCCCAGCCCTCAGC
m CACCTATGTCACTGAGGAAGAAGAGGAAGAGGAAGAGGCAGTGGGTCAGGAGGCTGAGGAAGAGGAAGCTGAGAACAACCCAGAACCATACAAAGACTCCATAGACTCCCAGCCCCAATC

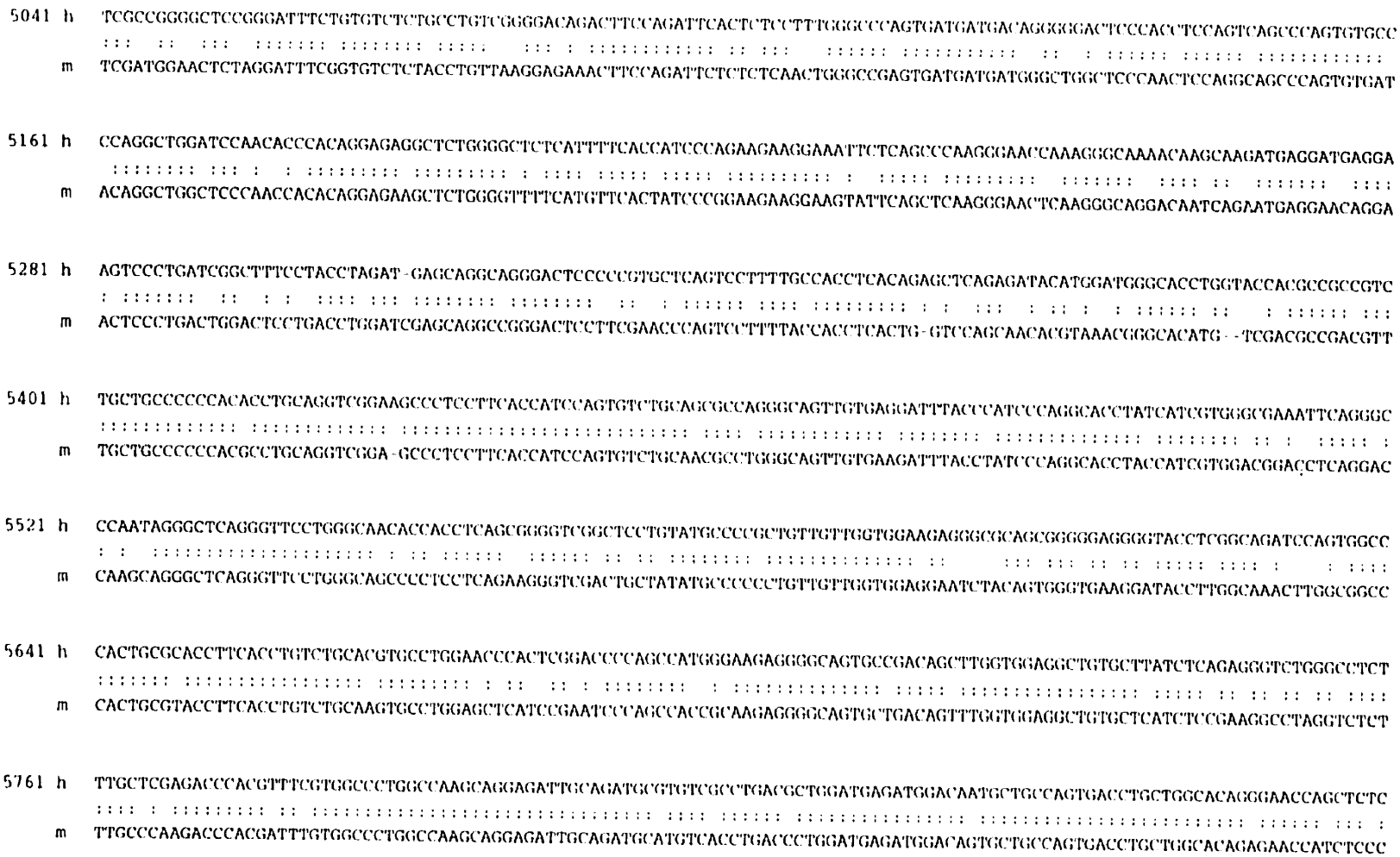
5041 h
m
5161 h
m
5281 h
m
5401 h
m
5521 h
m
5641 h
m
5761 h
m

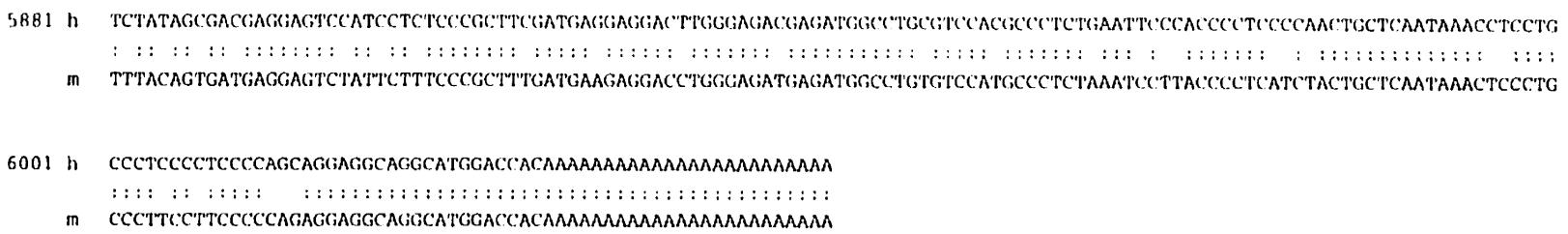
5881 h
TCTATAGCGACGAGGAGTCCATCCTCTCCCGCTTCGATGAGGAGGACTTGGGAGACGAGATGGCCTGCGTCCACGCCCTCTGAATTCCCACCCCTCCCCAACTGCTCAATAAACCTCCTG
m
TTTACAGTGATGAGGAGTCTATTCTTTCCCGCTTTGATGAAGAGGACCTGGGAGATGAGATGGCCTGTGTCCATGCCCTCTAAATCCTTACCCCTCATCTACTGCTCAATAAACTCCCTG
6001 h
CCCTCCCCTCCCCAGCAGGAGGCAGGCATGGACCACAAAAAAAAAAAAAAAAAAAAAAAA
m
CCCTTCCTTCCCCCAGAGGAGGCAGGCATGGACCACAAAAAAAAAAAAAAAAAAAAAAAA

Mapping of Cacna1f to the mouse X-chromosome

On the human X-chromosome, *CACNA1F* lies immediately adjacent to the synaptophysin gene (approximately 5 kb apart) in the Xp11.23 cytogenetic region of the X-chromosome. Due to the conservation of linkage in this region between the mouse and human, *Syp* and *Cacna1f* were expected to lie close together on the mouse X-chromosome. To prove that the mouse gene isolated in this study is indeed the orthologue of the human *CACNA1F* gene, it was decided to demonstrate that this gene maps to the mouse X-chromosome near the synaptophysin gene. To do this, a BAC clone that hybridised with a 3' end probe of *CACNA1F* was identified at the MRC Genome Centre in Toronto, as described in 'Materials and Methods'. PCR analysis of BAC334I19 was performed using for the mouse synaptophysin gene (*Syp*) and the human *CACNA1F* gene (Table 10). The *CACNA1F* primers were nearly identical to the mouse *Cacna1f* sequence (17/18 bases were the same). Amplification products were observed for both sets of primers showing that both of these genes are present on BAC334I19 (Figure 21). Sequencing of the PCR products yielded sequence that was identical to mouse *Syp* and mouse *Cacna1f*, thus confirming the identity of the PCR products.

Spatial expression of *Cacna1f* in the mouse retina

To determine the spatial expression of *CACNA1F* in the retina, *in situ* hybridisation was performed on mouse retinal sections. Probes from two different regions of *Cacna1f*, both having a lower degree of homology with other calcium channel α_1-subunits than with human *CACNA1F*, were used in these hybridisation experiments. One probe, mJM8Ex15-21 (755 bp), spanned the region that translates into the

Table 10 – Primer sets for amplification of *Cacna1f* and *Syp* on BAC334I19

Primer Set	Forward Primer Name	Forward Sequence	Reverse Primer Name	Reverse Sequence	Product size (bp)
hJMC8SV1b	hJMC8SV1bF	accaccccagagccccagt	hJMC8SV1bR	tccactccacgatgctgat	247
mSypEx6	mSyp-F	cttcctgaacctggtgctct	mSyp-R	aggagctggttgcttttctg	115

Figure 21. Amplification of *Syp* and *Cacnalf* on mouse BAC334I19. a) Amplification of *Cacnalf* using primer set SV1b (Table 10) yielded a 250 bp PCR product from BAC334I19 DNA (lanes 2 and 3). b) Amplification of *Syp* using primer set SypEx6 yielded a 115 bp PCR product from BAC334I19 DNA (lanes 2 and 3). Amplification using both sets of primers on a human BAC204-C16 representing Xp11.4 yielded no PCR products (lane 4). The marker in lane 1 of both a) and b) is the 1 kb ladder from GIBCO/BRL.

NB. BAC334I19-1 and BAC334I19–2 represent isolated clones of the BAC that were selected from an LB agar plate and grown individually.

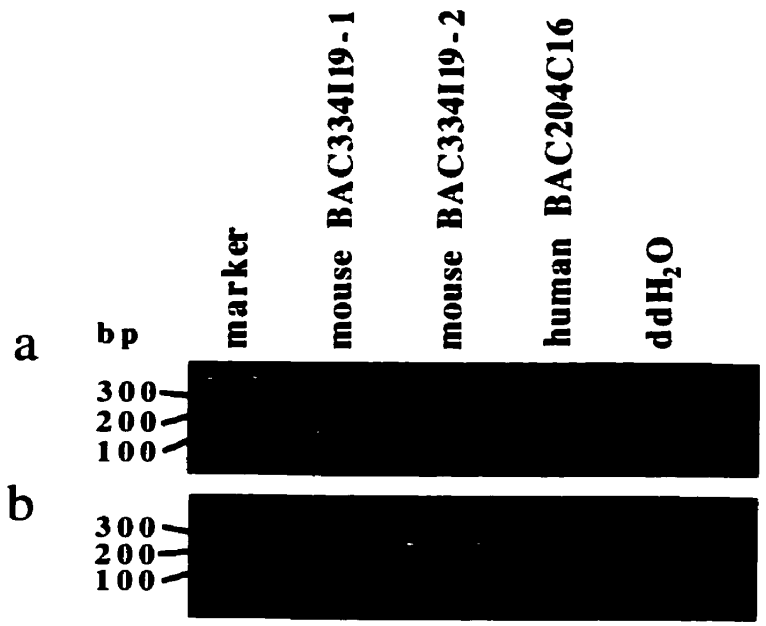
a
b
bp
300
200
100
300
200
100
marker
mouse BAC334I19-1
mouse BAC334I19-2
human BAC204C16
ddH_2O

cytoplasmic loop between internal homologous repeats II and III and the other probe, JM8Ex40-48 (948 bp), spanned the 3' end of the gene, the part corresponding to the COOH cytoplasmic portion of the $\alpha 1$ protein.

The hybridisation signal generated with the antisense versions of both probes was detected in three distinct retinal layers: the outer nuclear layer, the inner nuclear layer, and the ganglion cell layer (Figure 22a). To demonstrate that the signals elicited from the *Cacna1f* probes were specific: hybridisation with a rhodopsin cDNA antisense probe was also performed. This hybridisation yielded a signal in both the outer nuclear layer and the inner segment layer of the photoreceptor cells (Figure 22b). Hybridisation with the *Cacna1f* and *Rho* sense probes yielded no significant signal in any of the retinal layers (Figure 22c).

Figure 22. *in situ* hybridisation of *Cacna1f* transcripts in mouse retina. Sections of mouse retina were hybridised with riboprobes generated from mouse cDNA clones. The probes used for each section are as follows: a) antisense *Cacna1f*, showing hybridisation with the ONL (outer nuclear layer), INL (inner nuclear layer) and the GCL (ganglion cell layer), but not with the OS (outer segment) or IS (inner segment) b) antisense Rhodopsin, showing hybridisation with the ONL and IS only, and c) sense *Cacna1f*, showing no hybridisation with any of the retinal layers.

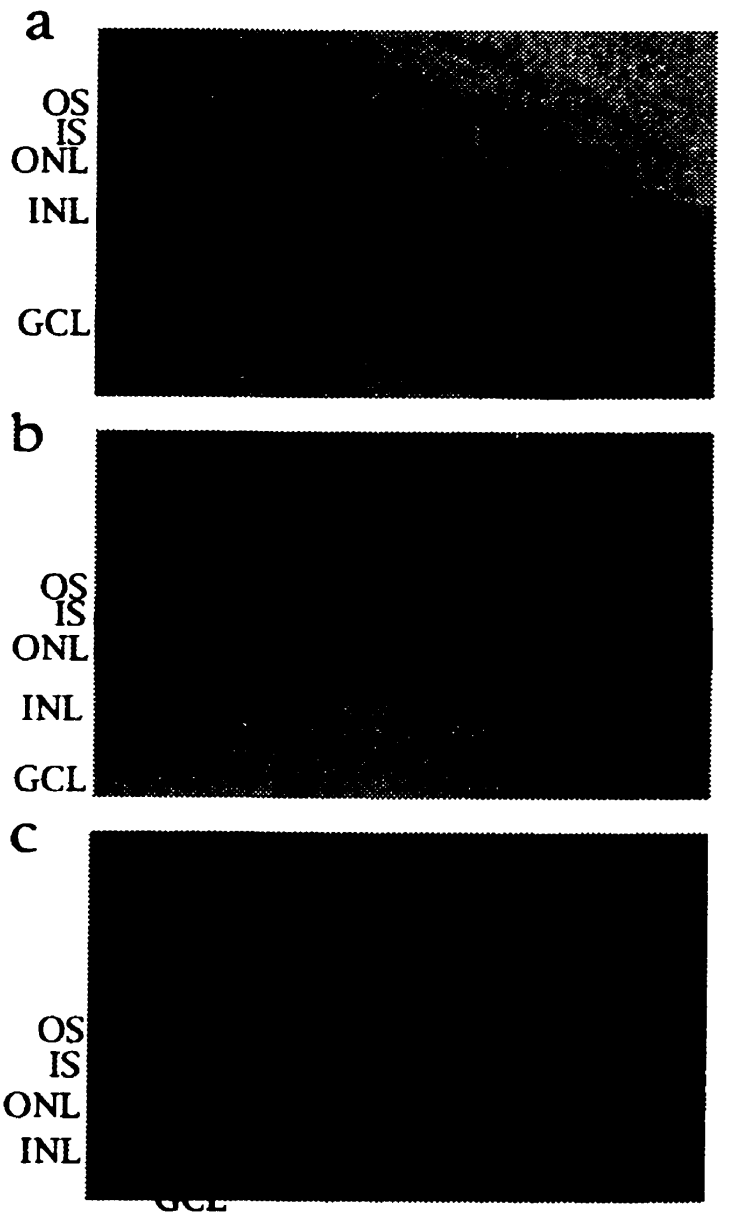
a
OS
IS
ONL
INL
GCL
b
OS
IS
ONL
INL
GCL
c
OS
IS
ONL
INL

CHAPTER 4 – DISCUSSION

CACNA1F is a calcium ion channel α_1-subunit

The detailed task of defining the total genomic organisation of the gene responsible for incomplete CSNB began when the JMC8 gene was identified by mutation analysis of candidate genes. Homologue analysis established JMC8 to be *CACNA1F* (Fisher et al., 1997) member of the calcium ion channel α_1-subunit family. This thesis research showed that the *CACNA1F* gene contains 48 exons which are distributed across 29 kb of genomic DNA in Xp11.23. The 6069 bp cDNA has an open reading frame of 5931 bp which translates into a 1977 amino acid protein. Comparison analysis of the full-length cDNA and amino acid sequences suggests that *CACNA1F*, by homology with similar calcium ion channels, is a novel α_1-subunit of a voltage-gated dihydropyridine-sensitive L-type calcium channel. Functional studies with an expressed protein are required to confirm the identity of *CACNA1F*.

Voltage-dependent calcium channels are found in the plasma membranes of various excitable cell-types and they function in the regulation of Ca^{++} entry into cells. Calcium channels are classified based on their electrophysiological and pharmacological properties. L-type calcium channels are high-voltage activated (>-30mV) and some of them are sensitive to dihydropyridines. The "L" stands for long-lasting, in other words they inactivate slowly. Dihydropyridine-sensitive L-type calcium channels are hetero-oligomeric and are comprised of five different subunits, α_1, α_2, β_1, δ, and γ (Puro et al., 1996); (Stea et al., 1995).

In comparing the cDNA and predicted protein structure of *CACNA1F* with other voltage-gated dihydropyridine-sensitive L-type calcium channel α_1-subunits, five distinct features of these types of channels were found in *CACNA1F*, strongly supporting the assertion that *CACNA1F* encodes an α_1-subunit of this type of ion channel (Figure 23).

1) *CACNA1F* has four internal homologous repeat domains (I-IV) that each have six alpha-helical membrane spanning segments (S1-S6). These transmembrane segments are highly homologous among the members of this α_1-subunit family (in some cases greater than 85%), and clusters of these segments called domains are separated by cytoplasmic loops which are comprised of stretches of amino acids.

2) The fourth transmembrane segment in each domain of *CACNA1F* has a set of positively charged residues and this feature is considered to be the voltage-sensor domain of the calcium channel.

3) The ion pore of the channel is formed by a hydrophobic linker of the amino acids between transmembrane segments five and six: this linker has a beta-hairpin structure (Doyle and Stubbs, 1998); (Stea et al., 1995).

4) Intracellular calcium levels regulate the opening and closing of this channel, thus controlling calcium entry into the cells. High levels of intracellular calcium ion result in the closing of the channels; whereas when the intracellular calcium levels are low, the channels open (de Leon et al., 1995). The EF-hand and the calmodulin binding region (the "IQ" motif) are two other features of *CACNA1F* that are highly conserved among the calcium channel α_1-subunit family. The EF-hand has been shown to be a calcium binding motif that functions in calcium-sensitive inactivation of the ion channel (de Leon et al., 1995). It is located on the cytoplasmic side of the membrane at the

Figure 23. Cartoon of the topology of the predicted protein expressed from *CACNA1F*. The typical features of a voltage-gated dihydropyridine-sensitive L-type calcium channel α_1-subunit can be seen in this illustration: a) four homologous repeat domains, each with six transmembrane segments, are separated by cytoplasmic loops; b) the fourth transmembrane segment of each domain has positively charged residues and act as voltage sensors; c) the hydrophobic linker between transmembrane segments 5 and 6 in each domain forms the ion channel pore and; d) the E-F hand is a calcium binding motif that functions in the calcium-sensitive inactivation of the calcium channel. The location of mutations in *CACNA1F* that have been found in the DNA of family members affected with incomplete CSNB are indicated by different symbols (Bech-Hansen et al., 1998).

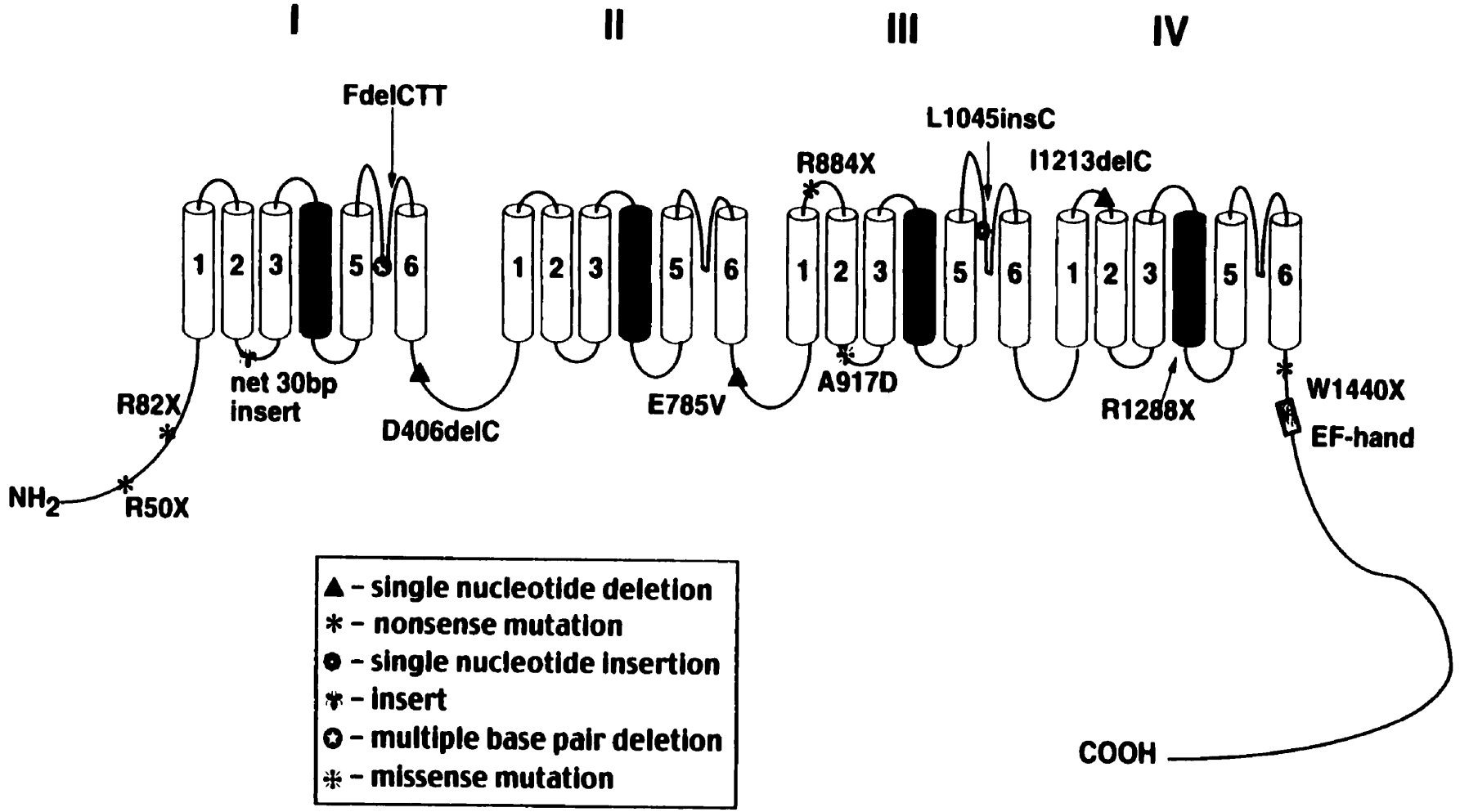
I
II
III
IV
FdelCTT
L1045insC
R884X
I1213delC
1 2 3 5 6
R82X
net 30bp insert
D406delC
E785V
A917D
R1288X
W1440X
EF-hand
NH2
R50X
COOH
▲ - single nucleotide deletion
* - nonsense mutation
● - single nucleotide insertion
* - insert
○ - multiple base pair deletion
* - missense mutation

carboxy-terminal tail region, only 18 amino acids away from the last membrane-spanning segment (IVS6). Deletion studies by de Leon et al. (1995) conveyed the importance of the EF-hand by demonstrating that it was necessary for calcium-mediated inactivation of the calcium channels and did not require the last two-thirds of the cytoplasmic tail for its function (de Leon et al., 1995). More recently, the IQ motif located in exon 40 immediately 3' of the EF-hand has been demonstrated to contain glutamine and isoleucine residues that bind calmodulin, which itself is a critical Ca2+ sensor involved in inactivation of the calcium channel (Figure 9) (Zuhlke et al., 1999), (Peterson et al., 1999). Calmodulin has been shown to bind to the cytoplasmic tail of the calcium channel α_1-subunit (Peterson et al., 1999).

5) Specific amino acids in IIS5, IIIS6, and IVS6 have been found to confer dihydropyridine-sensitivity to the calcium channel (Sinnegger et al., 1997). These amino acids are present in the predicted protein encoded by *CACNA1F* (Figure 24).

5' UTR

5' RACE was performed on *CACNA1F*, which extended the transcript sequence 62 bp upstream of the start codon (Strom et al., 1998). Analysis of the genomic DNA sequence upstream of the translation start site revealed a possible TATA box approximately 103 bp upstream of the start codon, which would place it at the expected position approximately 30 bp before the transcription start site (Strom et al., 1998). The GENSCAN prediction program includes promoter regions in the search for genes within genomic DNA, but as not all genes have similar promoters, the transcription start site cannot always be predicted (Burge and Karlin, 1997). In order to determine if the

Figure 24. Alignment of the mouse *Cacna1f* amino acid sequence with the human *CACNA1F* amino acid sequence. The upper sequence represents human *CACNA1F* (h) and each amino acid in the sequence is depicted by the single letter symbol for that amino acid. The lower sequence represents mouse *Cacna1f* (m) and the identical amino acids are depicted by two dots below the corresponding amino acid. The amino acids in the mouse sequence that differ from those in the human sequence are also depicted by a plus sign for conserved changes in the amino acid and by the single letter code for non-conserved changes in the amino acid. Dashes in either sequence introduce spaces in that sequence to maintain maximum homology between the two sequences. The transmembrane segments are marked with an underline and labeled. The EF-hand is shaded and labeled.

```
1    h  MSESEGGKDTTPEPSPANGAGPGPEWGLCPGPPAVEGESSGASGLGTPKRRNQHSKHKTV
        m  :::::V:::::::::::::T:::::::::::::T:GTD+:::::::::R::T::N:::::

                                                    IS1
61   h  AVASAQRSPRALFCLTLANPLRRSCISIVEWKPFDILILLLTIFANCVALGVYIPFPEDDS
        m  ::::::::::::::::::T::+::::::::::::::::::::::::::::::::::::::::

                          IS2                                   IS3
121  h  NTANHNLEQVEYVFLVIFTVETVLKIVAYGLVLHPSAYIRNGWNLLDFIIVVVGLFSVLL
        m  ::::::::::::::::::::::::::::::::::::::::::::::::::::::::::::::

                                        IS4
181  h  EQGPGRPGDAPHTGGKPGGFDVKALRAFRVLRPLRLVSGVPSLHIVLNSIMKALVPLLHI
        m  ::::::::::::::::::::::::::::::::::::::::::::::::+:::::::::::::

                IS5
241  h  ALLVLFVIIIYAIIGLELFLGRMHKTCYFLGSDMEAEEDPSPCASSGSGRACTLNQTECR
        m  ::::::::::::::::::::::::::::::::::::::::::::::::::::+::::H::::

                                                                IS6
301  h  GRWPGPNGGITNFDNFFFAMLTVFQCVTMEGWTDVLYWMQDAMGYELPWVYFVSLVIFGS
        m  ::::::::::::::::::::::::::-::::::::::::::::::::::::::::::::::

361  h  FFVLNLVLGVLSGEFSKEREKAKARGDFQKQREKQQMEEDLRGYLDWITQAEELDMEDPS
        m  ::::::::::::::::::::::::::::::L::::::::::::::::::::::+H:::

421  h  ADDNLGSMAEEGRAGHRPQLAELTNRRRGRLRWFSHSTRSTHSTSSHASLPASDTGSMTE
        m  V:G::A:+::::::::::::+::::::::::::::::::::::::::::::::::::::D

                                                            IIS1
481  h  TQGDEDEEEGALASCTRCLNKIMKTRVCRRLRRANRVLRARCRRAVKSNACYWAVLLLVF
        m  :P::::::::T+::::::::::::::I::HF:::::G::::::::::::::::::::::

                                        IIS2                    IIS3
541  h  LNTLTIASEHHGQPVWLTQIQEYANKVLLCLFTVEMLLKLYGLGPSAYVSSFFNRFDCFV
        m  ::::::::::::::+::::T::::::::::::::::::::::::V::+::::::::::

                                IIS4
601  h  VCGGILETTLVEVGAMQPLGISVLRCVRLLRIFKVTRHWASLSNLVASLLNSMKSIASLL
        m  ::::::::::::::::::::::::::::::::::::::::::::::::::::::::::::::

                IIS5
661  h  LLLFLFIIIFSLLGMQLFGGKFNFDQTHTKRSTFDTFPQALLTVFQILTGEDWNVVMYDG
        m  ::::::::::::::::::::::::::::::::::::::::::::::::::::::::::::::
```

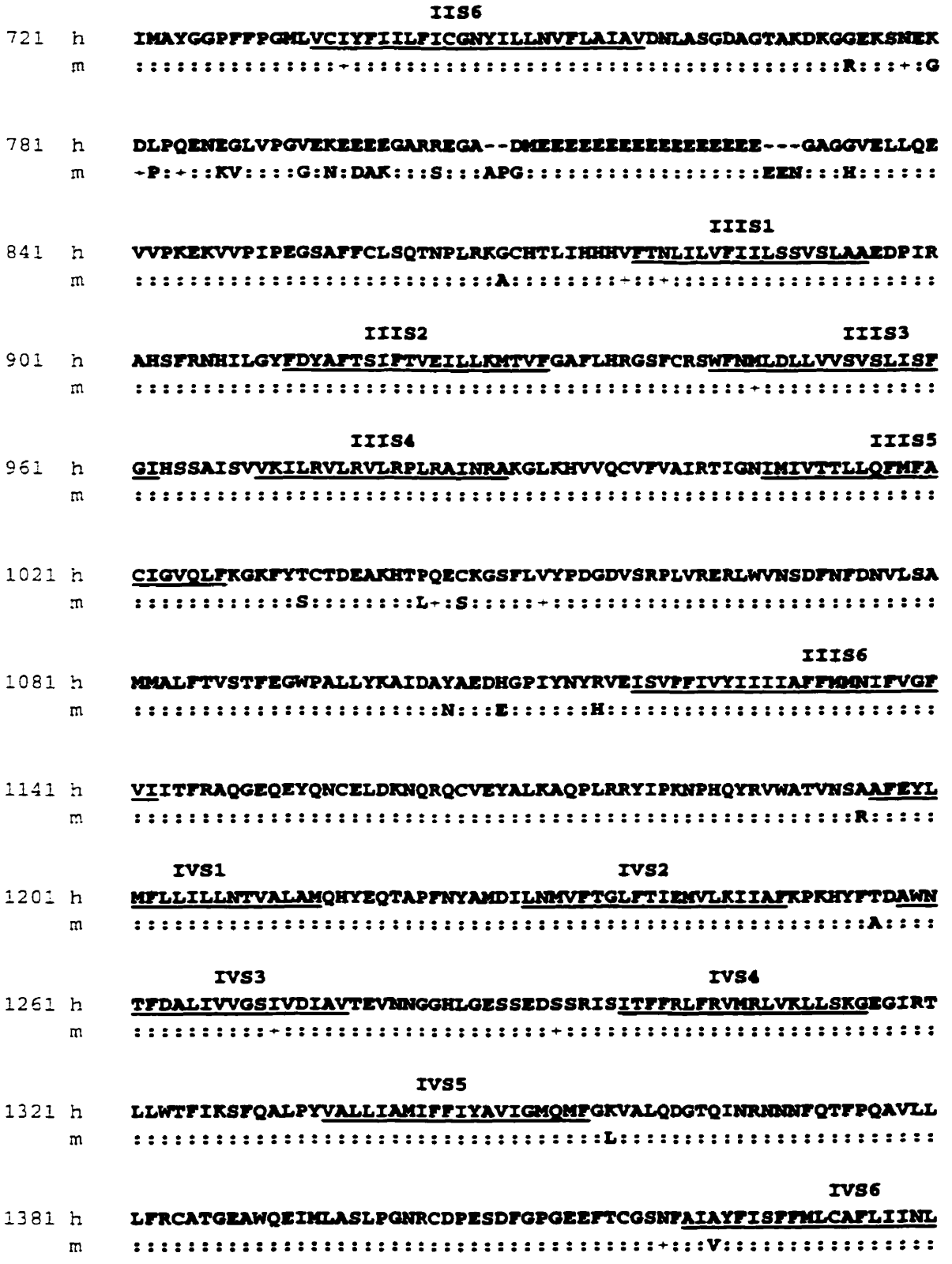
IIS6
721 h IMAYGGPFFPGMLVCIYFIILFICGNYILLNVFLAIAVDNLASGDAGTAKDKGGEKSNEK
m :::::::::::::::+:::::::::::::::::::::::::::::::::::::::R::::+:G
781 h DLPQENEGLVPGVEKEEEEGARREGA--DMEEEEEEEEEEEEEEEEEE---GAGGVELLQE
m -P:+::KV::::G:N:DAK:::S:::APG:::::::::::::::::::EEN:::H::::::
IIIS1
841 h VVPKEKVVPIPEGSAFFCLSQTNPLRKGCHTLIHHHVFTNLILVFIILSSVSLAAEDPIR
m :::::::::::::::::::::::::::::A:::::::::+::+::::::::::::::::::::
IIIS2 IIIS3
901 h AHSFRNHILGYFDYAFTSIFTVEILLKMTVFGAFLHRGSFCRSWFNMLDLLVVSVSLISF
m :::+:::::::::::::
IIIS4 IIIS5
961 h GIHSSAISVVKILRVLRVLRPLRAINRAKGLKHVVQCVFVAIRTIGNIMIVTTLLQFMFA
m ::
1021 h CIGVQLFKGKFYTCTDEAKHTPQECKGSFLVYPDGDVSRPLVRERLWVNSDFNFDNVLSA
m ::::::::::::S:::::::::L+:S::::+::::::::::::::::::::::::::::::
IIIS6
1081 h MMALFTVSTFEGWPALLYKAIDAYAEDHGPIYNYRVEISVFFIVYIIIIAFFMMNIFVGF
m ::::::::::::::::::::::N:::E::::::H::::::::::::::::::::::::::
1141 h VIITFRAQGEQEYQNCELDKNQRQCVEYALKAQPLRRYIPKNPHQYRVWATVNSAAFEYL
m ::R:::::
IVS1 IVS2
1201 h MFLLILLNTVALAMQHYEQTAPFNYAMDILNMVFTGLFTIEMVLKIIAFKPKHYFTDAWN
m ::A::::
IVS3 IVS4
1261 h TFDALIVVGSIVDIAVTEVNNGGHLGESSEDSSRISITFFRLFRVMRLVKLLSKGEGIRT
m ::::::::::+::::::::::::::::::::+::::::::::::::::::::::::::::::
IVS5
1321 h LLWTFIKSFQALPYVALLIAMIFFIYAVIGMQMFGKVALQDGTQINRNDNFQTFPQAVLL
m ::::::::::::::::::::::::::::::::::L::::::::::::::::::::::::
IVS6
1381 h LFRCATGEAWQEIMLASLPGNRCDPESDFGPGEEFTCGSNFAIAYFISFFMLCAFLIINL
m ::::::::::::::::::::::::::::::::::::::+:::V::::::::::::::::

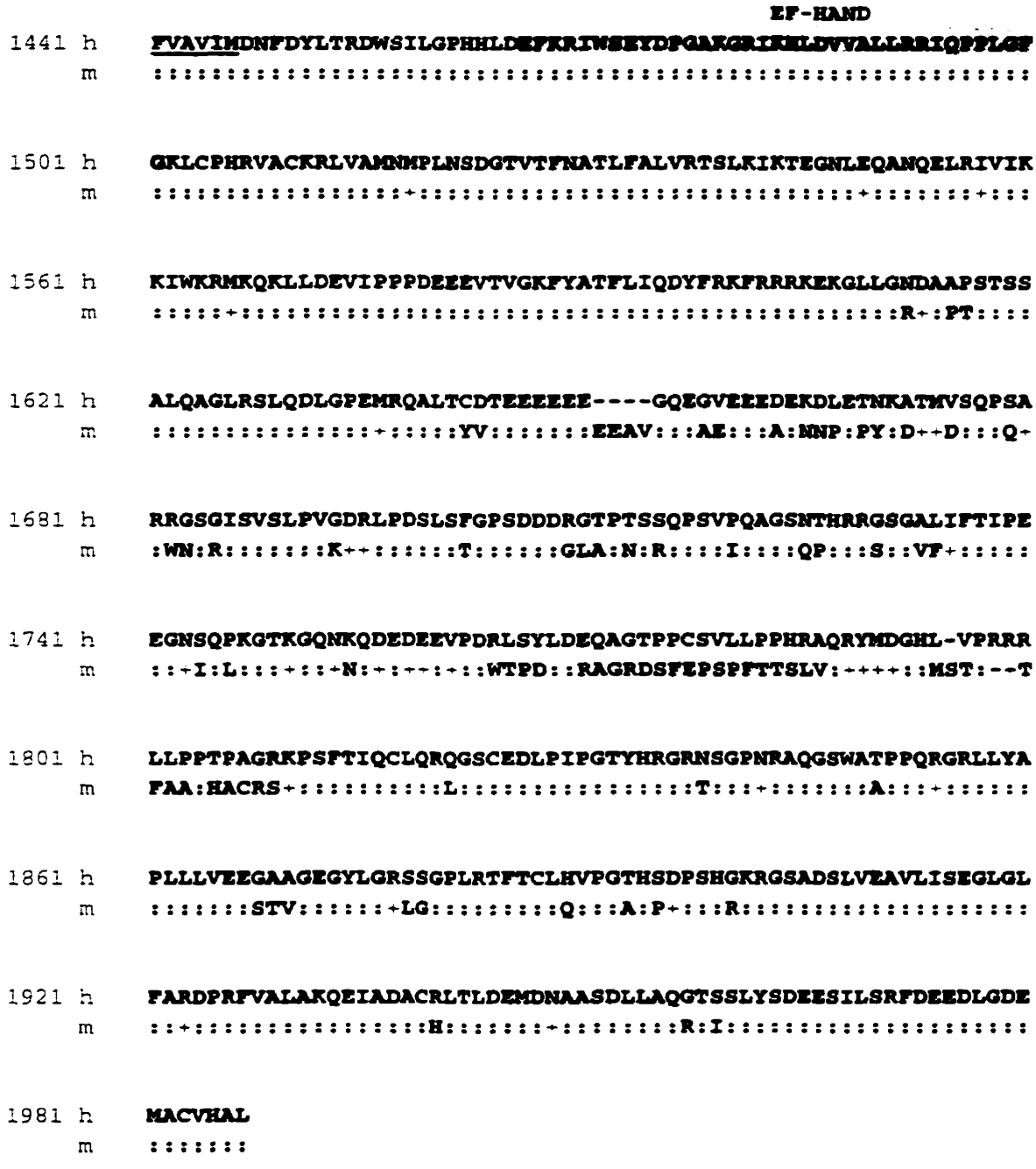
EF-HAND
1441 h
m
1501 h
m
1561 h
m
1621 h
m
1681 h
m
1741 h
m
1801 h
m
1861 h
m
1921 h
m
1981 h
m

transcript extends further. S1 nuclease protection of the 5' end of the RNA can be performed and the subsequent product can be sequenced. This eliminates the loss of the 5' that may occur in RT-PCR by hybridising genomic DNA to an RNA transcript pool, digesting it with nuclease and sequencing the remaining DNA.

Splice variants

Although several splice variants of *CACNA1F* were recognised (see 'Splice variants' in the 'Results' section) only two variants lead to complete proteins. As the PCR amplifications performed were not quantitative, two factors helped in determining the predominance of these splice variants. First of all, since only two combinations of variable exons yielded productive sequence, these were considered to be the predominant isoforms of *CACNA1F* cDNA. Secondly, mutation analysis of *CACNA1F* in patients with incomplete CSNB in the laboratory of Dr. Bech-Hansen has provided evidence that further suggests that the cDNA sequence containing exons 1 (short), 2 (long), and 3, is the prototypical *CACNA1F* cDNA. This mutation analysis has identified two separate mutations in the long form of exon 2, strongly suggesting that exon 2 is the predominantly expressed variant in this region (Figure 9 in 'Genomic organisation of *CACNA1F*' in the 'Results' section) (Bech-Hansen et al. unpublished data).

What is the reason for the transcription of these numerous splice variants? The explanation for the splice variants that yield complete proteins seems relatively simple, they may be differentially expressed, either spatially or temporally. For example, a splice variant of a neuronal α_1-subunit in the chicken is expressed in the cochlea, while its isoform is expressed in the brain (Kollmar et al., 1997). Splice variants may also provide

an alternate functionality to the tissue in which they are expressed. Calcium channels have very specific electrophysiological and pharmacological properties that control the calcium current. This functionality is derived from the specific amino acids in the resultant protein such as the voltage sensor, the EF-hand, and the DHP-sensitive features that were determined to be part of *CACNA1F*. The addition or removal of amino acids from these regions can affect the flow of calcium ions into the cell. one group even found an α_1-subunit isoform that lacked the voltage sensor domain in the IVS4 region in non-excitable cells (Brereton et al., 1997). At this point it is difficult to say what the functional differences between the isoforms of *CACNA1F* are and studies described later in this chapter would be required to determine these differences.

Alternative splicing may also play a role as a regulatory mechanism in development, which may account for the highly variable phenotype that is seen amongst patients with incomplete CSNB who have the same mutation. Splice variants may also provide diversity to an organism, allowing the organism to adapt more readily to new situations. Alternative splicing throughout evolution may be the reason for such large and diverse family of calcium channels, each with its specific function for its specific tissue and cell type, thus explaining the presence of *CACNA1F* solely in the retina.

The splice variants that are predicted not to yield complete proteins appear to be lower in abundance than the variants the are expected to yield proteins, as was seen by them appearing as a fainter sequence on the autoradiograms (see Figure 11). The presence of these variants is less clearly explained. These aberrant transcripts may result from "leaky splicing machinery" and may just be side products of transcription.

Alternatively, these transcripts, although not expected to produce a calcium channel α_1-subunit, may also add to the genetic diversity of the organism.

The mouse orthologue of *CACNA1F*

As part of the effort to determine spatial expression and function of *CACNA1F*, the mouse orthologue, *Cacna1f*, was defined. There is a high degree of cDNA sequence homology between human *CACNA1F* and mouse *Cacna1f* (as high as 95% in some regions). It shares highest homology with the longer isoform of *CACNA1F*, adding to the presumption that this isoform is the predominant species. In this thesis work *Cacna1f* was shown to be expressed in the mouse retina and demonstrated not to be present in RNA extracted from adult mouse brain. This expression pattern agrees with the tissue expression profile of human *CACNA1F*, which was also determined in this study (Figure 14 in "Results").

The regions of greatest homology between the mouse and human were those which encoded the transmembrane segments of domains I to IV (Figure 24), in agreement with the high degree of homology seen amongst the family members of α_1-subunits of calcium channels which function in forming the channel pore. Furthermore, these segments are even highly conserved between mammals and *Drosophila* (Bech-Hansen et al., 1998); (Smith et al., 1996). Translation of the 5956 bp *Cacna1f* open reading frame revealed a greater than 90% identity with the predicted protein sequence encoded by the human *CACNA1F* (Figure 24). Every feature of the voltage-gated L-type calcium

channel α_1-subunit described for *CACNA1F* is conserved in the predicted protein of this orthologue (Figure 23).

To confirm that the murine *Cacna1f* cDNA was truly the orthologue of human *CACNA1F*, this thesis work showed that *Cacna1f* was present on the mouse X-chromosome adjacent to the synaptophysin (*Syp*) gene. Based on the high degree of conservation of linkage and synteny on the mouse X-chromosome and, more specifically, the conservation of linkage in the region between *SYP/Syp* and *CLCN5/Clcn5*, *Cacna1f* was assumed to be present in this region on the mouse X-chromosome as had been shown for human *CACNA1F* on the human X-chromosome (Bech-Hansen et al., 1998). *Cacna1f* was expected to lie in the same relative position compared with the genes for synaptophysin (*Syp*), Dent's disease (*Clcn5*), and a *GATA* transcription factor (*Gata1*) on the mouse X-chromosome as the human orthologues do on the human X-chromosome. The evidence provided in this study showing that *Syp* and *Cacna1f* lie on the same mouse BAC demonstrates linkage between the two genes on the mouse X-chromosome. Showing the presence of both *Cacna1f* and *Syp* on the same mouse BAC suggests that synteny is conserved and that *Cacna1f* is the orthologue of *CACNA1F*.

A mouse model for the disease retinitis pigmentosa has been created by targeted disruption of the rhodopsin gene (Humphries et al., 1997). This model aided in the characterisation of the structural and functional differences between normal and affected retinas and provided a starting point for the study of the pathogenesis of retinitis pigmentosa (Humphries et al., 1997). Mouse models have also proven useful in the testing of potential therapies for diseases. By studying abnormal as well as normal states,

both physiologically and anatomically, we have learned much of what we know about human biology. The identification of the *Cacna1f* sequence in this study provides us with critical information for creating a mouse model for incomplete CSNB. Having a model for incomplete CSNB will provide us with the abnormal state of vision and will be useful in divulging information not only about this disorder, but also about the mechanisms of the visual pathway. A mouse model may also provide the potential to develop therapies and treatments for incomplete CSNB.

CACNA1F expression is localised to the retina

To gain insight into its function, the expression pattern of *CACNA1F* was examined. The demonstration that *CACNA1F* expression was limited to retinal tissue by RT-PCR laid the foundation for defining its specific expression pattern within this tissue. Northern blot analysis performed by Fisher et al. (1997) showed hybridisation of *CACNA1F* with skeletal muscle RNA, whereas a similar analysis performed by Strom et al. (1998) showed hybridisation with retina RNA, but not with skeletal muscle RNA. Only under less stringent conditions were they able to detect hybridisation with the skeletal muscle RNA, therefore the signal seen in the Northern blot by Fisher et al. (1997) must represent another member of the calcium channel α_1-subunit family. The results from this study with both *CACNA1F* and *Cacna1f* are consistent with *CACNA1F* expression being restricted to the retina (Figures 14 and 15).

In a thorough review of calcium channels, five types of voltage-gated calcium channels (T, L, N, P, and Q) and their known subunits were described and compared (Stea et al., 1995). *CACNA1F* most closely resembles the α_1-subunits of Class C

(cardiac) and Class D (neuronal) L-type calcium channels (Bech-Hansen et al., 1998). α1C subunits have also been found in a variety of other tissues, including brain, smooth muscle, adrenal glands and pituitary glands. The neuronal α1D subunits are present in the pancreas as well as in the brain (as reviewed by (Stea et al., 1995). More recently, α1D has been identified in the retina (Puro et al., 1996). This group found several subunits of Class D L-type calcium channels in the Müller (glial) cells of the retina, including the α_1-subunit (Puro et al., 1996). *CACNA1F* shares the greatest degree of homology with the neuronal form of the α_1-subunit, which is 70% overall, and as high as 84% between transmembrane segments. Because this neuronal gene is expressed in the retina, the experiments looking at the expression pattern of *CACNA1F* were carried out with this in mind, focussing on regions having lower homology with other calcium channel α_1-subunits.

Spatial expression of *Cacna1f* in the mouse

Hybridisation of mouse retinal sections with probes covering two different regions of *Cacna1f* revealed a specific expression pattern for this gene, in the outer nuclear layer (ONL), the inner nuclear layer (INL), and the ganglion cell layer (GCL) of the retina (Figure 22). This pattern is similar to the one seen on hybridisation of mouse retina with the human probe from a different region of the gene than the murine probe used in this study (Strom et al., 1998). As described in the introduction, the mouse has been used extensively to study retinal disorders, therefore using information gleaned from

the *in situ* hybridisation in mouse retinal sections using *Cacna1f* cRNA probes, we can infer that *CACNA1F* is also expressed in the INL, ONL and the GCL in the human retina.

In a similar study by Reid et al. (1999), the expression of the mouse gene for X-linked juvenile retinoschisis (XLRS) was localised to the outer nuclear layer and the inner segments of the photoreceptor cells. This group used this information to speculate on the function of the XLRS gene in the human disorder (Reid et al., 1999). Prior to the results obtained from the mouse *in situ* hybridisation, the defect for XLRS was thought to be in the Müller cells, but the localisation of expression to the ONL and inner segments told a different story. Based on this information, the authors proposed that the defect may lie in the interaction of the XLRS protein with the Müller cells (Reid et al., 1999). Similarly, comparing the localisation of *CACNA1F* expression with functional studies on the retina, will also allow us to infer a function for *CACNA1F*.

Notably, a group performing immunocytochemistry with an antibody (MANC-1, monoclonal antibody against calcium channels) to dihydropyridine-sensitive calcium channels on rat brain, spinal cord and retina, determined the presence of dihydropyridine-sensitive calcium channel subunits in the rat retina (Ahlijanian et al., 1990). They detected immunoreactivity in the ONL, INL and GCL (Ahlijanian et al., 1990), and since this is where the *CACNA1F* transcripts are located, this information suggests that the *CACNA1F* protein is located in these layers as well. Additionally, they found strong immunoreactivity with DHP-sensitive calcium channels in the inner segments of the photoreceptors. This supplements the information gained from the *in situ* hybridisation, which allowed for the localisation of the transcripts only.

The role of *CACNA1F* in night vision

The results obtained from this work entail the identification of *CACNA1F* as the gene responsible for incomplete X-linked CSNB, the determination of the complete sequence of the mouse orthologue, *Cacna1f*, and its spatial expression in the mouse retina. These results allow us to entertain informed speculation on the functional role of this gene in the visual pathway, in particular, the mechanism for dark adaptation in the retina.

Electroretinography in patients with incomplete CSNB yields an ERG with a reduced b-wave and psychophysical evaluations exhibit a decreased ability to dark-adapt (as reviewed by (Héon and Musarella, 1994). The b-wave in the ERG is thought to be generated by a transretinal current in the Müller cells (Miller and Dowling, 1970), but this current can be affected by upstream events in the ON-bipolar cells or the photoreceptor cells. The a-wave in the ERGs of patients with incomplete CSNB are normal, which is indicative of normal hyperpolarisation of the outer segments in response to light (as reviewed by (Stockton and Slaughter, 1989). This suggests that *CACNA1F* plays a role in the visual pathway somewhere between the outer segments and the Müller cells.

The hyperpolarisation of the photoreceptors leads to the closing of DHP-sensitive L-type calcium channels causing a decrease in the release of glutamate, which in turn causes the depolarisation of the ON-bipolar cells (Schmitz and Witkovsky, 1997). A defect at this step of the visual pathway would influence the signal received by the Müller cells, and would account for the ERG in patients with incomplete CSNB. Localisation of

CACNA1F by *in situ* hybridisation to the photoreceptor cell bodies suggests that *CACNA1F* could be the calcium channel responsible for regulating the release of glutamate. As transcripts of *CACNA1F* are also present in the inner nuclear layer and the ganglion cell layer, expression of the protein in these cells may add to the abnormal response in the visual pathway elicited by the defect in the photoreceptor cells. On the other hand, the defect within the photoreceptors themselves is more likely to disrupt the visual pathway, therefore may be sufficient to cause the abnormal ERG response in patients with incomplete CSNB.

Theoretically, in patients with incomplete CSNB, the mutations in *CACNA1F* might decrease or even completely prevent the normal influx of Ca^{++} in the dark-adapted eye. Concomitantly, the continuous glutamate release that normally occurs would also be decreased or terminated and the ON-bipolar cells wouldn't be maintained in a hyperpolarised state, which is required for increased sensitivity to light in darkened conditions. It can be presumed then that individuals with incomplete CSNB would not detect low levels of light even in darkened surroundings. This defect apparently does not affect normal day vision, presumably because it emulates light-adaptation. Patients are not able to completely dark-adapt since physiologically, the message perceived by the brain is that there is a light stimulus. By understanding the mechanisms of the defect that causes incomplete CSNB, we begin to learn more about the normal physiology of the retina, much of which remains to be unveiled. By determining the genomic organisation of *CACNA1F*, unveiling its expression pattern, identifying and sequencing the mouse orthologue, *Cacna1f*, and localising its transcripts to the three nuclear layers within the retina, this thesis research has provided the framework for shaping our understanding not

only of the pathogenesis of incomplete CSNB, but also of the *CACNA1F* gene and its role in the visual pathway.

Future studies

To further characterise *CACNA1F*, it is important to ascertain its true function as well as the location of the protein within the retina. In order to express a protein, the full-length cDNA of *CACNA1F* must first be cloned into an expression vector. By expressing *CACNA1F* in a human cell line, such as human embryonic kidney (HEK) cells, it can be tested for its function as a calcium channel. Details of its function can be elucidated by performing functional assays on specific mutants such as the experiments done to determine the IQ motif where specific amino acids were changed and calcium inactivation was measured (Peterson et al., 1999). Furthermore, the missense mutation observed in patients with incomplete CSNB can be tested to determine there functional effect.

By raising antibodies to the α_1F protein and performing immunohistochemistry on retinal sections, studies can also be performed to determine the specific cellular location of function of *CACNA1F*. Antibodies specific to different isoforms of *CACNA1F* may provide information on the function of particular isoforms, by showing with which cell-type they are associated. The splice variants can also be investigated by performing *in situ* hybridisation with riboprobe sequences that are specific to these variants. Additionally they can also be clone and expressed to determine their specific functions.

Another important study to be carried out is to create a mouse model for incomplete CSNB. A model of this disease can be used to learn more about the pathology of CSNB, to understand the mechanisms of the visual pathway, and to test potential therapies.

REFERENCES

Ahlijanian, M. K., Westenbroek, R. E., and Catterall, W. A. (1990). Subunit structure and localization of dyhidropyridine-sensitive calcium channels in mammalian brain, spinal cord and retina. Neuron *4*, 819-832.

Alitalo, T., Kruse, T. A., Forsius, H., Eriksson, A. W., and de la Chapelle, A. (1991). Localization of the Aland Island eye disease locus to the pericentromeric region of the X chromosome by linkage analysis. American Journal of Human Genetics *48*, 31-38.

Bech-Hansen, N. T., Boycott, K. M., Gratton, K. J., Ross, D. A., Field, L. L., and Pearce, W. G. (1998a). Localization of a gene for incomplete X-linked congenital stationary night blindness to the interval between DXS6849 and DXS8023 in Xp11.23. Hum Genet *Aug;103*, 124-30.

Bech-Hansen, N. T., Field, L. L., Schramm, A. M., Reedyk, M., Craig, I. W., Fraser, N. J., and Pearce, W. G. (1990). A locus for X-linked congenital stationary night blindness is located on the proximal portion of the short arm of the X chromosome. Hum Genet *84*, 406-408.

Bech-Hansen, N. T., Naylor, M. J., Maybaum, T. A., Pearce, W. G., Koop, B., Fishman, G. A., Mets, M., Musarella, M. A., and Boycott, K. M. (1998). Loss-of-function mutations in a calcium-channel alpha1-subunit gene in Xp11.23 cause incomplete X-linked congenital stationary night blindness. Nat. Genet. *Jul;19*, 264-267.

Bech-Hansen, N. T., and Pearce, W. G. (1993). Manifestations of X-linked congenital stationary night blindness in three daughters of an affected male: demonstration of homozygosity. Am J Hum Genet *52*, 71-77.

Bergen, A. A. B., Brink, J. B. t., Riemsiag, F., Schuurman, E. J. M., and Tijmes, N. (1995). Localization of a novel X-linked congenital stationary night blindness locus: Close linkage to the RP3 type retinitis pigmentosa gene region. Hum Mol Genet *4*, 931-935.

Blair, H. J., Ho, M., Monaco, A. P., Fisher, S., Craig, I. W., and Boyd, Y. (1995). High-resolution comparative mapping of the proximal region of the mouse X chromosome. Genomics *28*, 305-310.

Blanchard, M. M., Taillon, M., P., Nowotny, P., and Nowotny, V. (1993). PCR buffer optimization with uniform temperature regimen to facilitate automation. PCR Methods and Applications *2*, 234-240.

Bowes, C., Li, T., Danciger, M., Baxter, L. C., Applebury, M. L., and Farber, D. B. (1990). Retinal degeneration in the rd mouse is caused by a defect in the beta subunit of rod cGMP-phosphodiesterase. Nature *Oct 18;347*, 677-80.

Boycott, K. M., Pearce, W. G., Musarella, M. A., Weleber, R. G., Maybaum, T. A., Birch, D. G., Miyake, Y., Young, R. S. L., and Bech-Hansen, N. T. (1998). Evidence for genetic heterogeneity in X-linked congenital stationary night blindness. Am. J. Hum. Genet. *Apr;62*, 865-75.

Boycott, K. M., Zahorchak, R. J., Summer, C. G., Boycott, N. P., Kotak, V., Russell, C. G., and Bech-Hansen, N. T. (1998a). Construction of a 1.5-Mb bacterial artificial chromosome contig in Xp11.23, a region of high gene content. Genomics *Mar 15;48*, 369-72.

Brereton, H. M., Harland, M. L., Froscio, M., Petronijevic, T., and Barritt, G. J. (1997). Novel variants of voltage-operated calcium channel alpha1 subunit transcripts in a rat liver-derived cell line: deletion in the IVS4 voltage sensing region. Cell Calcium *22*, 39-52.

Buchberg, A. M., Bedigian, H. G., Taylor, B. A., Brownell, E., Ihle, J. N., Nagata, S., Jenkins, N. A., and Copeland, N. G. (1988). Localization of Evi-2 to chromosome 11: linkage to other proto-oncogene and growth factor loci using interspecific backcross mice. Oncogene Res *2*, 149-65.

Burge, C., and Karlin, S. (1997). Prediction of complete gene structures in human genomic DNA. J. Mol. Biol. *268*, 78-94.

Carr, R. E. (1974). Congenital stationary night blindness. Trans Am Ophthalmol Soc *72*, 449-487.

Collins, F. S. (1995). Positional cloning moves from perditional to traditional. Nat Genet *9*, 347-349.

Copenhagen, D. R. (1996). Retinal development: On the crest of an exciting wave. Curr Biol *6*, 1368-70.

de Leon, M., Wang, Y., Jones, L., Perez-Reyes, E., Wei, X., Soong, T. W., Snutch, T., and Yue, D. T. (1995). Essential Ca^{2+}-Binding Motif for Ca^{2+}-Sensitive Inactivation of L-type Ca^{2+} Channels. Science *270*, 1502-1506.

DeBry, R. W., and Seldin, M. F. (1996). Human/mouse homology relationships. Genomics *33*, 337-351.

Doyle, J. L., and Stubbs, L. (1998). Ataxia, arrhythmia and ion-channel gene defects. Trends Genet *Mar;14*, 92-8.

Eppig, J. T., and Nadeau, J. H. (1995). Comparative maps: the mammalian jigsaw puzzle. Curr. Op. in Genet. and Dev. *5*, 709-716.

Epstein, D. J., Malo, D., Vekemans, M., and Gros, P. (1991). Molecular characterization of a deletion encompassing the splotch mutation on mouse chromosome 1. Genomics *10*, 89-93.

Erhlich, J., Sankoff, D., and Nadeau, J. H. (1997). Synteny conservation and chromosome rearrangements during mammalian evolution. Genetics *147*, 289-296.

Farber, D. B., and Danciger, M. (1994). Inherited retinal degenrations in the mouse. In Molecular Genetics of Inherited Eye Disorders, A. F. W. a. B. Jay, ed.: Harwood Academic Publishers), pp. 126.

Fisher, S. E., Ciccodicola, A., Tanaka, K., Curci, A., Desicato, S., D'urso, M., and Craig, I. W. (1997). Sequence-based exon prediction around the synaptophysin locus reveals a gene-rich area containing novel genes in human proximal Xp. Genomics *Oct 15;45*, 340-7.

Fishman, G. A. (1985). Basic principles of clinical electroretinography. Retina *5*, 123-126.

Gal, A., Schinzel, A., Orth, U., Fraser, N. A., Mollica, F., Craig, I. W., Kruse, T., Machler, M., Neugebauer, M., and Bleeker-Wagemakers, L. M. (1989). Gene of X-chromosomal congenital stationary night blindness is closely linked to DXS7 on Xp. Hum Genet *81*, 315-318.

Heckenlively, J. R., Martin, D. A., and Rosenbaum, A. L. (1983). Loss of electroretinographic oscillatory potentials, optic atrophy, and dysplasia in congenital stationary night blindness. Am J Ophthalmol *96*, 526-534.

Héon, E., and Musarella, M. A. (1994). Congenital stationary night blindness: a critical review for molecular approaches. In Molecular Genetics of Inherited Eye Disorders, A. F. Wright and J. Barrie, eds.: Harwood Academic Publishers), pp. 277-301.

Humphries, M. M., Rancourt, D., Farrar, G. J., Kenna, P., Hazel, M., Bush, R. A., Sieving, P. A., Sheils, D. M., McNally, N., Creighton, P., Erven, A., Boros, A., Gulya, K., Capecchi, M. R., and Humphries, P. (1997). Retinopathy induced in mice by targeted disruption of the rhodopsin gene. Nat Genet *Feb;15*, 216-219.

Jeon, C.-J., Strettoi, E., and Masland, R. (1998). The major cell populations of the mouse retina. J Neurosci *Nov.1(18)*, 8936-46.

Jimenez-Sierra, J. M., and Ogden, T. E. (1989). Abnormalities of photoreceptors, rod system disorders (CSNB). In Inherited Retinal Disorders: A Diagnostic Guide, J. M.

Jimenez-Sierra, T. E. Ogden and G. B. Van Boemel, eds. (St. Louis: CV Mosby Company), pp. 175-187.

Khouri, G., Mets, M. B., Smith, V. C., Wendell, M., and Pass, A. S. (1988). X-linked congenital stationary night blindness: Review and report of a family with hyperopia. Arch Ophthalmol *106*, 1417-1422.

Kollmar, R., Fak, J., Montgomery, L., and Hudspeth, A. J. (1997). Hair cell-specific splicing of mRNA for the alpha 1D subunit of voltage-gated Ca^{2+} channels in the chicken's cochlea. Proc. Natl. Acad. Sci. USA *94*, 14889-14893.

Koutalos, Y., and Yau, K. W. (1996). Regulation of sensitivity in vertebrate rod photoreceptors by calcium. Trends Neurosci *Feb;19*, 73-81.

Krill, A. E. (1977). Hereditary retinal and choroidal diseases, Volume 2, a. D. B. A. A.E Krill, ed. (Hagerstown: Harper and Row).

Lyubarsky, A. L., Falsini, B., Pennesi, M. E., Valentini, P., and Pugh, E. N. J. (1999). UV- and midwave-sensitive cone-driven retinal responses of the mouse: a possible phenotype for coexpression of cone photopigments. J Neurosci *Jan 1;19*, 442-55.

McKusick, V. A. (1992). Mendelian inheritance in man, 10 Edition, Volume 2 (Baltimore, Md.: John Hopkins University Press).

Merin, S., Rowe, H., Auerbach, E., and Landau, J. (1970). Syndrome of congenital high myopia with nyctalopia. Am J Ophthalmol *70*, 541-547.

Miller, R. F., and Dowling, J. E. (1970). Intracellular responses of the Muller (glial) cells of mudpuppy retina: their relation to b-wave of the electroretinogram. J Neurophysiol *May;33*, 323-41.

Miyake, Y., Horiguchi, M., Ota, I., and Shiroyama, N. (1987a). Characteristic ERG flicker anomoly in incomplete congenital stationary night blindness. Invest Opthalmol and Vis Sci *28*, 1816-1823.

Miyake, Y., Yagasaki, K., and Horiguchi, M. (1987b). A rod-cone dysfunction syndrome with separate clinical entity: incomplete-type congenital stationary night blindness. In Degenerative Retinal Disorders: Clinical and Laboratory Investigations, J. G. Hollyfield, R. E. Anderson and M. M. LaVail, eds. (New York: Alan R. Liss.), pp. 137-145.

Miyake, Y., Yagasaki, K., Horiguchi, M., Kawase, Y., and Kanda, T. (1986). Congenital stationary night blindness with negative electroretinogram. Arch Ophthalmol *104*, 1013-1020.

Musarella, M. A., Weleber, R. G., Murphey, W. H., Young, R. S. L., Anson-Cartwright, L., Mets, M., Kraft, S. P., Polemeno, R., Litt, M., and Worton, R. G. (1989). Assignment

of the gene for complete X-linked congenital stationary night blindness (CSNB1) to Xp11.3. Genomics *5*. 727-737.

Nadeau, J. H. (1989). Maps of linkage and synteny homologies between mouse and man. Trends Genet *5*. 82-86.

Nadeau, J. H., and Taylor, B. A. (1984). Lengths of chromosomal segments conserved since divergence of man and mouse. Proc. Natl. Acad. Sci. USA *81*. 814-818.

O'Brien. (1995). Peripheral visual apparatus. In Gray's Anatomy. M. Berry, L. H. Bannister and S. M. Standring, eds. (New York: Churchill Livingstone, Medical Division of Pearson Professional Limited), pp. 1321-1352.

O'Connell, P., Cawthon, R. M., Viskochil, D., White, R., Carey, J. C., and Buchberg, A. M. (1991). The NF1 translocation breakpoint region. Ann N Y Acad Sci *615*. 319-31.

Ott, J., Bhattacharya, S., Chen, J. D., Denton, M. J., Donald, J., Dubay, C., Farrar, G. J., Fishman, G. A., Frey, D., Gal, A., Humphries, P., Jay, B., Jay, M., Litt, M., Machler, M., Musarella, M., Neugebauer, M., Nussbaum, R. L., Terwilliger, J. D., Weleber, R. G., Wirth, B., Wong, F., Worton, R. G., and Wright, A. F. (1990). Localizing multiple X

chromosome-linked retinitis pigmentosa loci using multilocus homogeneity tests. Proc Nat Acad of Sci USA *87*, 701-704.

Pearce, W. G., Reedyk, M., and Coupland, S. G. (1990). Variable expressivity in X-linked congenital stationary night blindness. Canadian Journal of Ophthalmology *25*, 3-10.

Peterson, B. Z., DeMaria, C. D., Adelman, J. P., and Yue, D. T. (1999). Calmodulin is the Ca2+ sensor for Ca2+ -dependent inactivation of L-type calcium channels. Neuron *Mar;22*, 549-58.

Polans, A., Baehr, W., and Palczewski, K. (1996). Turned on by Ca_2^+! The physiology and pathology of Ca_2^+-binding proteins in the retina. Trends Neurosci *19*, 547-554.

Puro, D. G., Hwang, J.-J., Kwon, O.-J., and Chin, H. (1996). Characterization of an L-type calcium channel expressed by human retinal Muller (glial) cells. Brain Res Mol Brain Res. *Apr;37*, 41-8.

Reeves, R. (1998). Exploring development and disease through germ-line genetic engineering in the mouse. Anat Rec *253*, 19-23.

Reid, S. N. M., Akhmedov, N. I. P., Piriev, N. I., Kozak, C. A., Danciger, M., and Farber, D. B. (1999). The mouse X-linked juvenile retinoschisis cDNA: expression in photoreceptors. Gene *227*, 257-266.

Rieke, F., and Baylor, D. A. (1998). Origin of reproducibility in the responses of retinal rods to single photons. Biophys J *Oct;75*, 1836-57.

Rieke, F., and Schwartz, E. A. (1994). A cGMP-gated current can control exocytosis at cone synapses. Neuron *13*, 863-873.

Rispoli, G. (1998). Calcium regulation of phototransduction in vertebrate rod outer segments. J Photochem Photobiol B *Jun 15;44*, 1-20.

Schmitz, Y., and Witkovsky, P. (1997). Dependence of photoreceptor glutamate release on a dihydropyridine-sensitive calcium channel. Neuroscience *Jun;78*, 1209-16.

Schwahn, U., Lenzner, S., Dong, J., Feil, S., Hinzmann, B., van Duijnhoven, G., Kirschner, R., Hemberger, M., Bergen, A. A., Rosenberg, T., Pinckers, A. J., Fundele, R., Rosenthal, A., Cremers, F. P., Ropers, H. H., and Berger, W. (1998). Positional cloning of the gene for X-linked retinitis pigmentosa 2. Nat Genet *Aug;19*, 327-32.

Schwartz, M., and Rosenberg, T. (1991). Aland Eye Disease: Linkage data. Genomics *10*, 327-332.

Sharp, P. A. (1994). Split genes and RNA splicing. Cell *77*, 805-815.

Sieving, P. A. (1993). Photopic ON- and OFF-pathway abnormalities in retinal dystrophies. Trans Am Opthalmol Soc *LXXXXI*, 701-773.

Sinnegger, M. J., Wang, Z., Grabner, M., Hering, S., Striessnig, J., Glossmann, H., and Mitterdorfer, J. (1997). Nine L-type amino acid residues confer full 1,4-dihydropyridine sensitivity to the neuronal calcium channel alpha1A subunit. Role of L-type Met1188. J Biol Chem *Oct 31;272*, 27686-93.

Smith, L. A., Wang, X., Peixoto, A. A., Neumann, E. K., Hall, L. M., and Hall, J. C. (1996). A Drosophila calcium channel alpha1 subunit gene maps to a genetic locus associated with behavioral and visual defects. J Neurosci *Dec 15;16*, 7868-79.

Stea, A., Soong, T. W., and Snutch, T. P. (1995). Handbook of receptors and channels: Ligand- and voltage-gated ion channels. In Handbook of receptors and channels, R. A. North, ed. (Boca Raton, Florida: CRC Press, Inc.), pp. 113-151.

Stephens, R. M., and Schneider, T. D. (1992). Features of spliceosome evolution and function inferred from an analysis of the information at human splice sites. J Mol Biol *Dec 20;228*, 1124-36.

Stockton, R. A., and Slaughter, M. M. (1989). A reflection of ON bipolar cell activity. J Gen Phys *93*, 101-122.

Strom, T. M., Nyakatura, G., Apfelstedt-Sylla, E., Hellebrand, H., Lorenz, B., Weber, B. H. F., Wutz, K., Gutwillinger, N., Ruther, K., Drescher, B., Sauer, C., Zrenner, E., Meitinger, T., Rosenthal, A., and Meindl, A. (1998). An L-type calcium channel gene mutated in incomplete X-linked congenital stationary night blindness. Nat Genet *19*, 260-263.

Tachibana, M., Okada, T., Arimura, T., Kobayashi, K., and Piccolino, M. (1993). Dihydropyridine-sensitive calcium current mediates neurotransmitter release from bipolar cells of the goldfish retina. J Neurosci *13*, 2898-2909.

Travis, G. H., and Hepler, J. E. (1993). A medley of retinal dystrophies. Nat Genet *Mar;3*, 191-2.

Wachtmeister, L. (1998). Oscillatory potentials in the retina: what do they reveal? Prog in Ret Eye Res *17*, 485-521.

Williams, P. (1995). Embryology and Development. In Gray's Anatomy, P. Collins, ed. (New York: Churchill Livingstone, Medical Division of Pearson Professional Limited), pp. 259.

Witkovsky, P., Schmitz, Y., Akopian, A., Krizaj, D., and Tranchina, D. (1997). Gain of rod to horizontal cell synaptic transfer: relation to glutamate release and a dihydropyridine-sensitive calcium current. J Neurosci *17*, 7297-7306.

Zuhlke, R. D., Pitt, G. S., Deisseroth, K., Tsien, R. W., and Reuter, H. (1999). Calmodulin supports both inactivation and facilitation of L-type calcium channels. Nature *399*, 159-62.